

**DOUBLE-ENCAPSULATION SYSTEM FOR DERMAL VACCINE DELIVERY**

A DISSERTATION

SUBMITTED ON THE EIGHTH DAY OF JANUARY 2013

TO THE DEPARTMENT OF CHEMICAL AND BIOMOLECULAR ENGINEERING

IN PARTIAL FULFILLMENT OF THE REQUIREMENTS

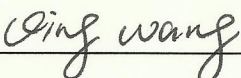
OF THE SCHOOL OF SCIENCE AND ENGINEERING

OF TULANE UNIVERSITY


FOR THE DEGREE OF

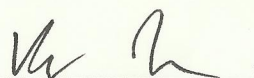
DOCTOR OF PHILOSOPHY

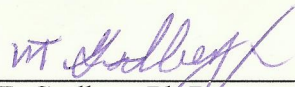
BY

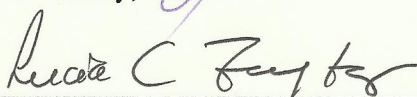
  
\_\_\_\_\_  
Qing Wang


APPROVED:

  
\_\_\_\_\_  
Kyriakos D. Papadopoulos, D. Eng. Sci.  
Director

  
\_\_\_\_\_  
Vijay T. John, D. Eng. Sci.

  
\_\_\_\_\_  
W T. Godbey, Ph.D.

  
\_\_\_\_\_  
Lucia C. Freytag, Ph.D.

  
\_\_\_\_\_  
Louise B. Lawson, Ph.D.

**DOUBLE-ENCAPSULATION SYSTEM FOR DERMAL VACCINE DELIVERY**

AN ABSTRACT

SUBMITTED ON THE EIGHTH DAY OF JANUARY 2013

TO THE DEPARTMENT OF CHEMICAL AND BIOMOLECULAR ENGINEERING

IN PARTIAL FULFILLMENT OF THE REQUIREMENTS

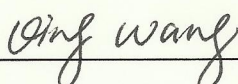
OF THE SCHOOL OF SCIENCE AND ENGINEERING

OF TULANE UNIVERSITY

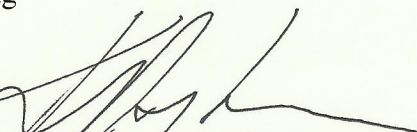
FOR THE DEGREE OF


DOCTOR OF PHILOSOPHY

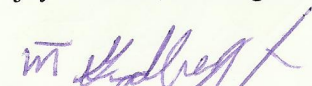
BY

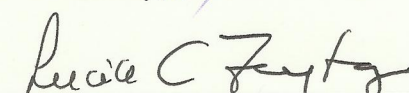
  
\_\_\_\_\_  
Qing Wang

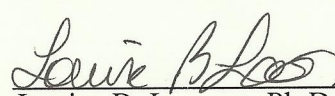
APPROVED:

  
\_\_\_\_\_  
Kyriakos D. Papadopoulos, D. Eng. Sci.  
Director

  
\_\_\_\_\_  
Vijay T. John, D. Eng. Sci.

  
\_\_\_\_\_  
W T. Godbey, Ph.D.

  
\_\_\_\_\_  
Lucia C. Freytag, Ph.D.

  
\_\_\_\_\_  
Louise B. Lawson, Ph.D.

## ABSTRACT

The objective of this study is to develop a colloid-based vaccine formulation that will be applied dermally to facilitate the permeation of macromolecules across the skin. Due to the high deformability and the compositions having the structural similarity with skin lipids, liposomes have shown promise in cutaneous delivery. However, their applications are limited due to the fact that they are susceptible to unfavorable physicochemical environment. Encapsulation of liposomes into micro-delivery systems allows the properties of liposomes to be protected while also controlling the time and rate of release during administration. Thus, a double-encapsulation system, in which liposomes containing a model active component were incorporated inside the internal aqueous phase ( $W_1$ ) of  $W_1/O/W_2$  double emulsions, was proposed and studied.

Capillary video-microscopy was used to study the behavior of the double-encapsulation system, and enabled direct monitoring of the individual globules from the moment of their preparation. Variations of Tween 80 concentration in the external aqueous phase ( $W_2$ ) or/and Span 80 concentration in the oil phase (O) controlled the release of liposomes from the  $W_1$  phase to the  $W_2$  phase. The major finding is that the sheer presence of liposomes in the  $W_1$  phase is by itself a stabilizing factor for double-emulsion globules. Additionally, the double-encapsulation formulation has been applied to skin-permeation *in vitro*; when combined with skin-treatment by use of a microneedle-

skinroller, the double-encapsulation formulation demonstrated high efficiency in delivering the model macromolecule across the skin. Results obtained from individual-globule experiments and *in-vitro* skin-permeation studies motivated us for the optimization of the double-encapsulation formulation in bulk. Cationic liposomes were selected since they have high penetration ability across the skin and hair follicles, as well as the adjuvant effect on the activation of antigen presenting cells. Bulk double-encapsulation formulations were fabricated using a two-step emulsification procedure, and subsequently stored at 5°C to obtain stable and cream-like formulations. With the aim of exploring how liposomes and their contents would be released after their application on the skin, the phase separation and release rate of double-encapsulation formulations were investigated upon the freeze-thaw process. By incorporating double emulsions and liposomes into one single delivery system, double-encapsulation formulations allow the liposomes and their contents to stay well protected, while also achieving a more efficient cutaneous delivery.

©Copyright by Qing Wang, 2013

**All Rights Reserved**

## **ACKNOWLEDGEMENTS**

I would like to express my sincere gratitude and appreciation to my advisor Dr. Kyriakos Papadopoulos for giving me the opportunity to pursue my Ph.D. degree at Tulane University, for introducing me to the fields of colloids and dermal vaccine delivery, and also for his unconditional support, guidance, patience and encouragement during my research. This work would not be completed without his guidance and help.

I would like to thank my important committee members, Dr. Vijay John, Dr. Lucia Freytag, and Dr. W Godbey, for offering me precious comments and suggestions on this work. Especially, I would like to thank Dr. Louise Lawson, from whom I received priceless training and advice on vaccinology. I would like to express my gratitude to Dr. Jibao He for his assistant with cryo-SEM and cryo-TEM, to Dr. Grace Tan for her contributions during experiments with the double-encapsulation system, and to Dr. Edith Rojas for her suggestions during the related experimentation. My appreciation is also extended to my friends and labmates in Chemical & Biomolecular Engineering Department, and Microbiology & Immunology Department at Tulane University.

Finally, I would like to dedicate my Ph.D degree to my parents and my parents in law for their influence and unconditional love. I thank my husband Wei for his love, sacrifice, encouragement, and support. Every bit of my progress comes with their deep love.

## TABLE OF CONTENTS

|   |      |
|---|------|
| LIST OF TABLES .....  | vii  |
| LIST OF FIGURES .....   | viii |
| Chapter   | Page |
| 1. INTRODUCTION .....   | 1    |
| 1.1 Dermal Immunization .....                                       | 1    |
| <i>Skin Structure</i> .....   | 1    |
| <i>Potential of Skin in Dermal Immunization</i> .....               | 3    |
| <i>Strategies for Dermal Vaccine Delivery</i> .....                 | 4    |
| 1.2 Double Emulsions .....  | 7    |
| <i>Preparation of <math>W_1/O/W_2</math> Double Emulsions</i> ..... | 10   |
| <i>Stability of <math>W_1/O/W_2</math> Double Emulsions</i> .....   | 10   |
| <i>Applications of Double Emulsions</i> .....                       | 13   |
| <i>Release Mechanism of Double Emulsions</i> .....                  | 14   |
| 1.3 Liposomes .....   | 16   |
| <i>Liposomes as Dermal Delivery Vehicle</i> .....                   | 16   |

|   |    |
|---|----|
| <i>Delivery Mechanisms of Liposomes in Dermal Delivery</i> .....                          | 19 |
| 1.4 Double-Encapsulation System .....   | 21 |
| 1.5 Significance of This Study .....  | 22 |
| 2. METHODOLOGY .....  | 23 |
| 2.1 Materials .....   | 23 |
| 2.2 Liposomes Fabrication.....  | 25 |
| 2.3 Preparation of Individual Double-Emulsion or Double-Encapsulation Globules<br>.....   | 25 |
| 2.4 Fabrication of Double Emulsions and Double-Encapsulation Formulations in<br>Bulk..... | 29 |
| 2.5 Cryogenic Transmission Electron Microscopy (Cryo-TEM).....                            | 29 |
| 2.6 Skin Preparation and Perforation by the Microneedle Skinroller .....                  | 32 |
| 2.7 Cryo-Scanning Electron Microscopy (Cryo-SEM) .....                                    | 33 |
| 2.8 <i>In-Vitro</i> Penetration Studies .....   | 33 |
| 2.9 Extraction of FITC-BSA from Skin.....   | 34 |
| 2.10 Confocal Microscopy.....   | 36 |
| 2.11 Encapsulation Efficiency of FITC-BSA in Liposomes .....                              | 37 |
| 2.12 Zeta Potential Analysis .....  | 37 |
| 2.13 Microscopy Observation .....   | 37 |
| 2.14 Release Rate of FITC-BSA from Formulations.....                                      | 38 |

|   |    |
|---|----|
| 2.15 Statistical Analysis .....   | 38 |
| 3. LIPOSOMES IN DOUBLE-EMULSION GLOBULES .....  | 39 |
| 3.1 Results and Discussion .....  | 42 |
| <i>Effect of Oil-Soluble Surfactant Span 80 on the Release of Liposomes</i> .....                 | 42 |
| <i>Effect of Water-Soluble Surfactant Tween 80 on the Release of Liposomes</i> .....              | 48 |
| <i>The Effect of Liposomes on External Coalescence</i> .....                                      | 50 |
| 3.2 Conclusions .....   | 55 |
| 4. IMPROVED DERMAL DELIVERY OF FITC-BSA USING A COMBINATION<br>OF PASSIVE AND ACTIVE METHODS..... | 56 |
| 4.1 Results.....  | 57 |
| <i>Passive Delivery of FITC-BSA via Different Formulations</i> .....                              | 57 |
| <i>Visualization of Microneedle Skinroller and Perforated Porcine Skin</i> .....                  | 57 |
| <i>Penetration Depth of FITC-BSA under Different Donor Formulations</i> .....                     | 61 |
| <i>Analysis of FITC-BSA Extracted from Skin</i> .....   | 63 |
| <i>Imaging Analysis on the Transport of FITC-BSA</i> .....  | 65 |
| <i>Studies on Fluorescent Intensity of FITC-BSA</i> .....   | 68 |
| 4.2 Discussion.....   | 70 |
| <i>Effect of Microneedle Skinroller on the Dermal Delivery of FITC-BSA</i> .....                  | 70 |
| <i>Effect of Formulations on the Dermal Delivery of FITC-BSA</i> .....                            | 71 |
| 4.3 Conclusions .....   | 73 |

|   |     |
|---|-----|
| 5. CATIONIC LIPOSOMES IN DOUBLE EMULSIONS FOR CONTROLLED<br>RELEASE .....                   | 75  |
| 5.1 Results and Discussions.....  | 76  |
| <i>Liposome Selection</i> .....   | 76  |
| <i>Microstructure Visualization of the Double-Encapsulation System</i> .....                | 79  |
| <i>Stability of Double-Encapsulation Formulations under Freeze-Thaw Treatment.</i><br>..... | 81  |
| <i>Release Rate of FITC-BSA from the Double-Encapsulation System</i> .....                  | 86  |
| <i>Release Mechanism of the Double-Encapsulation System</i> .....                           | 87  |
| 5.2 Conclusions .....   | 90  |
| 6. DISCUSSIONS AND FUTURE WORK.....   | 92  |
| 6.1 Discussions .....   | 92  |
| 6.2 Future Work .....   | 96  |
| <i>Adding Penetration Enhancer in the Double-Encapsulation Formulation</i> .....            | 96  |
| <i>In-Vitro Experiment</i> .....  | 96  |
| <i>In-Vivo Experiments</i> .....  | 97  |
| LIST OF REFERENCES .....  | 98  |
| BIOGRAPHY .....   | 111 |

## LIST OF TABLES

| Table   | Page |
|---|------|
| <b>2-1</b> Compositions of liposomes.....   | 26   |
| <b>2-2</b> Compositions of double emulsions and double-encapsulation formulations.....  | 31   |
| <b>4-1</b> Extraction of FITC-BSA from perforated porcine skin under different donor formulations (6-h experiment). The * symbol indicates that there is significant difference as compared to aqueous solution (ANOVA, $p < 0.05$ )..... | 64   |

## LIST OF FIGURES

| Figure   | Page |
|--|------|
| <b>1-1</b> Schematic illustration of the epidermis.....  | 2    |
| <b>1-2</b> Activation of the immune system after application of antigen and adjuvant.....  | 5    |
| <b>1-3</b> Schematic presentation of a $W_1/O/W_2$ double-emulsion globule.....  | 8    |
| <b>1-4</b> Schematic illustration of a two-step emulsification procedure to fabricate $W_1/O/W_2$ double emulsions.....  | 9    |
| <b>1-5</b> Fabrication of $W_1/O/W_2$ double emulsions by a “membrane emulsification technique”.....   | 11   |
| <b>1-6</b> Schematic illustration of the structure of liposomes.....   | 17   |
| <b>1-7</b> Possible mechanisms of action of liposomes as skin drug delivery systems. (A) the free drug mechanism, (B) the penetration enhancing process of liposome components, (C) vesicle adsorption to and/or diffusion with the <i>stratum corneum</i> , (D) penetration of intact vesicles into or through the intact skin, and (E) vesicles penetration across the skin through appendages, such as hair follicles, and sweat gland..... | 20   |
| <b>2-1</b> Chemical structures of L- $\alpha$ -phosphatidylcholine (A), hydrogenated soybean phosphatidylcholine (B), cationic lipid 1,2-dioleoyl-3-trimethylammonium-propane chloride salt (C), and Ceramide-VI (D).....  | 24   |
| <b>2-2</b> Setup of the capillary video-microscopy. The legend for this image is as follows: (1) compressed nitrogen-powered microinjection system; (2) a capillary holder carrying a microcapillary; (3) Optical microscope equipped with a high performance CCD camera; (4) PC with image processing software.....   | 27   |
| <b>2-3</b> Schematic illustration of the fabrication of the double-encapsulation formulation by a two-step emulsification procedure. $W_1$ is the liposome suspension; O is the oil phase; $W_2$ is the external aqueous phase.....  | 30   |

|            |   |    |
|------------|---|----|
| <b>2-4</b> | A: the arrangement of the Franz diffusion cell; B: setup for skin-permeation experiments.....   | 35 |
| <b>3-1</b> | Hypothesized model of the double-encapsulation delivery system. A: the double-encapsulation delivery system does not suffer any instability; B: by adding stimulus, external coalescence induces the release of liposomes from the $W_1$ phase to the $W_2$ phase in a $W_1/O/W_2$ double emulsion.....   | 40 |
| <b>3-2</b> | Cryo-TEM image of tubular liposomes encapsulating fluorescein sodium salt...41  |    |
| <b>3-3</b> | The stability of double-emulsion globules entrapping liposomes. $W_1$ phase: liposome suspension; O phase: 0.005 M Span80 in <i>n</i> -hexadecane; $W_2$ phase: water. The scale bar in (A) is applicable for both images.....  | 43 |
| <b>3-4</b> | Tubular liposomes inside the oil phase for 24 hours.....  | 45 |
| <b>3-5</b> | Average external-coalescence time at 0.01 M Tween 80 in the $W_2$ phase. $W_1$ phase: water (square) or liposome suspension (triangle); O phase: 0.005, 0.01, 0.02 and 0.03 M Span 80 in <i>n</i> -hexadecane; $W_2$ phase: 0.01 M Tween 80 in water.....   | 46 |
| <b>3-6</b> | The effect of Span 80 in the oil phase on the release of liposomes. $W_1$ phase: liposome suspension; O phase: 0.005 M (A) and 0.03 M (B) Span 80 in <i>n</i> -hexadecane; $W_2$ phase: 0.01 M Tween 80 in water. Average external-coalescence time: 387.67 s/droplet (A) and 1003.67 s/droplet (B). The scale bar in (A) is applicable for all images.....   | 47 |
| <b>3-7</b> | Average external-coalescence time at 0.02 M Span 80 in the O phase. $W_1$ phase: water (square) or liposome suspension (triangle); O phase: 0.02 M Span 80 in <i>n</i> -hexadecane; $W_2$ phase: 0.002, 0.005, 0.008 and 0.01 M Tween 80 in water.....  | 49 |
| <b>3-8</b> | The effect of Tween 80 in the $W_2$ phase on the release of liposomes. $W_1$ phase: liposome suspension; O phase: 0.02 M Span 80 in <i>n</i> -hexadecane; $W_2$ phase: 0.005 M (A) and 0.01 M (B) Tween 80 in water. Average external-coalescence time: 716.00 s/droplet (A) and 477.33 s/droplet (B). The scale bar in (A) is applicable for all images..... | 51 |
| <b>3-9</b> | Time elapsed images of a $W_1/O/W_2$ double-emulsion globule prepared with $W_1$ phase: water; O phase: 0.005 M Span 80 in <i>n</i> -hexadecane; $W_2$ phase: 0.01 M Tween 80 in water. Average external-coalescence time: 5.6 s/droplet. The scale bar is applicable for all images.....   | 53 |

|     |   |    |
|-----|---|----|
| 4-1 | Penetration depth of FITC-BSA transported through intact porcine skin under different donor formulations. Donor formulations are FITC-BSA aqueous solution, double emulsions, double-encapsulation formulations, and PC-liposome suspension, respectively. Data represents averages of $n \geq 3$ samples with standard deviation. (ANOVA, $p > 0.05$ ).....  | 58 |
| 4-2 | Visualization of the microneedle skinroller with 200 $\mu\text{m}$ needle length. (A) a 25-G hypodermic needle placed next to the microneedle skinroller; (B) the microneedle skinroller image captured by the vivacam.....   | 59 |
| 4-3 | Skin puncture marks by the microneedle skinroller with 200 $\mu\text{m}$ needle length. A: perforated porcine skin visualized by the methylene blue solution; B: cryo-SEM image of perforated porcine skin viewed from the <i>stratum corneum</i> (SC) side; C: cryo-SEM image showing the cross-section of perforated porcine skin.....  | 60 |
| 4-4 | Penetration depth of FITC-BSA transported through the perforated porcine skin under different donor formulations. Data represents averages of $n \geq 3$ samples with standard deviation. The * symbol identifies penetration depth of FITC-BSA in formulations is significantly greater than that in aqueous solution (ANOVA, $p < 0.05$ ). The + symbol indicates that penetration depth of FITC-BSA in double-encapsulation formulations is significantly enhanced by the incorporation of PC liposomes in the $W_1$ phase as compared to double emulsions (ANOVA, $p < 0.05$ )..... | 62 |
| 4-5 | The confocal images of FITC-BSA across the perforated porcine skin at $Z=0$ , 30 and 50 $\mu\text{m}$ . The fluorescence-emission signal of FITC-BSA is represented by green color. Four donor formulations, including FITC-BSA aqueous solution, double emulsions, double-encapsulation formulations, and PC-liposome suspension, were applied in the donor chambers, and microchannels created by the microneedle skinroller are indicated by white arrows. (6-h experiment; the scale bar is applicable for all images) .....  | 66 |
| 4-6 | Cross-section images of perforated porcine skin reconstructed based on the confocal image stacks. Images A, B, C and D illustrated perforated porcine skins treated with PC-liposome suspension, double-encapsulation formulations, double emulsions and FITC-BSA aqueous solution, respectively. (6-h experiment; the scale bar, 50 $\mu\text{m}$ , is applicable for all images) .....  | 67 |
| 4-7 | The fluorescent intensity profiles under different donor formulations at 0.5 h (A), 2 h (B) and 6 h (C). Donor formulations: PC-liposome suspension (■); double-  |    |

|            |  |    |
|------------|--|----|
|            | encapsulation formulations (●); double emulsions (▲); FITC-BSA aqueous solution (◆).....   | 69 |
| <b>5-1</b> | Cryo-TEM images of PC liposomes (A), hydrogenated PC liposomes (B) and DOTAP cationic liposomes (C).....   | 77 |
| <b>5-2</b> | Encapsulation efficiency of FITC-BSA in PC liposomes, hydrogenated PC liposomes and DOTAP cationic liposomes. Data represents the average of three samples with standard deviation.....  | 78 |
| <b>5-3</b> | Cryo-SEM images of (A) the cross section of double-encapsulation formulation and (B) closer observation of one $W_1$ droplet shown in Figure 5-3A. Liposomes within the $W_1$ droplet are pointed by white arrows.....   | 80 |
| <b>5-4</b> | Visual comparison of the effect of the freeze-thaw treatment on phase separation of the control double emulsion (A) and the double-encapsulation formulation (B); Aqueous bottom content in the control double emulsion and the double-encapsulation formulation after freeze-thaw treatment (C).....  | 82 |
| <b>5-5</b> | Microscopy observation of the top creamy layers of the control double emulsion and the double-encapsulation formulation after fabrication and freeze-thaw treatment. The scale bar is applicable to all images.....  | 83 |
| <b>5-6</b> | Release rate of FITC-BSA from the control double emulsion (◆), original double-encapsulation formulation (■) and modified double-encapsulation formulation (▲).....  | 85 |
| <b>5-7</b> | Real time observation of a typical double-emulsion globule right after preparation. $W_1$ phase: 2 mg/ml FITC-BSA in PB buffer, O phase: 0.05 M Span 80 in <i>n</i> -hexadecane, $W_2$ phase: 0.08 M Tween 80 in PB buffer; Real time observation of a typical double-encapsulation globule right after preparation. $W_1$ phase: Cationic C liposomes containing 2 mg/ml FITC-BSA in PB buffer, O phase: 0.05 M Span 80 in <i>n</i> -hexadecane, $W_2$ phase: 0.08 M Tween 80 in PB buffer..... | 89 |

## CHAPTER 1

### INTRODUCTION

#### 1.1 Dermal Immunization

##### *Skin Structure*

Being the largest human organ, skin acts as an excellent biological barrier to prevent the entry of pathogens into the body as the first line of defense. Such fact presents a great challenge to the delivery of substances through the skin.

The superstructure of the skin is composed of the epidermis, the dermis and the hypodermis. The hypodermis forms the lowest layer of the skin and is composed of fibroblasts and adipocytes [1]. The Dermis (1-2 mm thick), lies in-between hypodermis and epidermis, contains the lymphatic and blood vessels, serves as foundation for epidermal appendages such as hair follicles and sweat glands, and provides the mechanical support for the skin. As the outmost layer of the skin, the epidermis is typically 50-150  $\mu\text{m}$  thick in humans, and is composed of the *stratum corneum* and viable epidermis, as shown in Figure 1-1. The human *stratum corneum* is approximately 10-20  $\mu\text{m}$  thick, consisting of a dense layer of dead corneocyte cells surrounded by a lipophilic matrix made primarily of cholesterol, cholesterol esters, free fatty acid, and ceramide [2].

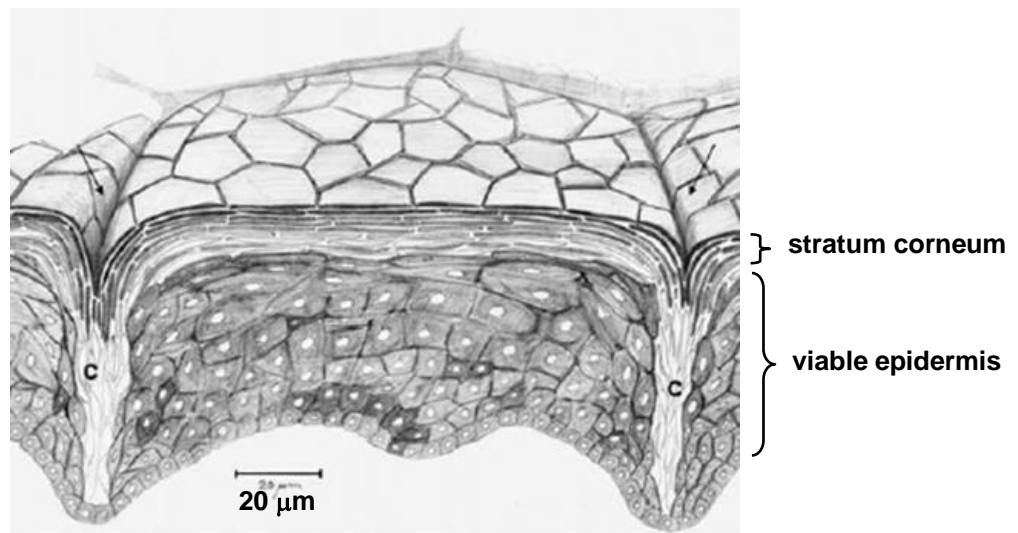


**Figure 1-1.** Schematic illustration of the epidermis [3].

The compact “brick and mortar” [4] arrangement of the corneocytes presents a great hindrance for substances across the skin, and thus protects against the entry of invaders. Underlying the *stratum corneum* is viable epidermis (50-100  $\mu\text{m}$  thick), which is responsible for generation of the *stratum corneum*. The viable epidermis is a stratified epithelium consisting of *stratum basale*, *stratum spinosum*, and *stratum granulosum*. The main cell type in the viable epidermis is the keratinocyte, which contains keratin filaments and constitutes approximately 90% of the viable epidermis [5]. Upon leaving the *stratum basale*, keratinocytes undergo a programmed process of differentiation, and start migration in the direction of the skin surface. During their migration through the *stratum spinosum* and *stratum granulosum*, keratinocytes experience changes in both structure and composition, resulting in their transformation into corneocyte cells of the *stratum corneum*. Other cells includes the melanocytes with the function of protecting all of the lower cells from ultraviolet light by their pigmentation, Merkel cells (sensation), and Langerhans cell (immunocompetent cell).

### ***Potential of Skin in Dermal Immunization***

The skin, as the site for vaccination, is mainly due to the presence of immunocompetent dendritic cells, Langerhans cells, in the basal layer of the viable epidermis. This type of cell, even though comprising 2%-4% of the cell population in the epidermis, covers approximately 20% of the surface area through their horizontal orientation and long protrusions [6], thus forming a meshwork that represents the second line of defense.

Pattern recognition receptors (Toll-like receptors) on keratinocytes play a great role in identifying microbial pathogens or their components. Upon activation by invaded

pathogens or antigens, keratinocytes secrete a wide variety of cytokines, chemokines and antimicrobial peptides [7]. Langerhans cells locate in the *stratum basale* of the epidermis, where Langerhans cells take up and undergo endocytosis of antigens or pathogens, as depicted in Figure 1-2. During their migration to the draining lymph node via the afferent lymphatics, these cells mature, express a variety of receptors (e.g. receptor for chemokines), and become highly effective antigen-presenting cells. In the lymph node, T cells are activated and interact with activated B cells, inducing an immune response [8].

As a non-invasive route, vaccine delivery via skin offers several advantages over traditional routes [9]. Compliance is very critical for successful immunization among children, a large portion of immunization population for whose needle-based administrations can be stressful [10]. Vaccine cream or skin patch-based vaccine may provide a self-administration capability, which reduces the need of clinical setting and medical assistant. Cutaneous immunization also has the potential to reduce and eliminate the spread of infections by accidental needle sticks and needle-reuse. And more importantly, self-immunization simplifies large-scale immunization programs and prompts widespread use of vaccines in developing countries. In addition, as compared to oral administration, dermal delivery may avoid the first-pass metabolism effects through the liver and lead to better bioavailability.

### ***Strategies for Dermal Vaccine Delivery***

Even though the skin is a site equipped with plenty of immunocompetent cells, it was believed that the drugs and bioactive molecules with molecular weight greater than 500 Dalton [11] have penetration difficulty through the *stratum corneum*. Therefore,

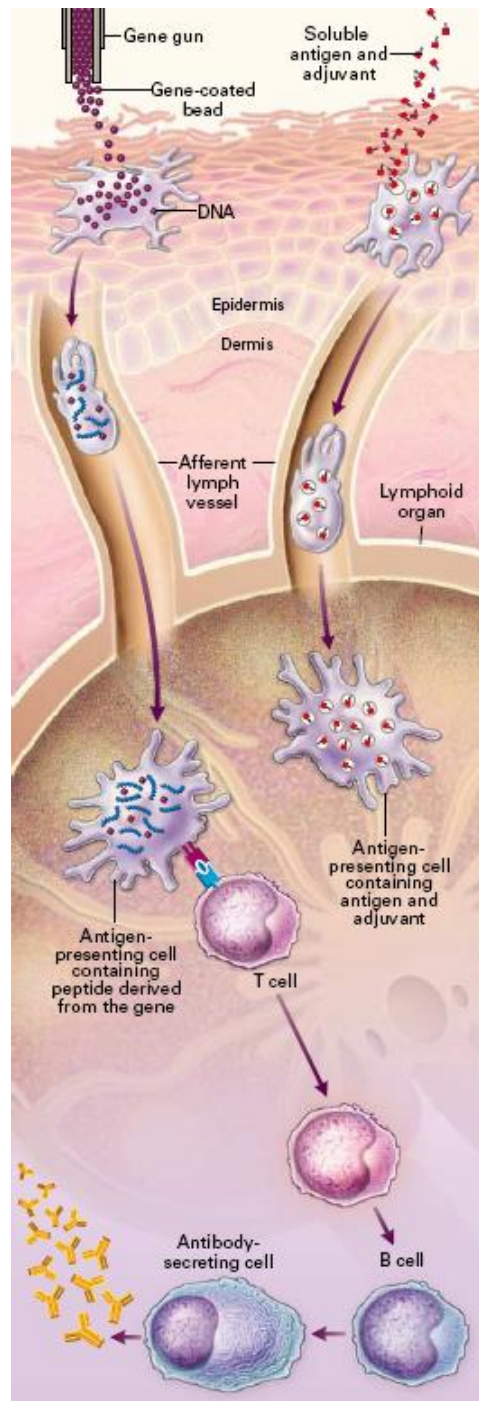


**Figure 1-2.** Activation of the immune system after application of antigen and adjuvant[8].

various passive or/and active methods [12] have been proposed in order to enhance the permeability of the *stratum corneum*.

Passive methods include the use of penetration enhancers [13-17] and ways of formulating suspensions/solutions of the active ingredient [18-20]. Water is the most natural and biocompatible penetration enhancer known to enhance the permeability of the *stratum corneum*. Occlusive hydration of porcine skin for 6 h results in that the thickness of the *stratum corneum* increases three to four folds to 30-40  $\mu\text{m}$  [17]. By use of cryo-scanning electron microscopy, it was observed that several locations in the *stratum corneum* lost their compact corneocyte structure, and small cisternae were formed within the intercellular space of the *stratum corneum*. Such alternations of the *stratum corneum* result in the significantly enhanced penetration of the protein though highly hydrated skin with penetration deep into the dermis [17]. The use of colloid-based system, such as negatively-charged latex nanoparticles with the sizes of 50 nm and 500 nm [21], has also shown high efficacy for transcutaneous immunization.

The limitation in the application of passive methods lies in that they can have a delivery time of up to several hours. Hence, active methods, such as iontophoresis [22], microscission [23], and microneedles [24-30], have been and are continually being explored. By adding an external force to disrupt the skin barrier physically, these methods can create micropores within the *stratum corneum*, thus facilitating dermal macromolecular transport. Microneedles were first proposed for cutaneous drug delivery in 1998 [24] and subsequently various microneedle systems have been developed and investigated. Studies from different research groups have proven the feasibility of microneedles, such as assembled microneedle arrays [26], biodegradable microneedles

[30], and solid or hollow microneedles made of silicon, metal and polymer [25], to deliver macromolecules through the skin. Theoretically, microneedles are designed to create a hole within the *stratum corneum*, but not to reach nerves in the deeper tissue so as to make their application painless. Through the superficial pathways created by the microneedles, antigens can reach the deeper region of the epidermis, leading to the uptake of antigens by Langerhans and other dendritic cells and the initiation of an immune response. Therefore, non-invasive vaccination via the skin can be achieved.

## 1.2 Double Emulsions

Double emulsions are termed “emulsions of emulsions”, which can be divided into two general types, water-in-oil-in-water ( $W_1/O/W_2$ ) and oil-in-water-in-oil ( $O_1/W/O_2$ ). In the case of the  $W_1/O/W_2$  double-emulsion system, small aqueous droplets ( $W_1$ ) are dispersed in oil globules (O), which are in turn confined in an external aqueous phase ( $W_2$ ). Only  $W_1/O/W_2$  double emulsions will be discussed in our study, since this type of double emulsions can act as a reservoir to store water-soluble substances in the internal aqueous phase ( $W_1$ ) safely or to release them at a controlled release rate. A schematic presentation of the  $W_1/O/W_2$  double-emulsion system is shown in Figure 1-3. In general, two types of surfactants, the oil-soluble and water-soluble surfactants, are required to stabilize the  $W_1/O/W_2$  double-emulsion system. Typically, the oil-soluble surfactant absorbs onto the  $W_1/O$  interface to stabilize the  $W_1$  droplets; the water-soluble surfactant adsorbs onto the  $O/W_2$  interface to prevent the coalescence of oil globules [31].

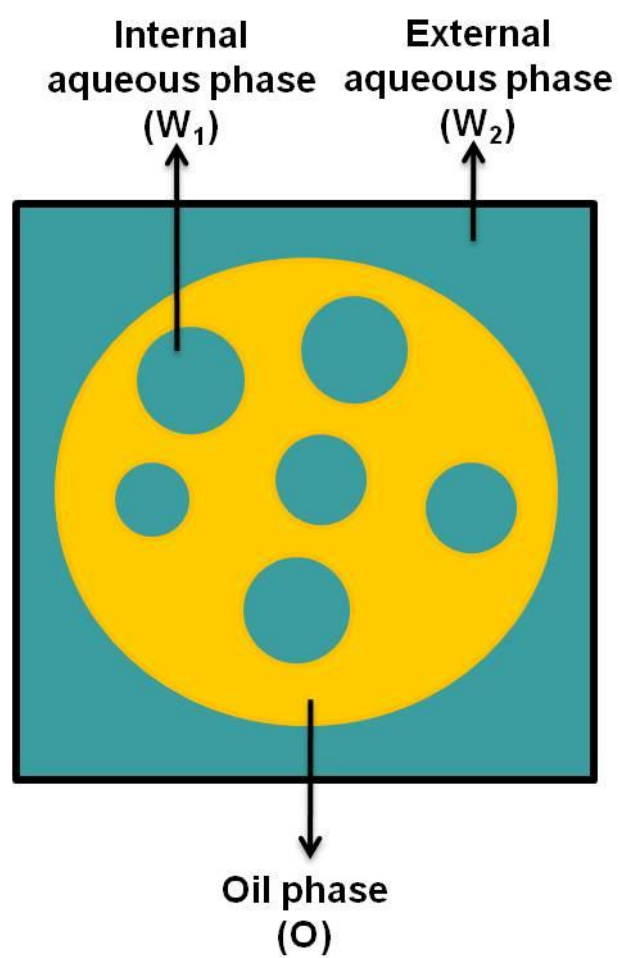


**Figure 1-3.** Schematic presentation of a  $W_1/O/W_2$  double-emulsion globule.

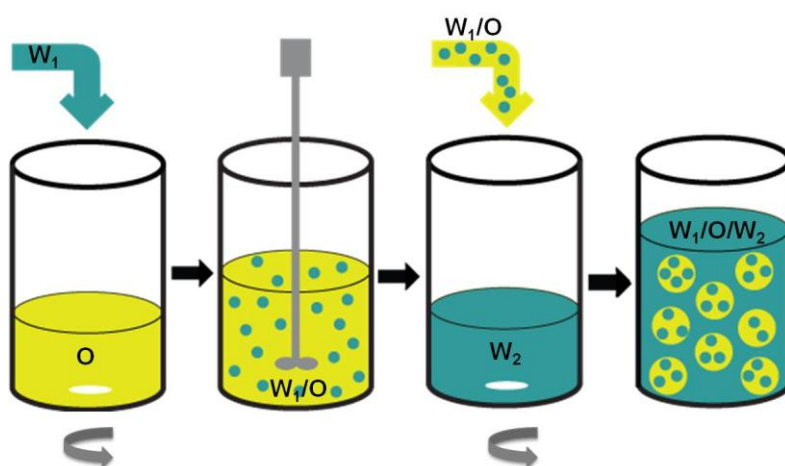


**Figure 1-4.** Schematic illustration of a two-step emulsification procedure to fabricate  $W_1/O/W_2$  double emulsions.

### ***Preparation of $W_1/O/W_2$ Double Emulsions***

The most common method for preparation of double emulsions is a two-step emulsification procedure [32], as shown in Figure 1-4. In the first step of the fabrication of  $W_1/O/W_2$  double emulsions, the  $W_1$  phase is added drop-by-drop to the O phase, in which an oil-soluble surfactant is dissolved. Subsequent high-shear homogenization is applied to obtain stable  $W_1/O$  single emulsions. In the second step, the  $W_1/O$  emulsions are emulsified in the  $W_2$  phase.

To scale up the fabrication of double emulsions, a membrane emulsification technique (Figure 1-5) has been proposed by Higashi *et al.* [33], which claimed to be used on the industrial scale. In this method, the  $W_1/O$  single emulsions are formed by sonication, and subsequently fill the upper chamber of this apparatus. The  $W_2$  phase is continuously injected into the lower chamber to create a continuous flow. A pressure is introduced to the upper chamber to transport the  $W_1/O$  emulsions through the controlled-pore glass membrane, resulting in the formation of  $W_1/O/W_2$  double emulsions. The emulsions are then progressively removed from the outlet of this apparatus.

Other promising methods have also been reported, such as oily isotropic dispersion process [34], and microchannel emulsification [35].

### ***Stability of $W_1/O/W_2$ Double Emulsions***

Due to the presence of large and polydispersed droplets, double emulsions are thermodynamically unstable with a great tendency to coalesce. The  $W_1/O/W_2$ -type double emulsions rupture through four possible mechanisms [36], including coalescence of the internal aqueous droplets (internal coalescence), coalescence of the oil globules,

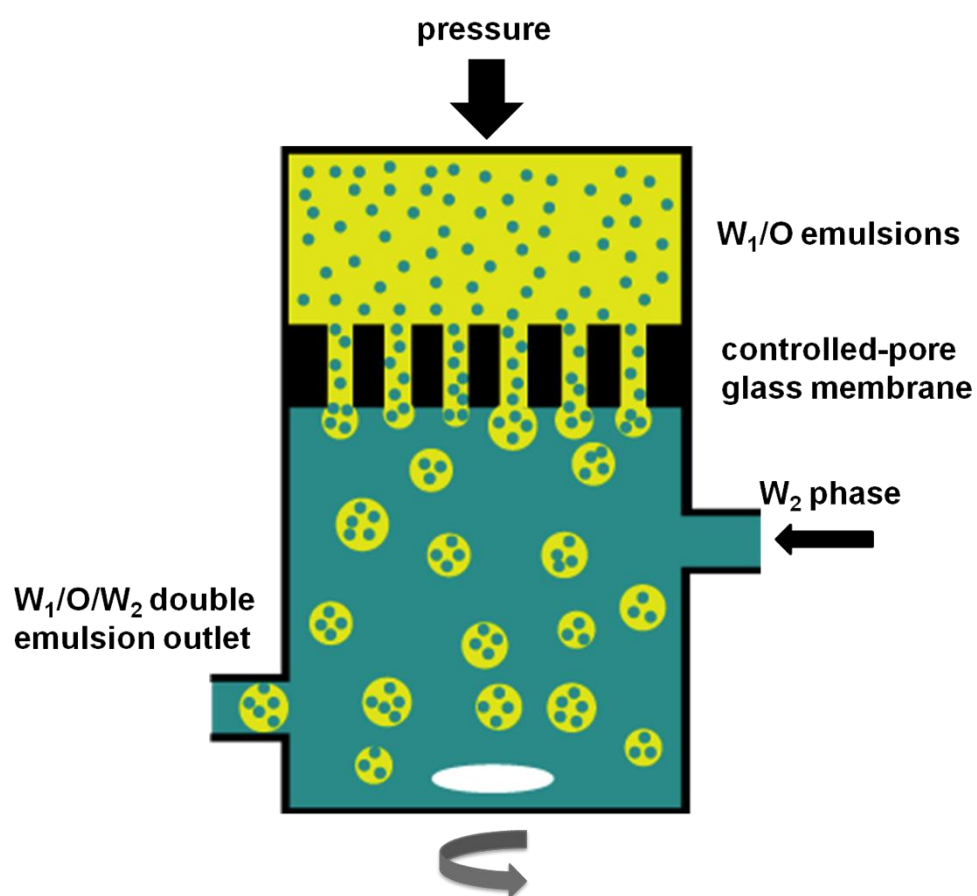


**Figure 1-5.** Fabrication of  $W_1/O/W_2$  double emulsions by a “membrane emulsification technique” [33].

coalescence of the internal aqueous droplets with the external aqueous phase (external coalescence), and transport of water to and from internal aqueous droplets through the oil layer. Thermodynamically unstable characteristic of double emulsions presents a great challenge for their successful applications. Therefore, numerous approaches have been investigated to improve the stability of double-emulsion system and slow down the release of active substances.

One strategy to improve the stability of the double-emulsion system is to utilize macromolecules, such as proteins or gums, as the emulsifier. Macromolecules have been widely adopted to stabilize emulsions since they might provide more interfacial coverage than monomeric emulsifiers. These macromolecular emulsifiers are strongly adsorbed at the interfaces to provide stability primarily through steric and mechanical effects. According to a study conducted by Garti et al. [37], the presence of a macromolecular emulsifier (bovine serum albumin), instead of a nonionic hydrophilic monomeric emulsifier, in the external aqueous phase retarded the release of NaCl from the internal aqueous phase. This retarded release was due to a “complex” formed by bovine serum albumin and lipophilic surfactant in the oil phase, which enhanced the stability and slowed down the release.

Obviously, increasing the viscosity of either the oil phase or the aqueous phase will restrict the mobility of active substances in compartments, and retard the transport of active substances through the oil membrane. Therefore, many attempts were made to increase the viscosity of emulsions, including (1) increasing the viscosity of the internal aqueous phase by adding gums or hydrocolloids to stabilize the  $W_1/O$  interface, (2)

increasing the viscosity of the oil phase, and (3) thickening or gelling the external aqueous phase by gums to block the coalescence of oil globules [38].

Solidifying of the oil phase is another effective method to maintain the stability of double emulsions [39-41]. The rigidity of oil was reported to retain the stability of the emulsions, and showed no release of active substances from the  $W_1$  phase to the  $W_2$  phase during long-time storage. However, release was triggered by the melting of the oil phase at the skin temperature, resulting in the instant release of active substances from the  $W_1$  phase. This concept could be applied to the administration of double-emulsion formulations dermally/topically. Thus, during the storage, no leakage of any active substance is occurred; the delivery of active substances only starts when the formulation is applied on the skin.

### ***Applications of Double Emulsions***

Since double emulsions are able to sustain and control the release of active matters which would then progressively release from the  $W_1$  phase to the  $W_2$  phase, much work has been devoted to drug-delivery studies, particularly through oral [42, 43], topical [44], intramuscular, and intravenous routes [45]. It has been proposed that the emulsion formulation could facilitate the permeation of drug across the intestinal membrane [46]. For the evaluation of molecular weight and antigenicity of the entrapped antigens, the work by Bozkir and Hayta showed that the  $W_1/O/W_2$  double-emulsion system has potential as the influenza vaccine delivery carrier [47]. In fact, from *in-vivo* experiments, it has been proven that the intramuscular administration of double-emulsion formulations stimulates a more effective immune response than conventional vaccination [48].

Other main advantages of  $W_1/O/W_2$  double emulsions, such as their protection for the fragile entrapped substances and their capacity to incorporate several active substances in one compartment, enable  $W_1/O/W_2$  double emulsions to be a more efficient delivery vehicle in dermal immunization. For instance,  $W_1/O/W_2$  double emulsions might protect fragile antigens in the  $W_1$  phase against the unfavorable physicochemical environment, as well as store stimuli or penetration enhancers in the  $W_2$  phase to initiate the release or facilitate the penetration of antigens across the skin [49-51].

Due to their multiphase and compartmentalized structure, double emulsions lend themselves to other potential applications, such as food [52, 53], cosmetics [54], and environment [55]. Depending on their different applications, active substances may also migrate from the  $W_2$  phase to the  $W_1$  phase, providing in that case a reservoir particular suitable for detoxification (a process to remove the toxic substances from a living organism), or the removal of toxic materials from wastewater [56].

### ***Release Mechanism of Double Emulsions***

Since double emulsions have been considered as a suitable delivery system, “how does the release occur from double emulsions?” becomes an important issue to understand. In general, the release of water-soluble substances from  $W_1/O/W_2$  double emulsions is dominated by two mechanisms: transport of active substances through the oil membrane and breakdown of double emulsions [57].

Several mechanisms are responsible for the release of water-soluble active substances from  $W_1/O/W_2$  double emulsions without rupture of double emulsions. Kita et al. [58] suggested two possible mechanisms for the transport of water and water-

soluble substances: (1) through thin lamellae of surfactants which partially form in the oil layer due to fluctuation of its thickness, and (2) by incorporating in reverse micelles. Colinart et al. [59] proposed another possible mechanism for water transport, which occurs through hydrated surfactant. According to studies conducted by use of capillary video-microscopy, a new mechanism, spontaneous emulsification of the  $W_1$  phase followed by migration of the formed droplets to the  $W_2$  phase, was observed [60]. This phenomenon is taken place, when the  $W_1$  phase and the  $W_2$  phase have a salt-concentration gradient, as well as the  $W_1/O$  and  $O/W_2$  interfaces are not in visual contact.

Swelling is one of the mechanisms to trigger the release of active substances by breakdown of the double-emulsion globules. As a consequence of different solute concentration between the  $W_1$  and  $W_2$  phases, water may transport through the oil phase from the  $W_2$  phase to the  $W_1$  phase to equilibrate the concentration of both phases, resulting in swelling of the  $W_1$  droplets until they eventually burst and release their contents [61]. Another available mechanism is shear-induced breakdown of double-emulsion globules. Shear-sensitive  $W_1/O/W_2$  double emulsions were formulated, in which the breakage of the droplets occurs only upon the application of a shear stress. This was achieved by adding a novel thermally reversible hydrogel, EMP hydrogel, as a thickener in the  $W_2$  phase, to facilitate bursting of double-emulsion globules upon topical application [62]. Due to the unique property of this hydrogel, double emulsions were free-flowing at ambient temperature and thickened at the temperature of human body. Upon the application of moderate shearing, a nearly complete release (99.6%) of the model drug in the  $W_1$  phase was reached at 35°C, whereas only 30% was released at 20°C. Freeze-thaw process is one more possible mechanism to induce release of active

substances from  $W_1/O/W_2$  double emulsions [39-41]. It has been demonstrated that the crystallization of the oil phase preserves the stability of double emulsions for at least 2 months, while subsequent thawing triggers external and internal coalescences, leading to release their contents up to 90% from the  $W_1$  phase. A possible explanation could be that a fast rate of oil-melting may not allow the oil-soluble surfactant having enough time to migrate back to the  $W_1/O$  and  $O/W_2$  interfaces and stabilize the globules prior to the occurrence of the coalescences.

### **1.3 Liposomes**

Liposomes are lipid-bilayer arrays separating an inner aqueous phase from the bulk aqueous phase, as shown in Figure 1-6. Typically, they are hollow sphere with their size ranging from 20 nm to 10  $\mu$ m. Properties, such as biocompatibility, high loading capacity, as well as simultaneous encapsulation of both, hydrophilic active components in the aqueous core and hydrophobic ones in the lipid bilayers, render liposomes versatile drug-delivery vehicles.

#### ***Liposomes as Dermal Delivery Vehicle***

Since the first description of epicutaneous application of liposomes 30 years ago [63], a great deal of work has been done in many laboratories around the world trying to improve and optimize the dermal delivery of active substances using liposomes [64-76] and also coming up with new liposomes-based delivery systems. Cevc and Blume [67] introduced a type of elastic liposomes, Transfersomes, with high shape adaptability and good colloidal stability. Usually, a component, such as bile salt or highly soluble phospholipid, is added to modify the elasticity and increase the deformability of the lipid bilayers. The ultra-deformable drug carriers, Transfersomes, have characteristics [77],

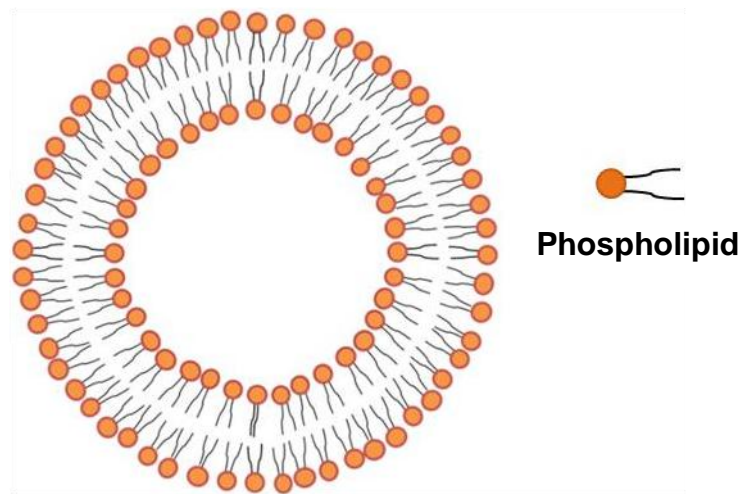


**Figure 1-6.** Schematic illustration of the structure of liposomes.

which include having (1) a very flexible lipid bilayer, (2) a capability to adapt the stress of the volume and the compressibility of the area, and (3) highly lipid bilayer surface hydrophilicity. Transport of Transfersomes across the skin is spontaneously driven by the naturally-occurring transcutaneous hydration gradient. Such “hydrotaxis” effect allows Transfersomes to facilitate more than 50% encapsulated substances across the skin. These ultradeformable liposomes have been used as carriers for the delivery of insulin[78], diclofenac [79], triamcinolone-acetonide [80] across the skin.

Similarly, other substances, such as ethanol [68] and cationic lipid 1,2-dioleoyl-3-trimethylammonium-propane (DOTAP) [81, 82], have been used to modify the properties of liposomes and enhance the permeation of active substances across the skin. Ethosomes are vesicles mainly consisted of phospholipid, ethanol and water [68, 83]. Due to the presence of penetration enhancer ethanol, ethosomes are shown enhanced penetration ability through the *stratum corneum*, as compared to conventional liposomes that are known to deliver drugs to the outer layer of skin. It has been proposed that cationic liposomes might potentially facilitate the initiation of an immune response and enhance the efficiency of dermal immunization, since they have an adjuvant effect on the activation of antigen-presenting cells [84]. In addition, high skin-penetration ability has been reported since cationic liposomes can bind the negatively-charged skin cells and hair follicles and thus achieve a high local concentration [81]. An average penetration depth of approximately 70% of the full hair follicle length was achieved followed by application of cationic liposomes.

### ***Delivery Mechanisms of Liposomes in Dermal Delivery***

As functions may vary with types and compositions of liposomes, mechanism of “how do liposomes facilitate the dermal substance delivery” can be controversial. As drug-delivery carriers, liposomes are non-toxic, biocompatible and biodegradable phospholipid vesicles that offer abilities to control the release of therapeutic agents and facilitate the drug adsorption. They may provide a localized depot in the skin to reduce the amount of drug penetrating through the skin thus minimizing systematic effects. They may also provide a targeted delivery to skin appendages, such as hair follicles and sweat glands. With such variety of functions, it is not surprising that the mechanisms of liposomes as dermal-delivery vehicles are still unclear.

According to El Maghraby et al. [85], several mechanisms are responsible for liposomes acting as dermal delivery vehicles. In the case depicted in Figure 1-7A, the drug, released from liposomes, can independently transport through the skin [86]. It has also been proposed that a penetration effect is generated by liposomes (Figure 1-7B). Such effect is caused by the changes in the ultrastructures of the intracellular lipids in the *stratum corneum* [87] or the fusion of vesicles' lipid components with skin lipids to loosen their structure [88]. In Figure 1-7C, liposomes may adsorb on the surface of the *stratum corneum*, followed by transfer of drug from liposomes to skin; liposomes may also fuse and mix with the lipids in the *stratum corneum*, increasing drug partitioning into the skin. Ultradeformable liposomes, as shown in Figure 1-7D, are able to transport intactly through the skin and permeate deep enough to be absorbed by the systematic circulation [67, 77, 78, 89]. Such ability is attributed to the high deformability of the liposomes, which are modified by adding “edge activator” molecules to conventional

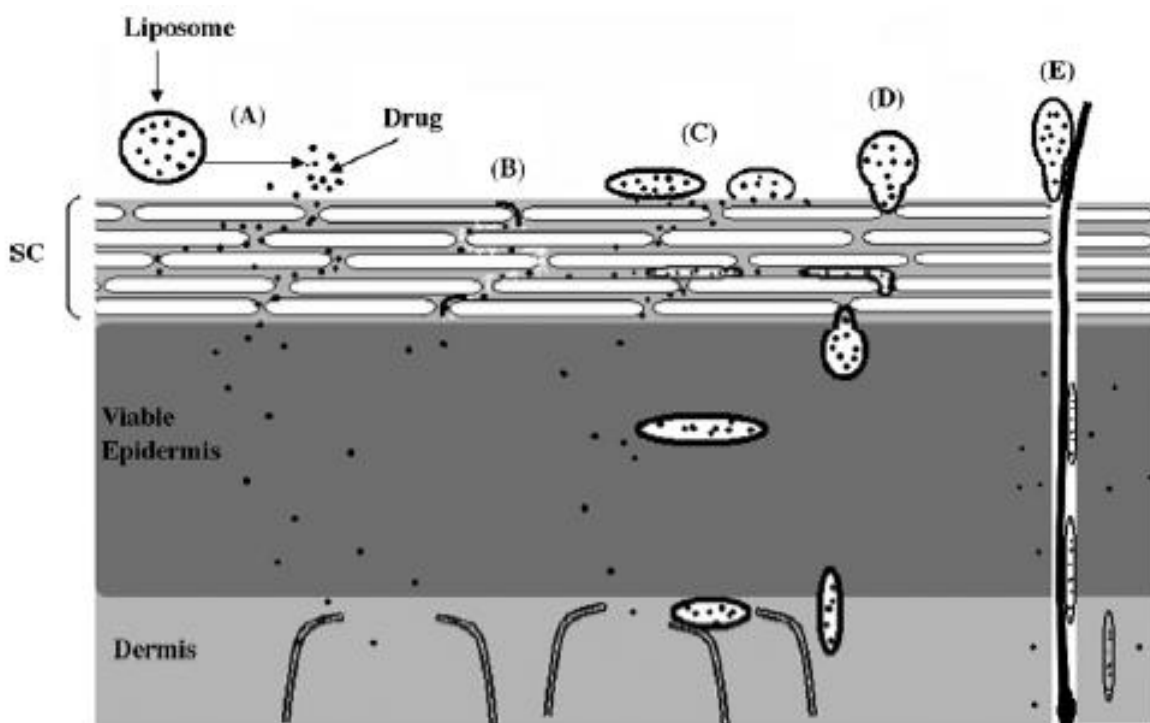


**Figure 1-7.** Possible mechanisms of action of liposomes as skin drug delivery systems. (A) the free drug mechanism, (B) the penetration enhancing process of liposome components, (C) vesicle adsorption to and/or diffusion with the *stratum corneum*, (D) penetration of intact vesicles into or through the intact skin, and (E) vesicles penetration across the skin through appendages, such as hair follicles, and sweat gland [85].

liposomes. One more possible route is via appendages, such as hair follicles, and sweat gland (Figure 1-7E).

#### **1.4 Double-Encapsulation System**

Even though liposomes have been evaluated as drug carrier for decades [90], their applications are often limited by the fact that they tend to aggregate, fuse with other liposomes, or leak entrapped substances [91]. Moreover, they are susceptible to factors such as changes in pH or temperature, or exposure to serum [92, 93]. Once exposed to unfavorable physicochemical conditions, their unique structures become unstable. Therefore, from an application point of view, it is necessary to retain the intactness of liposomes before they are administered to a specific target.

Coating the surface of liposomes with a biocompatible polymer like polyethylene glycol (PEG) has proven useful, since this protective layer allows for extended circulation of liposomes in human serum [94]. However, even though PEG was previously considered inert, it should be noted that the PEG-liposomes complex may still induce side effects upon activation of the complement system [95]. Another feasible method is the encapsulation of nano-scale liposomes within a micro-scale delivery system, so that double encapsulation of active ingredients enhanced their level of protection by keeping the liposomes intact. For instance, encapsulation of liposomes with a second bilayer [96], entrapment of liposomes in hydrogel microcapsules [97], vesicles in a water-in-oil emulsion system [98]. In all the above-cited studies, an additional layer led to better protection and controlled release of the encapsulated substances.

As part of this dissertation's work, we reported a new type of double-encapsulation system, in which liposomes are incorporated into the  $W_1$  phase of  $W_1/O/W_2$  double emulsions. By combining double emulsions and liposomes in a single delivery system, the double-encapsulation formulation allows the liposomes and their contents to stay well protected against the influence of unfavorable physicochemical conditions, while also achieving a more efficient cutaneous delivery. In the possible application of such formulations for dermal drug or vaccine delivery, the water or other penetration enhancers contained in the  $W_2$  aqueous phase of the  $W_1/O/W_2$  double emulsions would hydrate/disrupt the *stratum corneum*, thus facilitating the further interaction of liposomes with the skin.

### **1.5 Significance of This Study**

Dermal immunization provides a route to take advantages of the skin immune network by inducing an immune response against invaded antigens. The work presented here proposed a novel colloidal-based system, double-encapsulation formulation, which will be applied dermally to facilitate the transport of vaccines across the skin. Liposomes are entrapped inside the  $W_1$  phase of  $W_1/O/W_2$  double emulsions; therefore, the oil membrane of double emulsions can function as a protective layer to avoid the interactions between liposomes and unfavorable conditions. According to the studies we conducted, such system not only allows the liposomes and their contents to stay well protected, but also achieving a more efficient cutaneous delivery.

## CHAPTER 2

### METHODOLOGY

#### 2.1 Materials

Deionized (DI) water was generated from water purification system (Barnstead E-pure purifier or Medica 15 BP) to a resistivity of approximately 18 M $\Omega$ ·cm. *n*-Hexadecane (99%, Sigma-Aldrich, MO), as the model oil phase of double emulsions, was used in all experiments. Nonionic surfactants, sorbitan monooleate (Span 80, Sigma-Aldrich, MO) and polyoxyethylene sorbitan monooleate (Tween 80, Sigma-Aldrich, MO), were used in oil and aqueous phases, respectively. Fluorescein sodium salt (FSS, Sigma-Aldrich, MO, chapter 3) and fluorescein isothiocyanate-conjugated bovine serum albumin (FITC-BSA, Sigma-Aldrich, MO, chapter 4&5) were chosen as the model active substances. Methylene blue (chapter 4) as a stain was purchased from Sigma-Aldrich.

For liposome preparation, L- $\alpha$ -phosphatidylcholine (PC, Avanti Polar Lipids, AL), hydrogenated soybean phosphatidylcholine (hydrogenated PC, Lipoid GmbH, Germany), cationic lipid 1, 2-dioleoyl-3-trimethylammonium-propane chloride salt (DOTAP, Lipoid GmbH, Germany), and Ceramide-VI (Evonik Degussa Corporation, NJ) were used as the lipids, and their structures are shown in Figure 2-1. Organic solvents methanol and chloroform were purchased from Sigma-Aldrich. Triton X-100 (Sigma-Aldrich, MO) was used in chapter 5 to disrupt the lipid bilayer of liposomes.

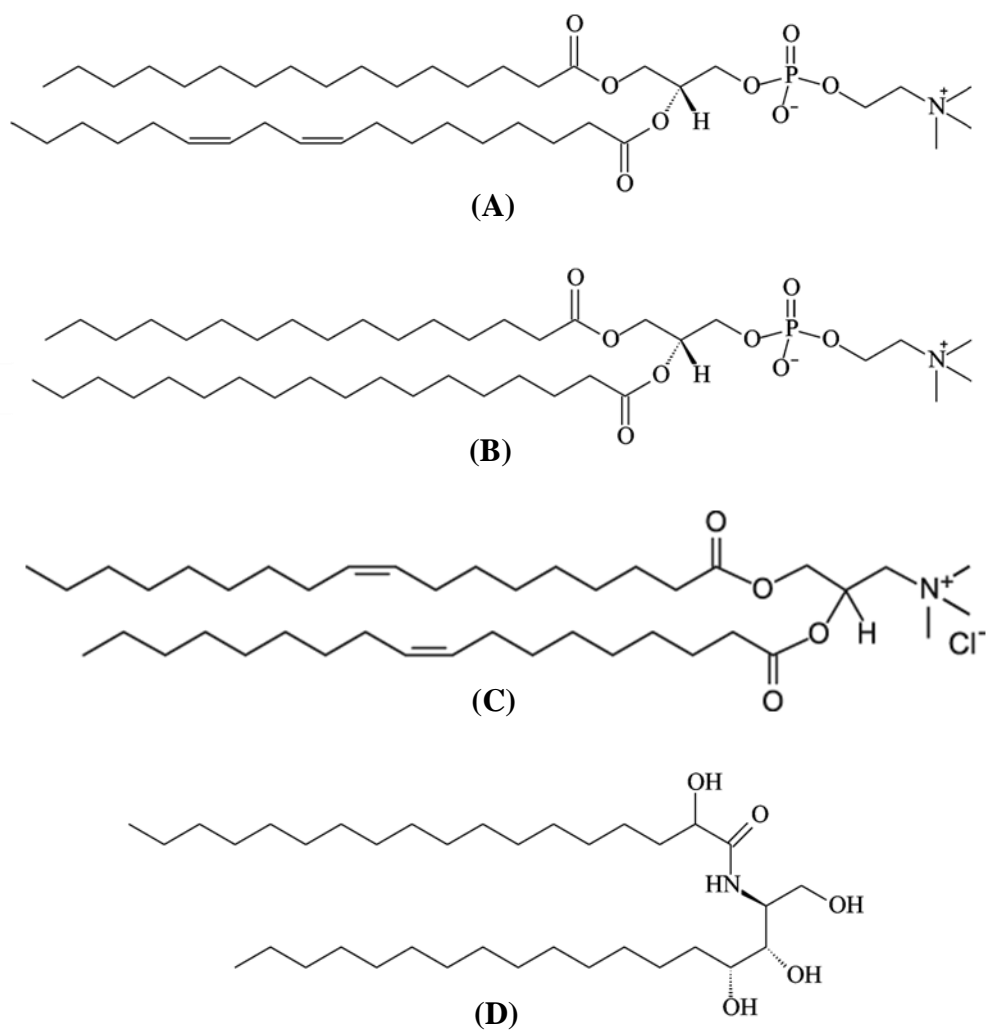


**Figure 2-1.** Chemical structures of L- $\alpha$ -phosphatidylcholine (A), hydrogenated soybean phosphatidylcholine (B), cationic lipid 1,2-dioleoyl-3-trimethylammonium-propane chloride salt (C), and Ceramide-VI (D).

Phosphate buffered saline pH=7.4 (PBS buffer, 1X, chapter 4) was composed of 136.89 mM NaCl, 2.68 mM KCl, 1.76 mM  $\text{KH}_2\text{PO}_4$  and 10.14 mM  $\text{NaH}_2\text{PO}_4$  (Sigma-Aldrich, MO). Phosphate buffer pH=7.4 (PB buffer, 10mM, chapter 5) was composed of 7.7 mM  $\text{Na}_2\text{HPO}_4$  and 2.3 mM  $\text{NaH}_2\text{PO}_4$  (Sigma-Aldrich, MO). All reagents were used as received without further purification.

## **2.2 Liposomes Fabrication**

Liposomes were prepared by using the lipid film hydration and extrusion method. The lipid or lipid mixture was dissolved in methanol and chloroform (1:2, v/v). The organic solvents were then removed by drying at 100 mbar to form a lipid film using a rotary evaporator (BÜCHI, Switzerland). Subsequently, the lipid film was hydrated with either FSS (chapter 3) or FITC-BSA (chapter 4&5) aqueous solution for 30 min above the phase transition temperature of the lipid. For preparation of tubular liposomes, vesicle suspension was probe-sonicated for 1/2 hour at room temperature ( $22\pm 1^\circ\text{C}$ ) right after hydration. All resulting vesicle suspensions were extruded for 11 passes through a series of 400 nm and 100 nm polycarbonate membranes (whatman, NJ) in order to reduce the size of vesicles. Following this procedure, different types of liposomes, which include tubular liposomes, PC liposomes, hydrogenated PC liposomes and DOTAP cationic liposomes, were fabricated. Lipid compositions of liposomes are shown in Table 2-1. After preparation, liposome samples were stored at  $5^\circ\text{C}$ .

## **2.3 Preparation of Individual Double-Emulsion or Double-Encapsulation Globules**

Individual  $W_1/O/W_2$ -type double-emulsion or double-encapsulation globules were prepared and monitored by use of capillary video-microscopy, as shown in Figure 2-2.

**Table 2-1.** Compositions of liposomes.

| <b>Liposomes</b> | <b>Lipid compositions</b> | <b>Model drug</b> | <b>Lipid amounts</b>           |
|------------------|---------------------------|-------------------|--------------------------------|
| Tubular [74]     | Ceramide-VI:PC (1:1)      | FSS               | 2% (chapter 3)                 |
| PC               | PC                        | FITC-BSA          | 2% (chapter 4); 1% (chapter 5) |
| Hydrogenated PC  | hydrogenated PC           | FITC-BSA          | 1% (chapter 5)                 |
| DOTAP cationic   | DOTAP:PC (1:9)            | FITC-BSA          | 1% (chapter 5)                 |

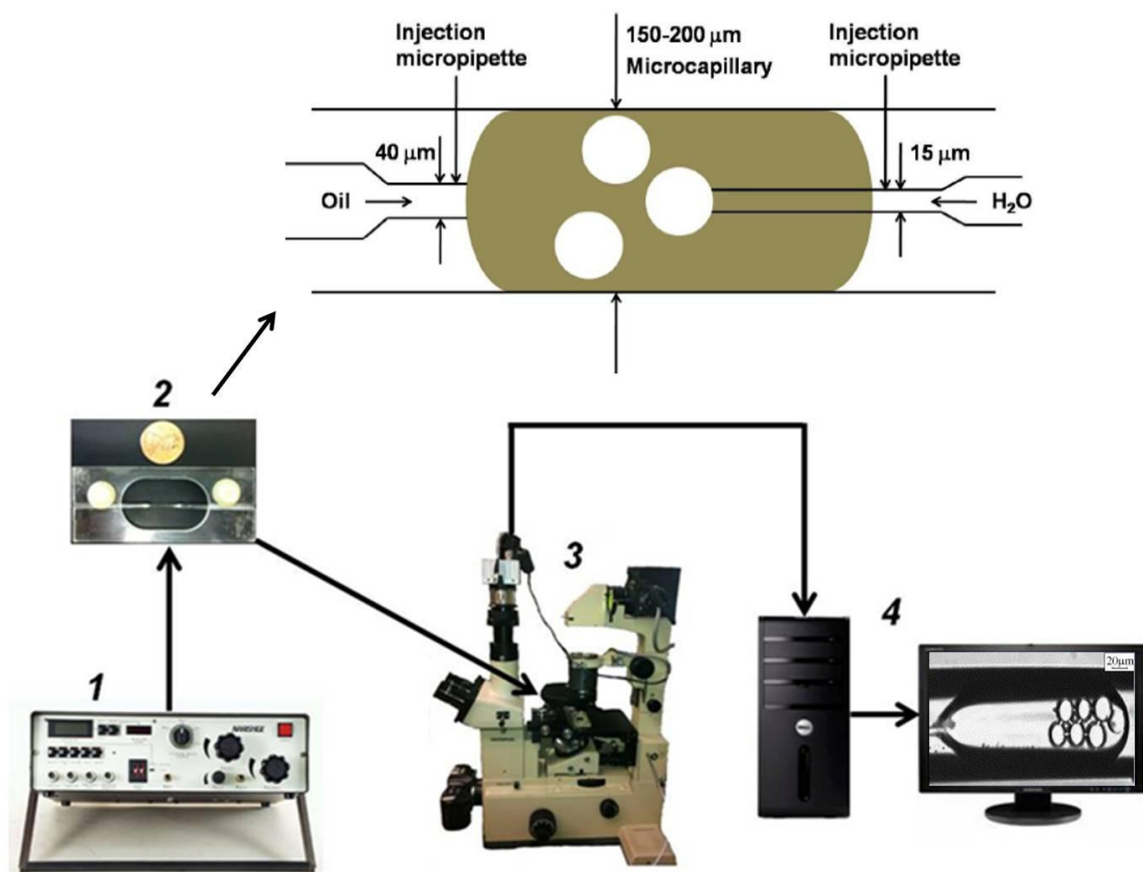


**Figure 2-2.** Setup of the capillary video-microscopy. The legend for this image is as follows: (1) compressed nitrogen-powered microinjection system; (2) a capillary holder carrying a microcapillary; (3) Optical microscope equipped with a high performance CCD camera; (4) PC with image processing software.

By using a micropipette puller (Narishige PB-7, Japan), the center of the microcapillary (1.5-1.8 mm i.d.  $\times$  100 mm length, Corning, NY) was pulled until the diameter was reduced to 150-200  $\mu\text{m}$ . Two three-dimensional hydraulic micromanipulators (Narishige, Japan) driven by compressed nitrogen-powered microinjection system (Narishige, Japan) were mounted on both sides of the microscope to allow the injection of oil globules and aqueous droplets precisely. Oil globules and the  $W_1$  droplets were injected into the thinnest part of the capillary from both sides of the microscope by micropipettes. One micropipette with an outer-diameter at the tip of approximately 40  $\mu\text{m}$  was filled with the oil phase. From this micropipette, individual oil globules were formed within the capillary by the microinjection system. A thinner micropipette with an outer-diameter at the tip of approximately 15  $\mu\text{m}$  was used to inject the  $W_1$  droplets within the oil globule. In order for the thinner micropipettes to penetrate the oil globules and for the injected  $W_1$  aqueous droplets to break from the tip of the micropipettes, the outer surface of the micropipette tips was rendered hydrophobic. The hydrophobicity was accomplished by immersing the micropipettes in a solution of siliclad (Gelest Inc., PA) for 30 seconds while nitrogen gas flowed through the micropipettes.

A high-performance CCD camera (Meyer Instruments, TX) with a frame rate of 30 frames-per-second connected to the microscope was used to observe double-emulsion globules. A high-resolution monitor and a S-VHS Hi-Fi VCR (Sony Electronics, CA) recorded all the experiments for further analysis by an image-analysis system (Media Cybernetics Inc., MD). The details of this equipment were published elsewhere [60].

## **2.4 Fabrication of Double Emulsions and Double-Encapsulation Formulations in Bulk**

Double emulsions were prepared by a two-step emulsification procedure (Figure 1-4) [32]. In the first step,  $W_1$  aqueous phase, containing the model active substance, was added to the O phase drop-by-drop under strong magnetic stirring. The O phase consisted of Span 80 in *n*-hexadecane. Subsequent high-shear homogenization (Silverson L4R laboratory mixer, East Longmeadow, MA) was applied for 5 min at the speed rate of 1000 rpm to obtain  $W_1/O$  emulsions. In the second step, the  $W_1/O$  emulsions were added to the  $W_2$  aqueous phase under gentle stirring. The volumetric ratio of  $W_1:O:W_2$  was 2:2:1.

As shown in Figure 2-3, the double-encapsulation formulations were prepared by the incorporation of liposome suspension containing the model active substance as the  $W_1$  phase of double emulsions. The rest of the preparation procedure followed the same as that of double emulsions. The compositions of both formulations are summarized in Table 2-2. After preparation, they were kept either at room temperature to evaluate the stability, or at 4°C to obtain stable cream-like formulations by freezing of the oil phase (melting point of *n*-hexadecane: 18°C).

## **2.5 Cryogenic Transmission Electron Microscopy (Cryo-TEM)**

The morphology of liposomes was determined by cryogenic transmission electron microscopy. Briefly, a drop of liposome suspension was placed on a formvar-coated copper TEM grid. The grid was blotted to form a thin film and rapidly vitrified in liquid ethane. After transferring to a microscope (JEOL 2010, Japan) equipped with a cold

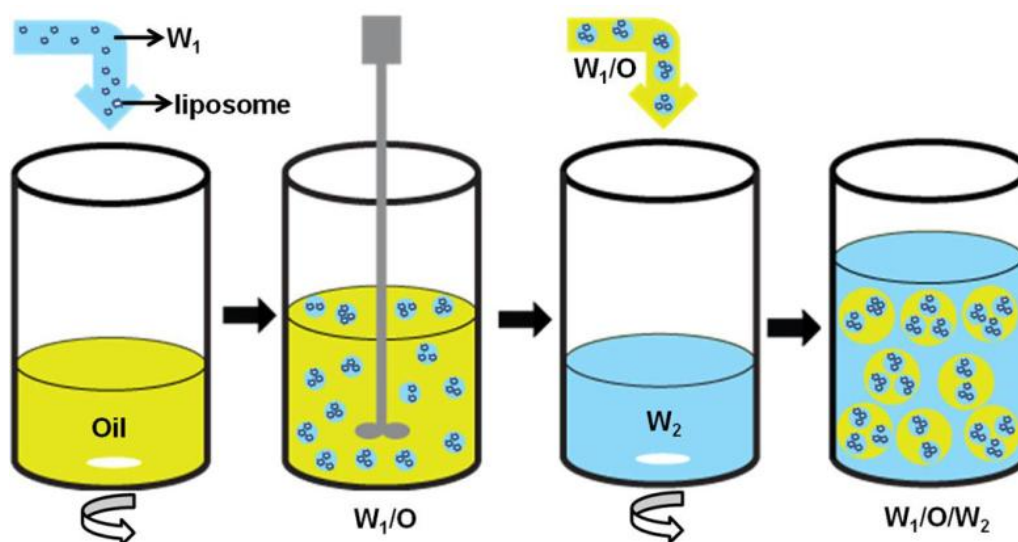


**Figure 2-3.** Schematic illustration of the fabrication of the double-encapsulation formulation by a two-step emulsification procedure.  $W_1$  is the liposome suspension; O is the oil phase;  $W_2$  is the external aqueous phase.

**Table 2-2.** Compositions of double emulsions and double-encapsulation formulations.

| <b>Formulations</b>               | <b>W<sub>1</sub></b>          | <b>O</b>                               | <b>W<sub>2</sub></b>               |
|-----------------------------------|-------------------------------|--|------------------------------------|
| double emulsions                  | FITC-BSA in buffer solution   | 0.05 M Span 80 in <i>n</i> -hexadecane | 0.08 M Tween 80 in buffer solution |
| double-encapsulation formulations | liposomes entrapping FITC-BSA | 0.05 M Span 80 in <i>n</i> -hexadecane | 0.08 M Tween 80 in buffer solution |

stage (Gatan Inc., CA) under the protection of liquid nitrogen, the grids were examined at an operating voltage of 120 kV.

## 2.6 Skin Preparation and Perforation by the Microneedle Skinroller

The needle length of the microneedle skinroller (Clinical Resolution Laboratory Inc., CA) is selected at 200  $\mu\text{m}$ . Since the needles are made of stainless steel and thus are not easily damaged, the same microneedle skinroller was used for several experiments. The intactness of the needles was checked by the vivacam of a VivaScope<sup>®</sup> confocal imager (Lucid Inc., NY) frequently.

Full-thickness porcine skin samples were selected from newborn pigs (three weeks or younger), and stored at  $-20^{\circ}\text{C}$  for a maximum of one month. Prior to experiments, a piece of skin was thawed at room temperature. The subcutaneous fat tissue was carefully removed, and the hair was trimmed short with a clipper. Subsequently, the skin was cut to the required area ( $4\text{ cm} \times 8\text{ cm}$ ), washed with PBS buffer, and dried with a tissue.

For perforation, a piece of treated porcine skin was stretched on parafilm to counteract the elasticity of the skin. The skin and parafilm were placed on styrofoam in order to protect the microneedle skinroller from damage [26], and fixed by pins. The same area of the skin was rolled vertically and horizontally three times by the microneedle skinroller. By mounting the porcine skin on a scale (Ohaus Co., NJ), the force applied to perforate the skin was controlled at  $22 \pm 2\text{ N}$ . Subsequently, the skin was cut to three small pieces ( $2\text{ cm} \times 2\text{ cm}$ ) and was ready to be used in penetration studies. Right after perforation, the skin was stained by applying a 1% (w/v) methylene blue solution on the *stratum corneum* side for 2 min, and then excess dye was carefully

removed by ethanol swabs. Images of the microneedle skinroller and of stained skin were taken by the vivacam and a Canon digital camera.

## **2.7 Cryo-Scanning Electron Microscopy (Cryo-SEM)**

In chapter 4, perforated skin samples were visualized by cryo-SEM. Samples were cut to a small piece (3 mm  $\times$  4 mm) and processed as described by Tan et al. [17]. Briefly, the skin sample was mounted on the cryo-SEM sample holder by use of a small amount of Tissue-Tek adhesive (Ted Pella Inc., CA). The sample was then fixed by plunge-freezing in liquid nitrogen slushed lower than  $-190^{\circ}\text{C}$  (Gatan Inc., CA), withdrawn into a vacuum transfer device under the protection of high vacuum, and transferred to the cryo-preparation chamber ( $-130^{\circ}\text{C}$ ). After sputter coated with platinum at 10 mA for 100 s, the sample was transferred into the main chamber of the Field Emission SEM (Hitachi S-4800) via an interlocked airlock and mounted onto a cold stage module ( $-130^{\circ}\text{C}$ ) fitted to the SEM stage. Images were acquired at a voltage of 3 kV and at a working distance of about 6 mm. Similarly, the cross-section of the microchannels was observed by vertically mounting a strip of skin (1.5 mm  $\times$  4 mm) on the sample holder. Then, the strip was fractured by the flat edge of a knife at  $-130^{\circ}\text{C}$  and sublimated for 5 min to etch away surface water at  $-95^{\circ}\text{C}$ . The temperature was then changed back to  $-130^{\circ}\text{C}$  before sputter coating. In chapter 5, the microstructure of the double-encapsulation system was also observed by cryo-SEM.

## **2.8 *In-Vitro* Penetration Studies**

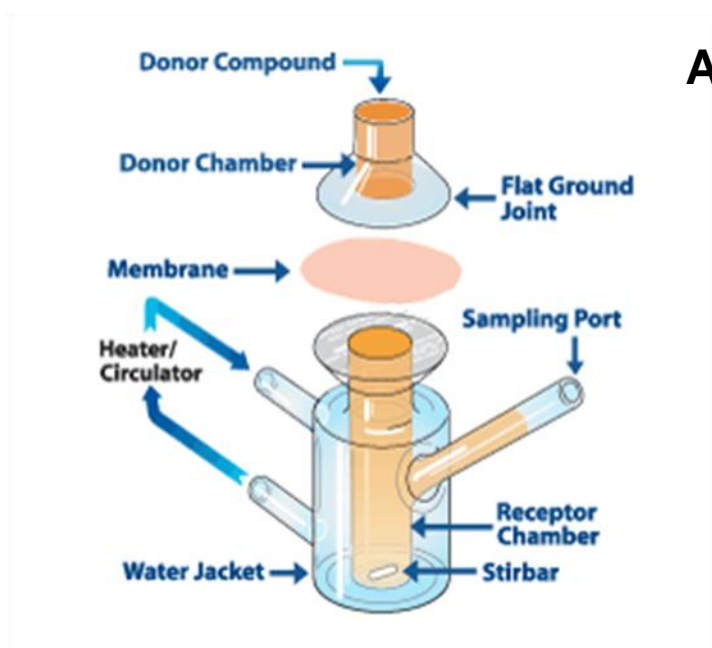
Experiments were performed on Franz diffusion cells (FDC, PermeGear, PA) with a receptor volume of 5 ml and a donor volume of 1 ml. The available diffusion area was  $0.64\text{ cm}^2$ . After the perforation, skin samples were mounted on the FDC, as illustrated in

Figure 2-4A. The epidermal side of the skin was exposed to the donor chamber whereas the dermal side was exposed to the receptor medium containing PBS pH=7.4 with constant magnetic stirring at 450 rpm. The temperature for the experiments was maintained at  $37 \pm 0.1^{\circ}\text{C}$ . To attain thermal equilibrium, 0.5 ml PBS buffer was added to every donor chamber for 20 min prior to the experiments. Subsequently, the donor chamber was emptied, and the formulation was placed inside. Volumes of formulations were 0.5 ml FITC-BSA aqueous solution (5 mg/ml FITC-BSA in PBS buffer), 0.5 ml PC-liposome suspension, 0.833 ml double emulsions and 0.833 ml double-encapsulation formulations. The volume of each formulation added to the donor chamber was chosen such as to have 3.91 mg FITC-BSA per  $\text{cm}^2$  of exposed skin. Additionally, continuous magnetic stirring ( $\sim 90$  rpm) was provided on the donor chamber to maintain homogeneous concentration and minimize the boundary layer effect on the *stratum corneum* side [99], as shown in Figure 2-4B.

For each formulation, experiments were conducted over periods of 0.25, 0.5, 2 and 6 h. After experiments, excess formulations were removed from the skin surface. Each skin was washed three times with PBS buffer, and gently dried with a tissue. As a control experiment, the passive delivery of FITC-BSA through the intact porcine skin via different formulations was also studied.

## 2.9 Extraction of FITC-BSA from Skin

Using a procedure, similar to Lopes et al [100], after 6 h of *in-vitro* experiment, skin pieces were collected for each formulation, and washed with PBS buffer. *Stratum*



**Figure 2-4.** A: the arrangement of the Franz diffusion cell; B: setup for skin-permeation experiments.

*corneum* was obtained by tape stripping. In this procedure, a piece of 3M Transpore<sup>TM</sup> tape (1 cm × 1 cm) was pressed onto the skin, and a force applicator (D-SQUAME<sup>®</sup> Disc Applicator, CuDerm Corp., TX) was applied for 5 s with a pressure of approximately 2.21 N/cm<sup>2</sup>. The tape was then removed, and 15 pieces of tape were collected for each skin sample. Subsequently, tape pieces were immersed in 3 ml of ethanol/PBS buffer (1:1, v/v) solution, and mixed by a vortex mixer for 2 min. After passing through a 0.2 µm filter, the resulting solution was analyzed with a fluorimeter (PTI Inc., NJ). Viable skin was cut into small pieces, transferred into a vial containing 1.0 ml of ethanol/PBS buffer solution, and homogenized over ice for 2 min by use of a homogenizer (IKA Works Inc., NC). The resulting suspension was then centrifuged at 13,000 rpm for 10 min at 4 °C, and the supernatant was analyzed.

In order to measure extraction efficiency, 25 µl of 0.2 mg/ml FITC-BSA was slowly injected into a piece of skin (1 cm × 1 cm). After the equilibrium of 2 h at room temperature, skin was cut into small pieces. Following the above procedure, extraction efficiency was calculated to be  $62.92 \pm 5.3\%$ .

## 2.10 Confocal Microscopy

A confocal microscope (LSM 510 META) was employed for the observation of the FITC-BSA transported through perforated porcine skin. The system is equipped with an argon laser, which is used to monitor FITC-BSA penetration. The fluorescent emission signals of FITC-BSA are represented by the green color. For microscopic observation, the skin was mounted between a glass slide and a cover glass, in which the *stratum corneum* side was faced downwards. Images were acquired by using a 20× objective lens. The pinhole was adjusted to 66 µm. Z-stacks profiles of porcine skin sample were

generated by taking individual pictures from the surface of the skin (*stratum corneum*) to the interior (dermis), with a Z-step of 1  $\mu\text{m}$ .

Image J software (National Institute of Health, MD) was applied to analyze the fluorescent intensity of images captured by the confocal microscope. For all images, each of the sites was  $460.68 \times 460.68 \mu\text{m}^2$  in size, and each image field associated with the 512 by 512 pixel.

### **2.11 Encapsulation Efficiency of FITC-BSA in Liposomes**

PC liposomes, hydrogenated PC liposomes and DOTAP cationic liposome were loaded separately into centrifuge tubes (Quick-Seal<sup>TM</sup> Beckman, CA) and spun in a Beckman Coulter ultracentrifuge (Fullerton, CA) at 100,000  $g$  for 1.5 h. FITC-BSA was collected from the supernatant and quantified by a UV-Vis Spectrophotometer (Shimadzu, Japan) at an adsorption wavelength of 495 nm. The encapsulation efficiency (EE) is defined as  $EE = 100\% \times (M_T - M_S) / M_T$ , where  $M_T$  is the total amount of FITC-BSA in the liposome preparation and  $M_S$  is the amount of FITC-BSA in the supernatant.

### **2.12 Zeta Potential Analysis**

Zeta potential of DOTAP cationic liposomes was measured using ZetaPALS Zeta Potential Analyzer (Brookhaven Instruments, USA). Prior to experiments, DOTAP cationic liposomes were diluted 50 folds with PBS buffer. Measurements were carried out under room temperature ( $22 \pm 1^\circ\text{C}$ ).

### **2.13 Microscopy Observation**

After preparation and freeze-thaw treatment, double-encapsulation formulations were studied microscopically and compared against control double emulsions. Aliquots

of formulations were diluted 20 times with the  $W_2$  phase and gently stirred for a few seconds. Subsequently, 5  $\mu$ l of the diluted sample were placed onto a concave glass slide, covered with a coverslip, and observed under a Leica DM IRE2 inverted microscope equipped with a fluorescence illuminator. The images were captured by a high-performance camera (Leica, Germany), and analyzed by the Image-Pro Plus image-analysis software (Media cybernetics Inc., MD).

#### **2.14 Release Rate of FITC-BSA from Formulations**

After fabrication, double emulsions or double-encapsulation formulations were split in 1 mL glass vials and stored at 5°C in a refrigerator. For the FITC-BSA release studies, formulations were subsequently thawed by transferring them to a water bath (35°C) for 5 min, and were thereafter kept at room temperature ( $22 \pm 1^\circ\text{C}$ ). Upon phase separation, aqueous samples were collected from the bottom of the vials by use of a 1 mL gastight<sup>®</sup> syringe (Hamilton Co., NV) at different time intervals. The collected aqueous bottoms were diluted 20 times with PB buffer containing 1% Triton X-100 in order to disrupt the liposome structure [101]. Samples were then analyzed by use of a UV-Vis spectrophotometer to quantify the FITC-BSA.

#### **2.15 Statistical Analysis**

In order to ensure the reproducibility of the results, each experiment was conducted at least three times. The statistical significance of the differences among the penetration depth of FITC-BSA and the amount of FITC-BSA delivered into the skin under different donor formulations was evaluated. A single-factor Analysis of Variance (ANOVA,  $\alpha=0.05$ ) was performed.  $p < 0.05$  was considered to be statistically significant.

## CHAPTER 3

### LIPOSOMES IN DOUBLE-EMULSION GLOBULES

This chapter presents a double-encapsulation system, as shown in Figure 3-1. The hypothesized model of this delivery system illustrates that active molecules are entrapped inside the liposomes, which are in turn confined in the  $W_1$  phase of  $W_1/O/W_2$  double emulsions. Our motivation in the development of this system is to prevent liposomes from interacting with external conditions and to ultimately apply this system by taking advantages of both double emulsions and liposomes in dermal delivery.

In the present study, tubular liposomes [74] containing FSS (Figure 3-2) were encapsulated inside the  $W_1$  phase of  $W_1/O/W_2$  double emulsions. Capillary video-microscopy, described in Chapter 2, was used to study the behavior of individual  $W_1/O/W_2$  double-emulsion globules. We visually monitored the release of tubular liposomes from double-emulsion globules with varying the concentration of surfactants in the oil phase or the  $W_2$  phase, as well as the intrinsic effect liposomes may themselves have on the stability of the globules. The latter was accomplished by comparison of liposome-containing- $W_1$ -phase globules to pure-water- $W_1$ -phase globules.

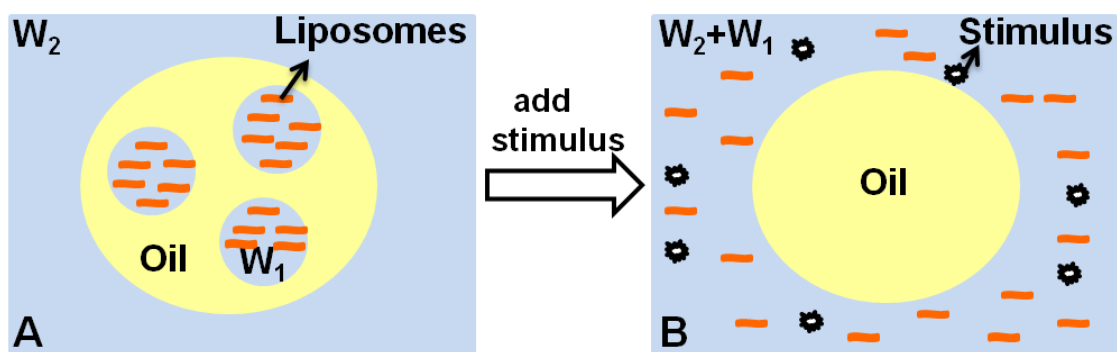


**Figure 3-1.** Hypothesized model of the double-encapsulation delivery system. A: the double-encapsulation delivery system does not suffer any instability; B: by adding stimulus, external coalescence induces the release of liposomes from the  $W_1$  phase to the  $W_2$  phase in a  $W_1/O/W_2$  double emulsion.

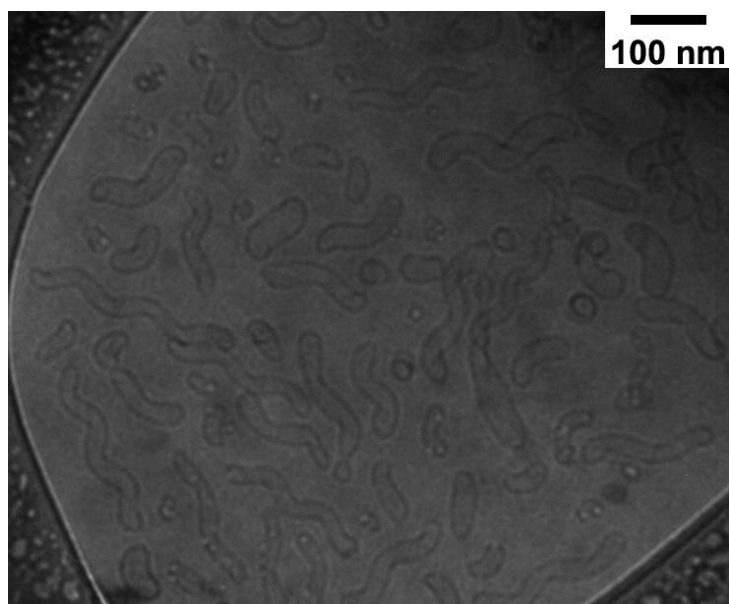


**Figure 3-2.** Cryo-TEM image of tubular liposomes encapsulating fluorescein sodium salt.

### 3.1 Results and Discussion

In our experiment, external coalescence was investigated as the mechanism for release of liposomes from the  $W_1$  phase to the  $W_2$  phase. The concentration of Span 80 in the O phase or Tween 80 in the  $W_2$  phase was varied to determine how surfactant concentration may influence liposome release. In experiments performed for each oil globule, three  $W_1$  droplets were formed inside the O phase. Since the size of globules and droplets is one of the factors that influence external coalescence, the ratio of the  $W_1$  droplet diameter to the effective diameter of the oil globule was maintained at  $0.4 \pm 0.05$ . The average external-coalescence time was calculated by the lifetime of all droplets divided by the number of the droplets.

#### *Effect of Oil-Soluble Surfactant Span 80 on the Release of Liposomes*

O phases were prepared with 0.005, 0.01, 0.02 and 0.03 M Span 80 in *n*-hexadecane. Tween 80 in all  $W_2$  phases was fixed at 0.01 M in water and the  $W_1$  phase was either liposome suspension or water. Since the critical micelle concentration of Span 80 is approximately 18  $\mu$ M in various alkane oils [102], the concentrations used in this study are sufficient to form reverse micelles within the *n*-hexadecane oil phase. With Span 80 as the only surfactant in the system, i.e., no Tween 80 in the  $W_2$  phase, double-emulsion globules entrapping liposomes or water in the  $W_1$  phase were stable at all Span 80 concentrations used in the O phase. This is in agreement with Hou and Papadopoulos's findings that report Span 80 alone can stabilize double-emulsion globules against external coalescence if the concentration of Span 80 is more than  $10^{-3}$  M [103]. For a double-emulsion globule with a Span 80 concentration of 0.005 M in the oil phase, Figure 3-3 shows three stable liposome droplets at 5.5 h. Because an uneven presence of

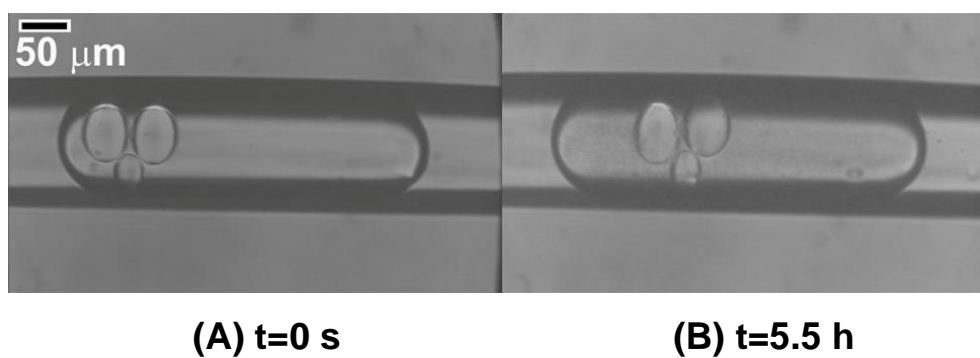


**Figure 3-3.** The stability of double-emulsion globules entrapping liposomes.  $W_1$  phase: liposome suspension; O phase: 0.005 M Span80 in *n*-hexadecane;  $W_2$  phase: water. The scale bar in (A) is applicable for both images.

salt in the  $W_1$  and  $W_2$  phases may induce water flow from the lower-salt-concentration water phase to the higher-salt-concentration water phase [60, 104], the existence of FSS in the  $W_1$  phase and its absence in the  $W_2$  phase resulted in spontaneous emulsification of the  $W_2$  phase into the oil phase. As seen in Figure 3-3B, at 5.5 h tiny water droplets appeared inside the oil membrane, however the diameters of the  $W_1$  droplets did not show a measurable change. Therefore the migration of water from the  $W_2$  to the  $W_1$  phase is not expected to influence the findings of our study because the duration of each experiment is less than 5.5 h. In addition, a cryo-TEM image (Figure 3-4) shows that tubular liposomes are stable for up to at least 24-hour storage when stored within the oil phase composed of 0.005 M Span 80 in *n*-hexadecane.

When 0.01 M Tween 80 is present in the  $W_2$  phase, the results of average external-coalescence time for water and liposome suspension in the  $W_1$  phase are summarized in Figure 3-5. As expected, for water in the  $W_1$  phase, external coalescence slows down as the concentration of Span 80 increases. For double-emulsion globules with the  $W_1$  phase consisting of liposome suspension, external coalescence follows the same trend as globules of pure water in the  $W_1$  phase. For example, when the oil phase contained 0.005 M Span 80 and the  $W_1$  phase was a liposome suspension, average external-coalescence time was 387.67 s/droplet for 0.01 M Tween 80 in the  $W_2$  phase (Figure 3-6A). When the concentration of Span 80 in the oil phase was increased to 0.03 M, the average external-coalescence time also rose to 1003.67 s/droplet under the same conditions in the  $W_1$  and  $W_2$  phases (Figure 3-6B). The fluorescent-light images before any of the droplets have coalesced are there to confirm that the internal aqueous phase consisted of a liposome suspension.

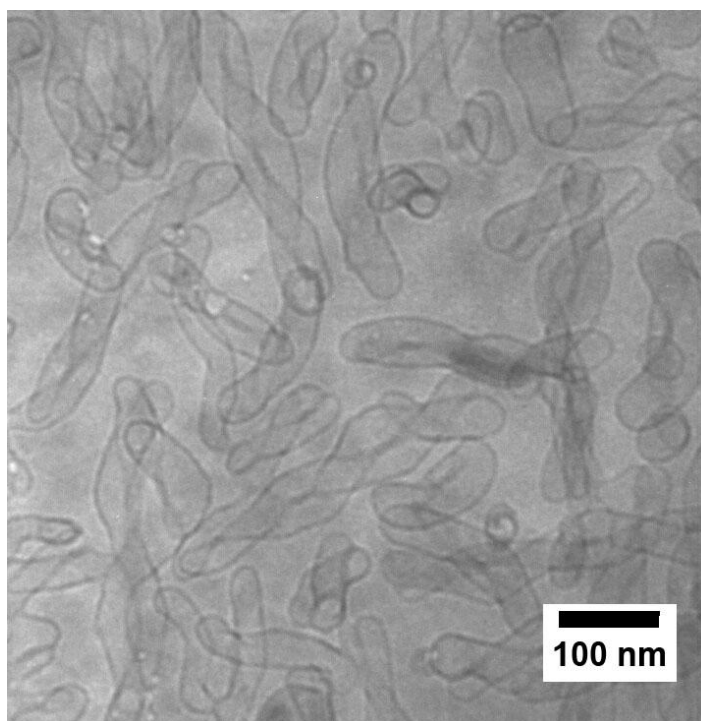


**Figure 3-4.** Tubular liposomes inside the oil phase for 24 hours.

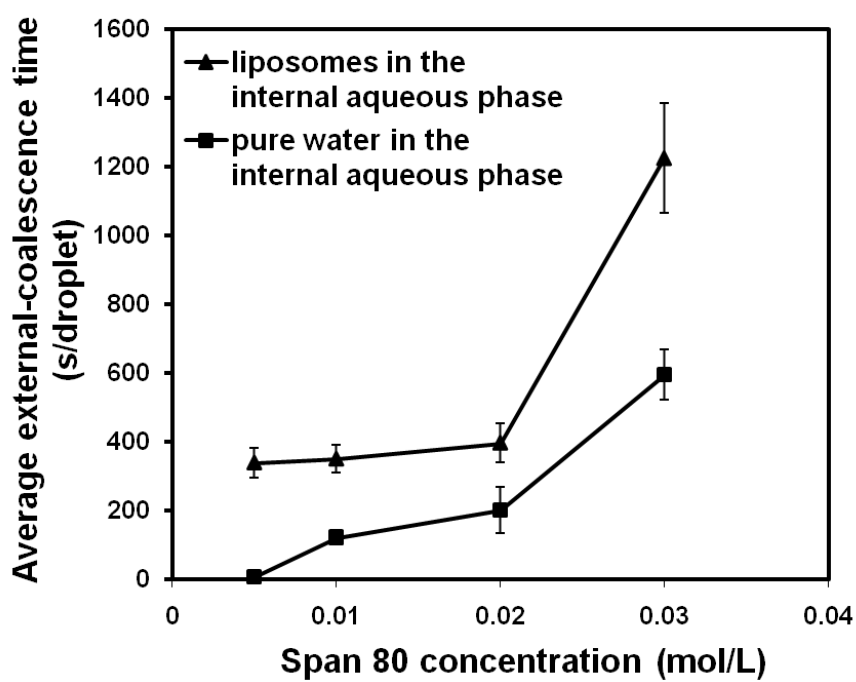


**Figure 3-5.** Average external-coalescence time at 0.01 M Tween 80 in the  $W_2$  phase.  $W_1$  phase: water (square) or liposome suspension (triangle); O phase: 0.005, 0.01, 0.02 and 0.03 M Span 80 in *n*-hexadecane;  $W_2$  phase: 0.01 M Tween 80 in water.

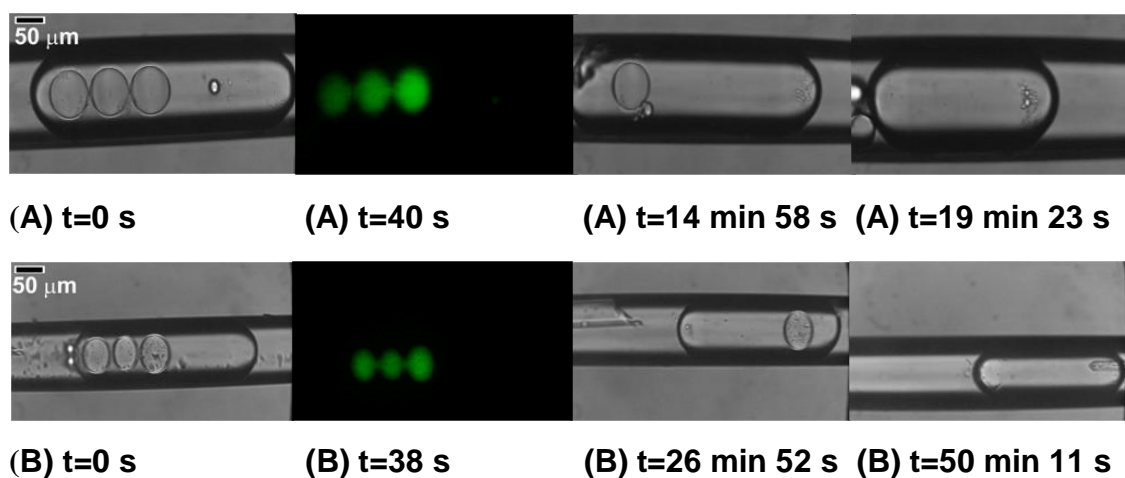


**Figure 3-6.** The effect of Span 80 in the oil phase on the release of liposomes.  $W_1$  phase: liposome suspension; O phase: 0.005 M (A) and 0.03 M (B) Span 80 in *n*-hexadecane;  $W_2$  phase: 0.01 M Tween 80 in water. Average external-coalescence time: 387.67 s/droplet (A) and 1003.67 s/droplet (B). The scale bar in (A) is applicable for all images.

The concentration of Span 80 plays a significant role on the stability of double emulsions. As suggested in previous work, the amount of the oil-soluble surfactant may be modeled by the effective thickness of adsorbed layers on the  $O/W_2$  and  $W_1/O$  interfaces. A higher Span 80 concentration in the oil phase corresponds to thicker adsorbed layers that produce a greater repulsive force to stabilize the double emulsions [105]. Therefore, as the concentration of Span 80 increased, the stability of double emulsions increased [32, 103, 106]. One recently proposed by Santini et al. [107] also suggests that the barrier against droplet coalescence becomes stronger due to the increase of the Span 80 concentration, thus enhancing the stability of emulsions.

#### ***Effect of Water-Soluble Surfactant Tween 80 on the Release of Liposomes***

The amount of Tween 80 in the  $W_2$  phase was varied in order to observe how Tween 80 may influence the release of water and liposome suspension in the  $W_1$  phase. Tween 80 in the  $W_2$  phase was incorporated at 0.002, 0.005, 0.008 and 0.01 M, while Span 80 in the oil phase for all experiments was 0.02 M. Several previous studies have discussed how external coalescence becomes faster with increasing Tween 80 concentration in the  $W_2$  phase [103, 108]. Also in the current study, when the concentration of Tween 80 in the  $W_2$  phase increased, external coalescence became faster for both water and liposome suspension in the  $W_1$  phase, as shown in Figure 3-7. At 0.005 M Tween 80 in the  $W_2$  phase and a liposome suspension in the  $W_1$  phase, average external-coalescence time was 716.00 s/droplet (Figure 3-8A). For the same conditions in the  $W_1$  and oil phase, but with Tween 80 concentration increased to 0.01 M in the  $W_2$  phase, average external-coalescence time decreased to 477.33 s/droplet (Figure 3-8B).

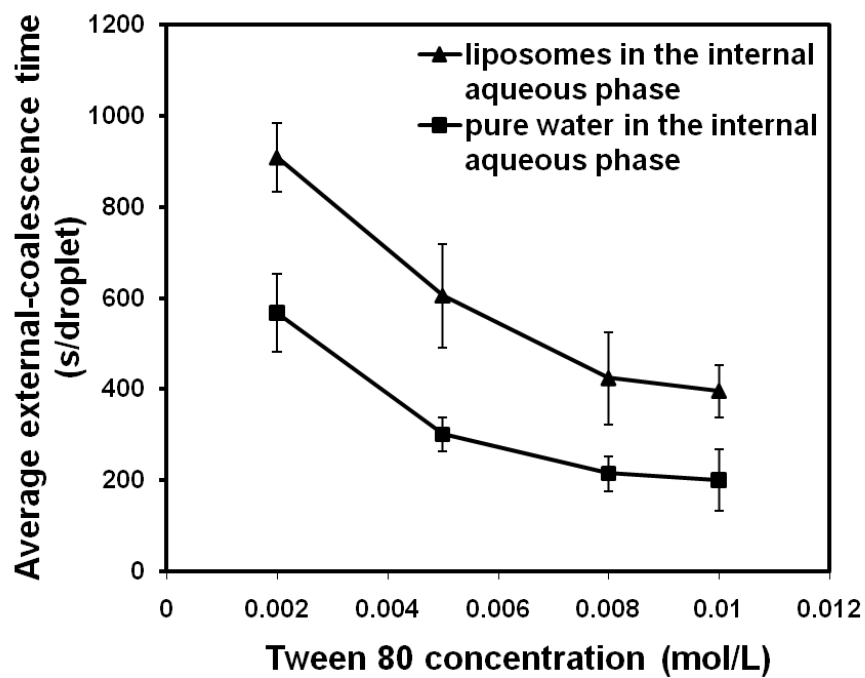


**Figure 3-7.** Average external-coalescence time at 0.02 M Span 80 in the O phase.  $W_1$  phase: water (square) or liposome suspension (triangle); O phase: 0.02 M Span 80 in *n*-hexadecane;  $W_2$  phase: 0.002, 0.005, 0.008 and 0.01 M Tween 80 in water.

In double-emulsion systems, water-soluble surfactant, such as Tween 80, plays a minor or negative effect on controlling the stability. At a low Tween 80 concentration in the  $W_2$  phase, a necessary amount of Tween 80 is essential to avoid coalescences of oil globules, contributing to stability of double emulsions [31]. However, a high concentration of Tween 80 in the  $W_2$  phase will lead to the rupture of double emulsions [109]. In exploring some basic rules to govern the stability of double emulsions, Ficheux et al. reported that there exists a threshold concentration for water-soluble surfactants in the  $W_2$  phase. When the concentration of water-soluble surfactant is lower than this threshold value, double emulsion globules remain stable without any release for a month; if the concentration is above this value, the release occurs after a few minutes [109]. A work conducted by Matsumoto et al. has indicated that the large amount of water-soluble surfactant in the  $W_2$  phase solubilized some of the oil-soluble surfactant [32], thereby decreasing the repulsive force between the  $W_1$  droplets and the  $O/W_2$  interface. Previous studies have provided other possible mechanisms for the action of water-soluble surfactants in the  $W_2$  phase [103, 108], and the same behavior was confirmed in our current results when the  $W_1$  phase contained liposomes.

### ***The Effect of Liposomes on External Coalescence***

Generally,  $W_1/O/W_2$  double emulsions require two types of surfactants, an oil-soluble surfactant and a water-soluble surfactant [38]. For instance, a water-soluble surfactant in the  $W_2$  phase is necessary to prevent globule-globule coalescence; however such surfactant at a high concentration has also been shown to induce external coalescence [103, 108, 110]. Based on the research of Kabalnov and Wennerström [111], Pays et al. [108] proposed a mechanism for external coalescence by relating it to the

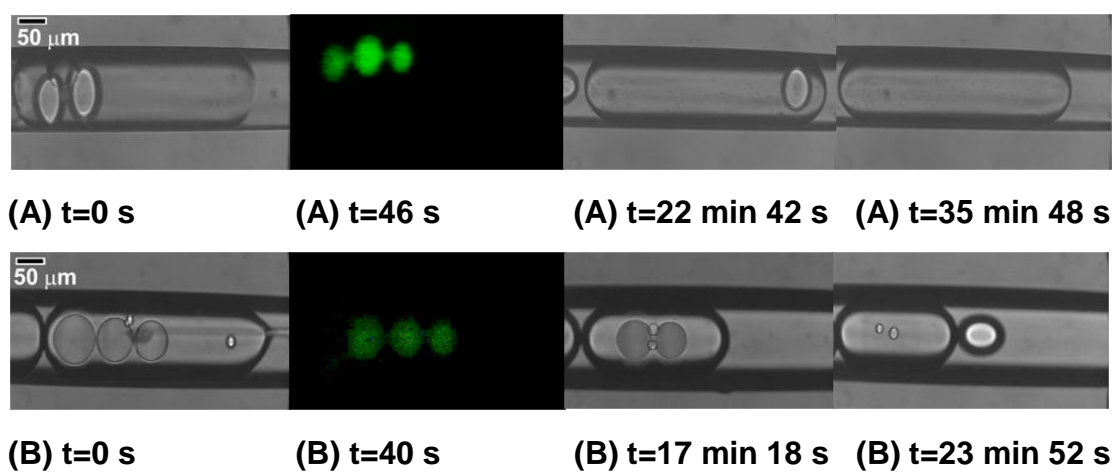


**Figure 3-8.** The effect of Tween 80 in the  $W_2$  phase on the release of liposomes.  $W_1$  phase: liposome suspension; O phase: 0.02 M Span 80 in  $n$ -hexadecane;  $W_2$  phase: 0.005 M (A) and 0.01 M (B) Tween 80 in water. Average external-coalescence time: 716.00 s/droplet (A) and 477.33 s/droplet (B). The scale bar in (A) is applicable for all images.

activation energy needed by the double-emulsion system to form a hole in the oil film. Their study showed that the presence of a high amount of water-soluble surfactant in the aqueous phases lowers the energy barrier for forming a hole within the oil film, thereby facilitating coalescence events between the aqueous phases. In our experiments, it should be noted that internal coalescence among the  $W_1$  droplets within double-emulsion globules did not occur at all. This was expected based on the results of the previous studies [103, 109, 110], according to which internal coalescence is an unlikely event, occurring only when there is significantly more water-soluble surfactant in the  $W_1$  phase than in the  $W_2$  phase.

To determine the effect of liposomes on external coalescence, globule behavior with a pure-water  $W_1$  phase was compared to that of the  $W_1$  phase being composed of a liposome suspension. Tween 80 concentration in the  $W_2$  phase was held at 0.01 M while Span 80 concentration in the oil phase was 0.005 M. Inspection of the coalescence times in Figures 3-6A and 3-9 shows that the coalescence of the three  $W_1$  liposome droplets with  $W_2$ , compared to the time needed for pure-water  $W_1$ , is delayed by approximately 19 minutes. Therefore, we propose that the existence of liposomes in the  $W_1$  phase has a stabilizing effect on the double-emulsion system. This observation agrees with the stabilizing effect of phospholipids from liposomes on the W/O-type emulsions reported by Muderhwa et al. [112]. They demonstrated that liposomes destroyed by emulsification in a bulk experiment donated phospholipid molecules to assist the stabilization effect of the oil-soluble surfactant Arlacel A. O/W liposomal emulsions in which the oil phase is emulsified by phospholipids in liposomes was also developed by this group [113].

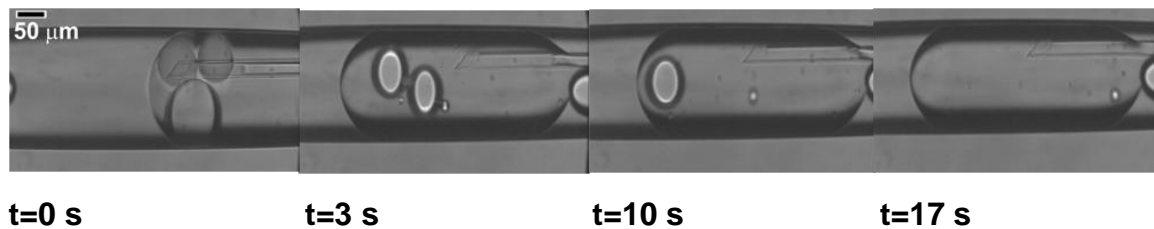


**Figure 3-9.** Time elapsed images of a  $W_1/O/W_2$  double-emulsion globule prepared with  $W_1$  phase: water; O phase: 0.005 M Span 80 in *n*-hexadecane;  $W_2$  phase: 0.01 M Tween 80 in water. Average external-coalescence time: 5.6 s/droplet. The scale bar is applicable for all images.

The tubular liposomes in our experiments are prepared with L- $\alpha$ -phosphatidylcholine and Ceramide-VI. The importance of phospholipids as components of all biological systems may also lie in the fact that they form stable adsorption layers in the oil/water interfaces and reduce the interfacial tension of all interfaces in such systems [114, 115]. Phospholipids, being effective emulsifiers and/or stabilizers, are the molecules used to make liposomes, which have been peripherally used to stabilize or co-stabilize W/O emulsions, O/W emulsions and  $W_1/O/W_2$  double emulsions, showing potential use in vaccine delivery [112, 113, 116]. In the liposome suspension reported in our study, there are some free phospholipid molecules resulting from preparation and storage. When the liposome suspension is injected into an oil globule, the free L- $\alpha$ -phosphatidylcholine molecules in the  $W_1$  phase will adsorb onto the  $W_1/O$  interface and provide more stability by increasing the overall surfactant concentration at the water/oil interfaces of the system. In other words, after the adsorption of L- $\alpha$ -phosphatidylcholine on the  $W_1/O$  interface, the activation energy for the rupture of oil film is increased. Therefore, external coalescence for the liposome-containing  $W_1$  droplets with  $W_2$  phase is delayed. For all our experiments, the existence of liposome suspension in the  $W_1$  phase showed a delayed external coalescence of approximately 10-30 minutes when compared to the case where the  $W_1$  phase consisted only of water.

With the aim to confirm the effect of L- $\alpha$ -phosphatidylcholine on the double emulsions, we did experiments with the  $W_1$  phase containing L- $\alpha$ -phosphatidylcholine instead of liposomes, and the total amount of lipids was about 0.0125% (w/v). The concentration of Span 80 in the oil phase was 0.02 M while the Tween 80 concentration in the  $W_2$  phase was at 0.005 M. Comparing with the average external-coalescence time

of pure water  $W_1$  phase ( $300.22 \pm 37.17$  s/droplet), the average external-coalescence time for three  $W_1$  droplets containing L- $\alpha$ -phosphatidylcholine was increased to  $702.22 \pm 112.05$  s/droplet (images not shown).

As reported by McConnell [117], unsaturated phospholipids are good fluidizers when compared to saturated ones, and spread more rapidly to the air/liquid interface due to their low phase transition. Since the phase-transition temperature of L- $\alpha$ -phosphatidylcholine is about 19°C, it is expected to adsorb on the W/O interface rapidly. In addition, the concentrations of Span 80 used in the study are sufficient to form reverse micelles within the *n*-hexadecane oil phase. Reverse micelles of the oil-soluble surfactant have been reported to facilitate the diffusion of molecules across the oil phase [58, 60, 118]. Therefore, it is possible that the reverse micelles of Span 80 incorporate L- $\alpha$ -phosphatidylcholine molecules to facilitate their adsorption on the interface.

### 3.2 Conclusions

Liposomes containing the model compound fluorescein sodium salt (FSS) were entrapped into the  $W_1$  phase of double-emulsion globules, thus providing a possible double-encapsulation delivery system. Liposomes may thus be protected against the influence of unfavorable physicochemical conditions. The release of liposomes from double-emulsion globules can be controlled from seconds to hours, by varying the water-soluble and/or oil-soluble surfactant concentrations in the  $W_2$  phase or oil phase. The findings also indicate that the mere presence of liposomes in the  $W_1$  phase extends the external-coalescence time in  $W_1/O/W_2$  double-emulsion globules due to the adsorption of free L- $\alpha$ -phosphatidylcholine molecules on the  $W_1/O$  interface.

## **CHAPTER 4**

### **IMPROVED DERMAL DELIVERY OF FITC-BSA USING A COMBINATION OF PASSIVE AND ACTIVE METHODS**

The previous chapter provided insights of the double-encapsulation system in a micro-capillary level. Due to the presence of liposomes in the  $W_1$  phase of double-emulsion system, the double-encapsulation system might have potential application in dermal delivery of macromolecules.

In this chapter, FITC-BSA (68 kDa), which has excitation and emission wavelengths at 485 and 520 nm respectively, was used as a model macromolecule for dermal delivery. A microneedle skinroller with 200  $\mu\text{m}$ -length needles was utilized to perforate newborn-porcine skin in order to be minimally invasive. With the hypothesis that faster delivery of macromolecules through the skin would be accomplished, the combined use of microneedle skinroller and novel formulations, including L- $\alpha$ -phosphatidylcholine liposomes (PC liposomes), double emulsions and double-encapsulation formulations, was investigated, and their efficacies were compared.

## 4.1 Results

### *Passive Delivery of FITC-BSA via Different Formulations*

By use of confocal microscopy, the delivery of FITC-BSA through the intact porcine skin was investigated under different donor formulations. It was found for all formulations studied that FITC-BSA cannot passively penetrate through the *stratum corneum* within 6 h. As shown in Figure 4-1, for four different donor formulations, all the penetration depths of FITC-BSA are  $\sim 10\ \mu\text{m}$  (ANOVA,  $p > 0.05$ ).

### *Visualization of Microneedle Skinroller and Perforated Porcine Skin*

The microneedle skinroller used in this study was composed of 200 extremely fine needles. As shown in Figure 4-2A, compared to a hypodermic needle, the microneedle skinroller has quite short needles which may cause less or no damage on the nerves in the deeper tissues during its use. The needle length of the microneedle skinroller was verified to be  $\sim 200\ \mu\text{m}$  (Figure 4-2B).

The ability of the microneedle skinroller to create microchannels was tested by applying methylene blue solution on the *stratum corneum* of the perforated porcine skin. According to Figure 4-3A, the microneedle skinroller with  $200\ \mu\text{m}$  needle length perforated the skin, and the presence of microchannels was confirmed by the appearance of blue dots inside the skin. The surface morphology and cross-section of the puncture mark were observed by high-resolution cryo-SEM. As shown in Figure 4-3B, the microneedle skinroller created a conduit. Within the epidermis, the skin tissue treated by

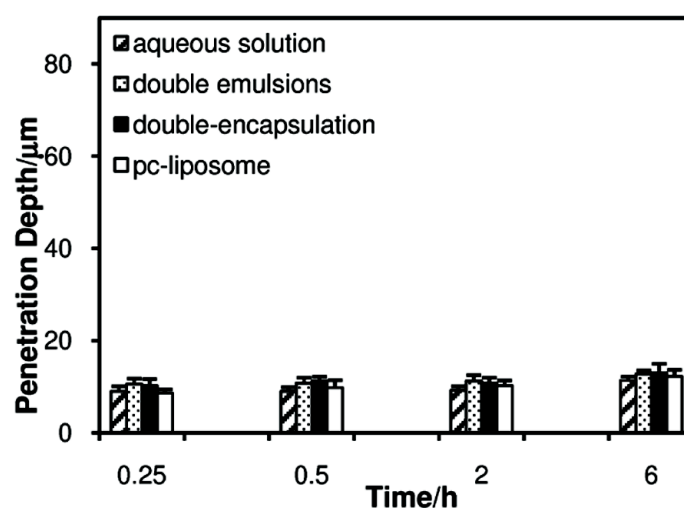


**Figure 4-1.** Penetration depth of FITC-BSA transported through intact porcine skin under different donor formulations. Donor formulations are FITC-BSA aqueous solution, double emulsions, double-encapsulation formulations, and PC-liposome suspension, respectively. Data represents averages of  $n \geq 3$  samples with standard deviation. (ANOVA,  $p > 0.05$ )

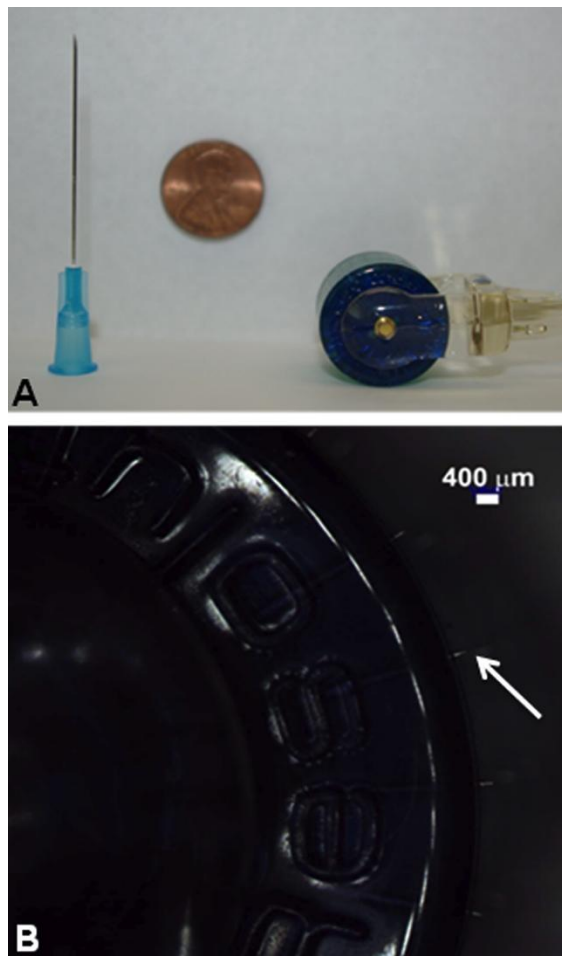


**Figure 4-2.** Visualization of the microneedle skinroller with 200  $\mu\text{m}$  needle length. (A) a 25-G hypodermic needle placed next to the microneedle skinroller; (B) the microneedle skinroller image captured by the vivacam.

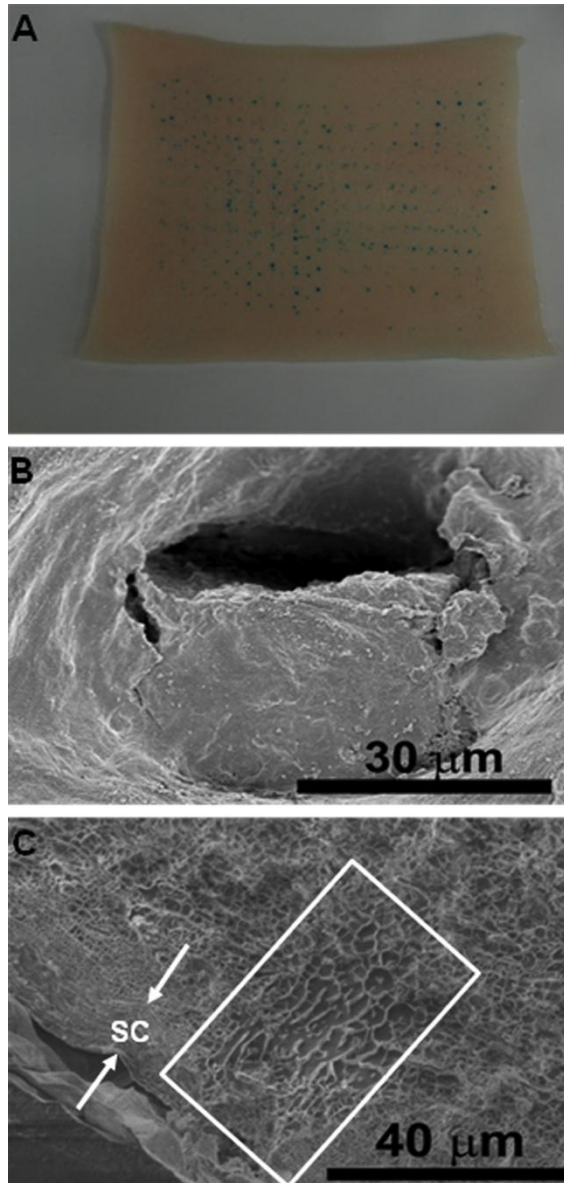


**Figure 4-3.** Skin puncture marks by the microneedle skinroller with 200 μm needle length. A: perforated porcine skin visualized by the methylene blue solution; B: cryo-SEM image of perforated porcine skin viewed from the *stratum corneum* (SC) side; C: cryo-SEM image showing the cross-section of perforated porcine skin.

the microneedle skinroller exhibited a less compact structure when compared to the non-treated region (Figure 4-3C).

### ***Penetration Depth of FITC-BSA under Different Donor Formulations***

To investigate the effect of the carrier on the transport of FITC-BSA through the perforated porcine skin, different formulations were applied in the donor chambers of FDC. Penetration depth of FITC-BSA under four donor formulations at 0.25, 0.5, 2 and 6 h are summarized in Figure 4-4. It was determined that FITC-BSA from all donor formulations penetrated through the *stratum corneum* within 0.25 h for those skin samples treated with the microneedle skinroller (ANOVA,  $p > 0.05$ ). Increasing the experimental time from 0.25 h to 6 h produced an enhancement in the penetration depth of FITC-BSA through the perforated porcine skin in the order of PC-liposome suspension (225.69%) > double-encapsulation formulations (199.06%) > double emulsions (143.43%) > aqueous solution (107.62%). Compared to aqueous solution, FITC-BSA in PC-liposome suspension and double-encapsulation formulations shows higher penetration depth at the time intervals of 0.5 h, 2 h and 6 h (ANOVA,  $p < 0.05$ ). The penetration depth of FITC-BSA in PC-liposome suspension and double-encapsulation formulations does not show significant differences (ANOVA,  $p > 0.05$ ). In addition, when compared to double emulsions, the penetration depth of FITC-BSA in double-encapsulation formulations is significantly enhanced by the incorporation of PC liposomes in the  $W_1$  phase at the time intervals of 0.5, 2 and 6 h (ANOVA,  $p < 0.05$ ).

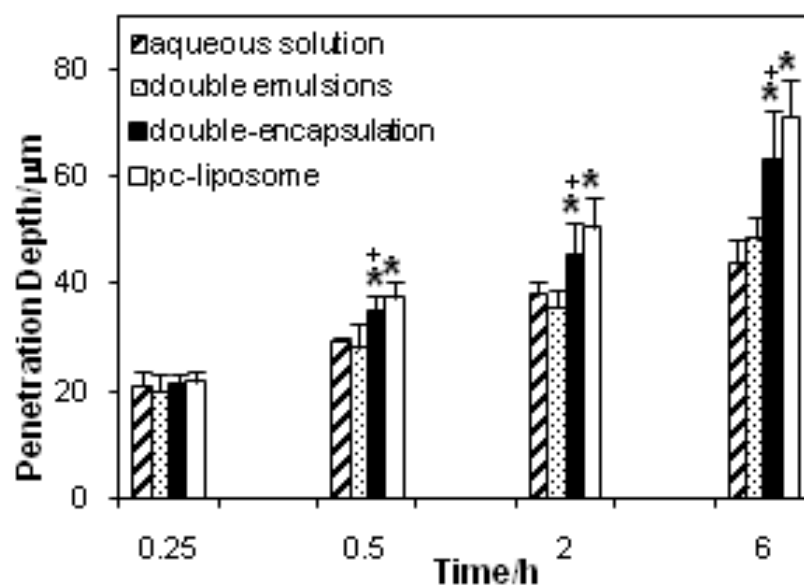


**Figure 4-4.** Penetration depth of FITC-BSA transported through the perforated porcine skin under different donor formulations. Data represents averages of  $n \geq 3$  samples with standard deviation. The \* symbol identifies penetration depth of FITC-BSA in formulations is significantly greater than that in aqueous solution (ANOVA,  $p < 0.05$ ). The + symbol indicates that penetration depth of FITC-BSA in double-encapsulation formulations is significantly enhanced by the incorporation of PC liposomes in the  $W_1$  phase as compared to double emulsions (ANOVA,  $p < 0.05$ ).

### ***Analysis of FITC-BSA Extracted from Skin***

Since the appearance of FITC-BSA in the receptor chambers, indicating transdermal (trans-cutaneous) as opposed to simply dermal (cutaneous) transport, was not observed in all of the experiments, the measurement of FITC-BSA entrapped in the *stratum corneum* and viable skin provides direct information on the amount of FITC-BSA that has permeated into the skin. Table 4-1 shows the amount of FITC-BSA retained in the *stratum corneum* and viable skin after administration of different donor formulations for 6 h. Compared to aqueous solution, the amount of FITC-BSA from the *stratum corneum* exposed to PC-liposome suspension was significantly higher:  $0.82 \pm 0.13 \mu\text{g}/\text{cm}^2$  (aqueous solution) versus  $1.19 \pm 0.06 \mu\text{g}/\text{cm}^2$  (PC-liposomes). For the *stratum corneum* exposed to double emulsions or double-encapsulation formulations, the difference between both formulations and aqueous solutions was not significant.

For FITC-BSA extracted from viable skin (without the *stratum corneum*), the amounts of FITC-BSA are  $7.76 \pm 1.0 \mu\text{g}/\text{cm}^2$ ,  $8.15 \pm 1.78 \mu\text{g}/\text{cm}^2$ ,  $10.47 \pm 0.80 \mu\text{g}/\text{cm}^2$ , and  $12.90 \pm 1.25 \mu\text{g}/\text{cm}^2$  for aqueous solution, double emulsions, double-encapsulation formulations, and PC-liposome suspension, respectively. While there was no significant difference between the amounts of FITC-BSA extracted from viable skin that was exposed to double-encapsulation formulations and PC-liposome suspension ( $p > 0.05$ ), these formulations did show significant increases as compared to transport of FITC-BSA administered in aqueous solution. In addition, it should be noted that the amount of FITC-BSA retained in the viable skin is greater than that in the *stratum corneum* for each piece of skin.

**Table 4-1.** Extraction of FITC-BSA from perforated porcine skin under different donor formulations (6-h experiment). The \* symbol indicates that there is significant difference as compared to aqueous solution (ANOVA,  $p < 0.05$ ).

| Donor Formulations   | Amount of FITC-BSA ( $\mu\text{g}/\text{cm}^2$ ) |             |
|----------------------|--|-------------|
|                      | <i>Stratum Corneum</i>                           | Viable Skin |
| Aqueous solution     | 0.82±0.13  | 7.76±1.0    |
| Double emulsions     | 1.07±0.14  | 8.15±1.78   |
| Double encapsulation | 1.09±0.18  | 10.47±0.80* |
| PC liposomes         | 1.19±0.06*                                       | 12.90±1.25* |

### ***Imaging Analysis on the Transport of FITC-BSA***

The Z direction is defined as perpendicular to the skin surface (into the dermis). The skin surface ( $Z=0$ ) is considered as the layer which shows the highest fluorescent intensity. In Figure 4-5, the distribution of FITC-BSA at skin depth of 0, 30 and 50  $\mu\text{m}$  is shown for each formulation (6-h experiment). The analysis of Figure 4-5 might provide additional information about the amount of penetrated FITC-BSA. At  $Z=0$   $\mu\text{m}$ , corneocytes on the surface of the *stratum corneum* were recognized by their characteristic polygonal shape. At the skin depth of  $Z=30$   $\mu\text{m}$ , the microchannels created by the microneedle skinroller are still visible, which are indicated by white arrows. At  $Z=50$   $\mu\text{m}$ , there is trace amount of green color for double-encapsulation formulations and PC-liposome suspension, but the microchannels cannot be observed. These results are in accordance to the designing purpose of microneedles, which is to disrupt the epidermis but not to reach the nerves in the deeper tissue.

Additionally, for 6-h experiment, cross-section images were reconstructed based on the individual Z-stacks confocal images. According to Figure 4-6, most of the FITC-BSA traveled through the *stratum corneum* along the microchannels created by the microneedle skinroller and into the deeper epidermis. It is also worth noting that, after passing through the *stratum corneum*, FITC-BSA began diffusing around the microchannels. Within the viable epidermis, it shows that the diffusion of FITC-BSA is fast for the formulations incorporating PC liposomes.

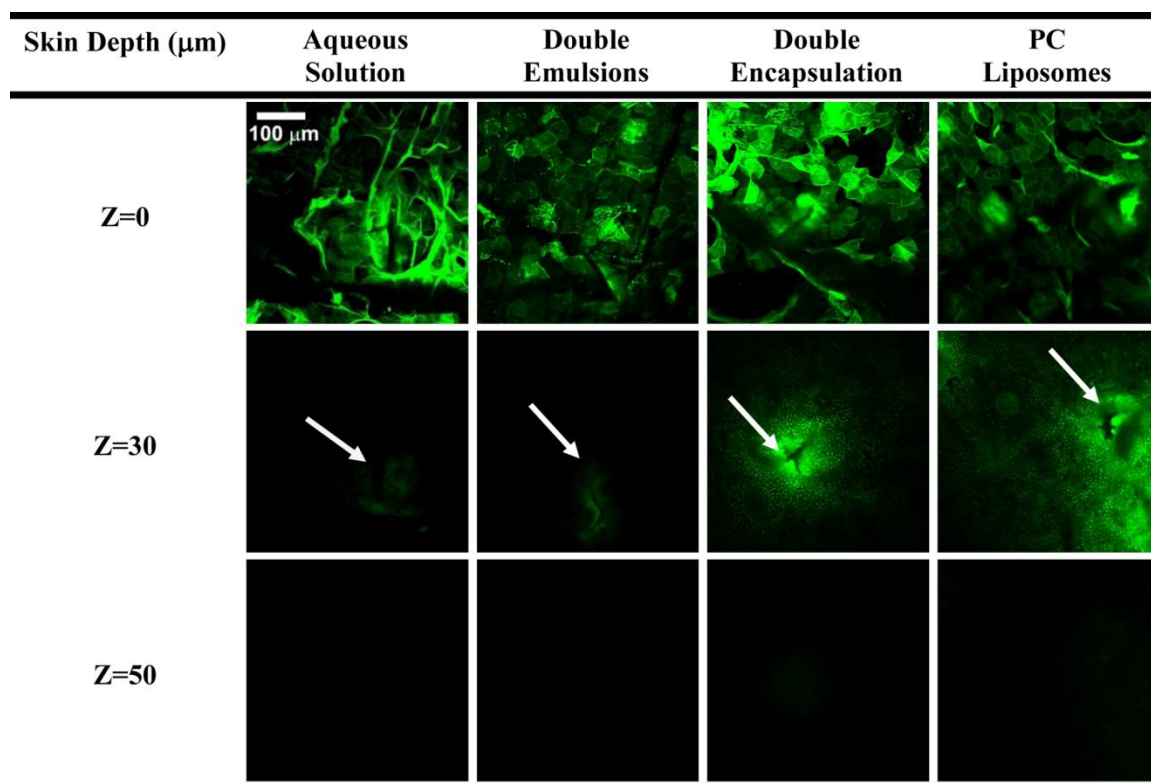


**Figure 4-5.** The confocal images of FITC-BSA across the perforated porcine skin at Z=0, 30 and 50  $\mu\text{m}$ . The fluorescence-emission signal of FITC-BSA is represented by green color. Four donor formulations, including FITC-BSA aqueous solution, double emulsions, double-encapsulation formulations, and PC-liposome suspension, were applied in the donor chambers, and microchannels created by the microneedle skinroller are indicated by white arrows. (6-h experiment; the scale bar is applicable for all images)

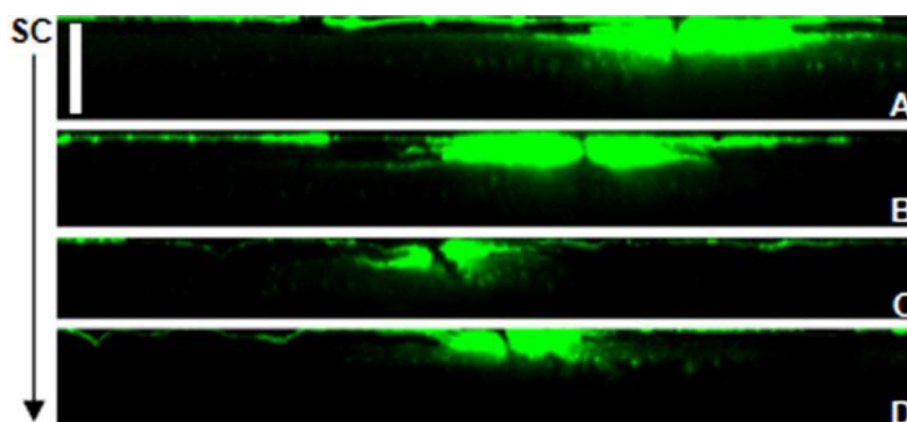


**Figure 4-6.** Cross-section images of perforated porcine skin reconstructed based on the confocal image stacks. Images A, B, C and D illustrated perforated porcine skins treated with PC-liposome suspension, double-encapsulation formulations, double emulsions and FITC-BSA aqueous solution, respectively. (6-h experiment; the scale bar, 50  $\mu\text{m}$ , is applicable for all images)

### ***Studies on Fluorescent Intensity of FITC-BSA***

The analysis of fluorescent intensity provided a simple method to express the relative amount of FITC-BSA on every 1  $\mu\text{m}$  layer of the skin. In Figure 4-7, the fluorescent intensity profiles of FITC-BSA under four donor formulations at 0.5, 2 and 6 h are shown. In general, the perforated porcine skin exposed to PC-liposome suspension showed the highest fluorescence intensity when compared to all other studied formulations. In the case of 0.5-h experiment, fluorescent intensity of FITC-BSA in all formulations decayed with the increase of skin depth (Figure 4-7A). For 2-h and 6-h experiments (Figure 4-7B and 4-7C), the fluorescent intensity of FITC-BSA in some formulations decreased at the beginning, and then a peak appeared at around 10-15  $\mu\text{m}$ , where the boundary between the *stratum corneum* and viable epidermis is located. Finally, fluorescent intensity decreased with skin depth again. The reason for the appearance of the peak could be explained by the different transport coefficients of molecules in the *stratum corneum* and viable epidermis. After the application of donor formulations, FITC-BSA penetrated through the *stratum corneum* along the microchannels. Very little fluorescence was observed around the microchannels located within the *stratum corneum* due to slower transport, especially that of hydrophilic macromolecules such as FITC-BSA, in the *stratum corneum*. Within the viable epidermis, FITC-BSA diffused around the microchannels, and more fluorescence was observed. This observation is consistent with the results observed from Table 4-1, and agrees with the conclusions drawn by Tojo et al., as they indicated that the diffusivity of drug molecules within the *stratum corneum* is 500-10,000 times lower than within the

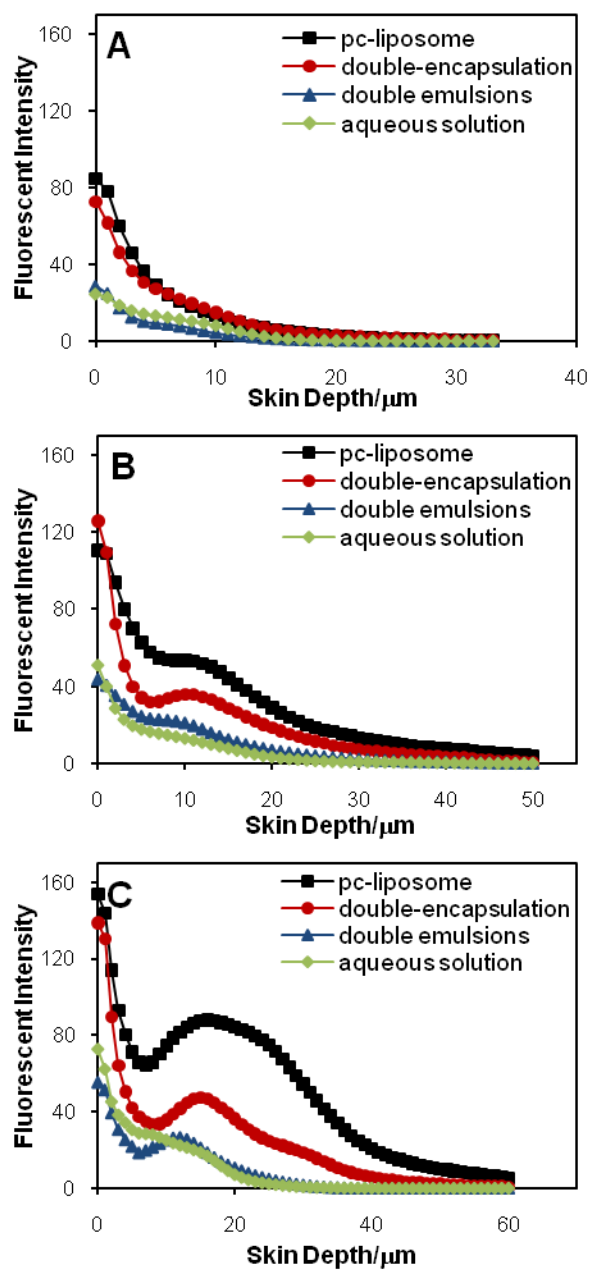


**Figure 4-7.** The fluorescent intensity profiles under different donor formulations at 0.5 h (A), 2 h (B) and 6 h (C). Donor formulations: PC-liposome suspension (■); double-encapsulation formulations (●); double emulsions (▲); FITC-BSA aqueous solution (◆).

viable skin [119]. No peak appears at 0.5 h for all donor formulations, which means that the diffusion of FITC-BSA within the viable epidermis has not occurred yet.

## 4.2 Discussion

### *Effect of Microneedle Skinroller on the Dermal Delivery of FITC-BSA*

In order to be minimally invasive, a commercially available microneedle skinroller with 200  $\mu\text{m}$  needle length was used to enhance the skin permeability. The perforation ability of the microneedle skinroller was confirmed by the application of methylene blue solution on the *stratum corneum* of the perforated skin, following by the appearance of blue dots. Although it was reported that the microneedle arrays with needle length of 300  $\mu\text{m}$  were not able to pierce the human skin *in vitro* [26], porcine skin was successfully perforated by a microneedle skinroller with the 200  $\mu\text{m}$  needle length in our studies. It should be noted that the way to disrupt the skin by the microneedle arrays and the microneedle skinroller is quite different. It has been reported that the cylindrical geometry of the microneedle skinroller perforates the skin by rolling it on the skin surface, leading to the generation of a tension between adjacent needles which facilitates the perforation [29]. In addition, the strength of the force used might be another reason to achieve porcine skin perforation. Clinical studies on pain and sensation have showed that less pain and discomforting sensation are caused by 180  $\mu\text{m}$  and 280  $\mu\text{m}$  microneedles compared to the use of hypodermic needle [120]. Moreover, it has been reported that the microchannels created by the microneedles repaired and resealed after 8-24 hours post application [120].

The surface morphology and cross-section of the microchannels were visualized by use of high-resolution cryo-SEM. The compact structure of epidermis is altered after perforating the porcine skin with the microneedle skinroller, and the depth of the microchannels is near 50  $\mu\text{m}$ . Since the thickness of human *stratum corneum* is about 10-20  $\mu\text{m}$ , following by the viable epidermis being 50-100  $\mu\text{m}$  [121], the needle length of the microneedle skinroller should be sufficient to penetrate through the *stratum corneum* without reaching the nerves and blood vessels. When compared to non-perforated porcine skin, the penetration depth of FITC-BSA increased with a maximum of 7 folds for a 6-h experiment.

#### ***Effect of Formulations on the Dermal Delivery of FITC-BSA***

While the microneedles are an active method to enhance the skin permeability, the use of novel formulations could be another approach. In this study, after the skin was perforated with the microneedle skinroller, a series of novel formulations, such as PC-liposome suspension, double-encapsulation formulations and double emulsions, were selected and compared.

Liposomes, which have been widely used in the immunization studies as the delivery/adjuvant system [122-124], have also shown promise in cutaneous delivery [4, 74, 85, 125-129]. Due to the high deformability and their compositions having the structural similarity to skin lipids, liposomes offer many benefits in the dermal delivery. In order to prevent the interaction of liposomes with an unfavorable physicochemical environment [91-93], double-encapsulation formulation, in which liposomes were

encapsulated inside the oil membrane of double emulsions, was proposed and studied by our group [49].

By combining the benefits of liposomes and double emulsions, our double-encapsulation formulations present promising potential in dermal delivery. Firstly, as with double emulsions [40, 41], by storing liquid double-encapsulation formulations at a temperature below the freezing point of the oil phase, solidification/freezing of *n*-hexadecane made the formulations cream-like and successfully preserved their stability; when the solid emulsions returned to room temperature and the oil phase thawed, a large amount of the  $W_1$  phase is released to the  $W_2$  phase instantly. For application, the solid double-encapsulation formulations can be applied in the same way as with cosmetic creams. The contact of double-encapsulation formulations with the skin will melt the oil phase and trigger the release of proteins and liposomes from the  $W_1$  phase. Secondly, since the exposure of proteins to the water/oil interface may result in a loss of biological activity or conformational changes [130], the adsorption of phospholipids from disassembled liposomes onto the  $W_1/O$  interface prevents the interaction between proteins and oil phase. Thus, with double-encapsulation formulations, not only is the cutaneous delivery more efficient, but protein stability should also be improved.

It was found that FITC-BSA cannot passively penetrate beyond the intact *stratum corneum*, though the combination of microneedle skinroller and formulations resulted in both a greater penetration depth and a higher fluorescent intensity of FITC-BSA. To analyze the penetration of FITC-BSA through the perforated porcine skin under different donor formulations, confocal microscopy was utilized. The confocal images indicated that PC liposomes have the greatest efficiency in delivering FITC-BSA into the viable

epidermis. By the incorporation of liposomes in the  $W_1$  phase, FITC-BSA in double-encapsulation formulations showed a similar penetration depth as that in PC liposomes (ANOVA,  $p > 0.05$ ). Also, there is no significant difference for FITC-BSA from viable skin exposed to PC-liposome suspension and double-encapsulation formulations (ANOVA,  $p > 0.05$ ). As reported, hydrophilic molecules entrapped inside phospholipid vesicles have higher penetration ability into the deeper skin layers [129]. FITC-BSA in formulations containing the PC liposomes transported more quickly through the viable epidermis as compared to that in double emulsions and aqueous solution as indicated in Figures 4-5 and 4-6. Since the lipids in the PC liposomes have similar structure with skin lipids, an expected fusion between PC liposomes and the skin lipids may facilitate the delivery of FITC-BSA in the PC-liposome suspension and double-encapsulation formulations. On the other hand, the fusion and aggregation of liposomes with epidermal cells may have induced an increased liposome-flow towards the epidermis [29]. Therefore, formulations incorporating liposomes may continuously deliver the protein to the epidermis of the skin.

### 4.3 Conclusions

Macromolecules were delivered to skin effectively by combining passive and active methods. Following the perforating action of a microneedle skinroller by applying novel formulations, the dermal delivery of FITC-BSA was enhanced significantly when compared to passive methods alone or microneedle skinroller-effected transport of aqueous solutions of macromolecules. With the perforated porcine skin, FITC-BSA in all formulations penetrated through the *stratum corneum* within 15 min. The penetration pathway of FITC-BSA under different donor formulations was analyzed by confocal

microscopy. Because of the incorporation of PC liposomes in the  $W_1$  phase of double-encapsulation formulations, FITC-BSA shows greater penetration depth and diffusibility as compared to FITC-BSA in aqueous solutions or in double emulsions, presumably due to the structural similarity of phospholipids with skin lipids. Because of the different transport coefficients of molecules in the *stratum corneum* and viable epidermis, the amount of FITC-BSA retained in the viable skin is larger than that in the *stratum corneum*. Although the combination of microneedle skinroller and novel formulations makes the delivery of macromolecules more efficient, there are still other factors which should be considered in the future, such as the force applied on the microneedle skinroller and phospholipid type.

## CHAPTER 5

### CATIONIC LIPOSOMES IN DOUBLE EMULSIONS FOR CONTROLLED RELEASE

Our previous work on individual double-encapsulation globules demonstrated that the release of liposomes and their contents can be controlled by varying the concentration of oil-soluble and/or water-soluble surfactant in the O phase or the W<sub>2</sub> phase, and indicated the presence of liposomes in the W<sub>1</sub> phase delays the occurrence of external coalescence [49]. Skin-permeation studies via double-encapsulation formulations were also performed *in vitro* [51]. Combined with the treatment of microneedle-skinroller, double-encapsulation formulations were confirmed to have a high efficiency in delivering macromolecules across the porcine skin.

In this chapter, cationic liposomes were selected among several liposome types to fabricate double-encapsulation formulations. Our motivation for current study is that positively charged liposomes are more readily taken up via phagocytosis (one of the first lines of defense against invading microorganisms), which might facilitate the initiation of the immune response. Other effects, such as high encapsulation efficiency and great penetration ability [81], were also reported. FITC-BSA (MW: 68 kDa; isoelectric point: 4.7) was used as a model active substance and encapsulated inside cationic liposomes.

Double-encapsulation formulations were successfully fabricated in bulk by the incorporation of cationic liposomes in the  $W_1$  phase of  $W_1/O/W_2$  double emulsions using a two-step emulsification procedure. Upon the freeze-thaw treatment, stability of double-encapsulation formulations, FITC-BSA release mechanism and FITC-BSA release rate were revealed.

## 5.1 Results and Discussions

### *Liposome Selection*

The morphology of three types of liposomes was studied by use of cryo-TEM. According to cryo-TEM images, PC liposomes (Figure 5-1A), hydrogenated PC liposomes (Figure 5-1B) and DOTAP cationic liposomes (Figure 5-1C) are mainly unilamellar and vesicular. Because of the high phase-transition temperature of the hydrogenated PC lipid ( $51^{\circ}\text{C}$ ), hydrogenated PC liposomes are angular in shape [131]. Furthermore, an important finding is the better dispersibility of the DOTAP cationic liposomes, compared to PC liposomes and hydrogenated PC liposomes, which is due to repulsive electrostatic forces.

As illustrated in Figure 5-2, the encapsulation efficiencies of FITC-BSA in PC liposomes, hydrogenated PC liposomes and DOTAP cationic liposomes were  $29.73 \pm 1.12\%$ ,  $35.58 \pm 0.22\%$  and  $93.67 \pm 0.23\%$ , respectively. In contrast to PC liposomes and hydrogenated PC liposomes, DOTAP cationic liposomes have an extremely high encapsulation capacity for negatively-charged FITC-BSA due to charge interactions; this

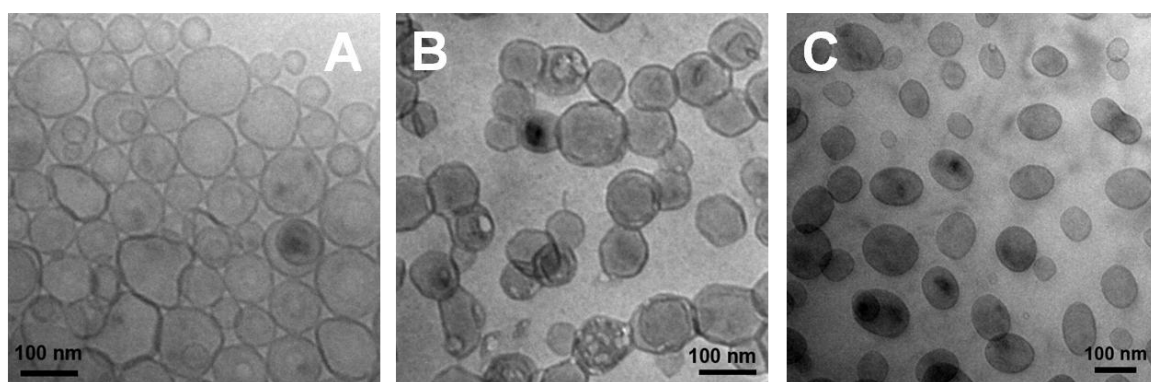


**Figure 5-1.** Cryo-TEM images of PC liposomes (A), hydrogenated PC liposomes (B) and DOTAP cationic liposomes (C).

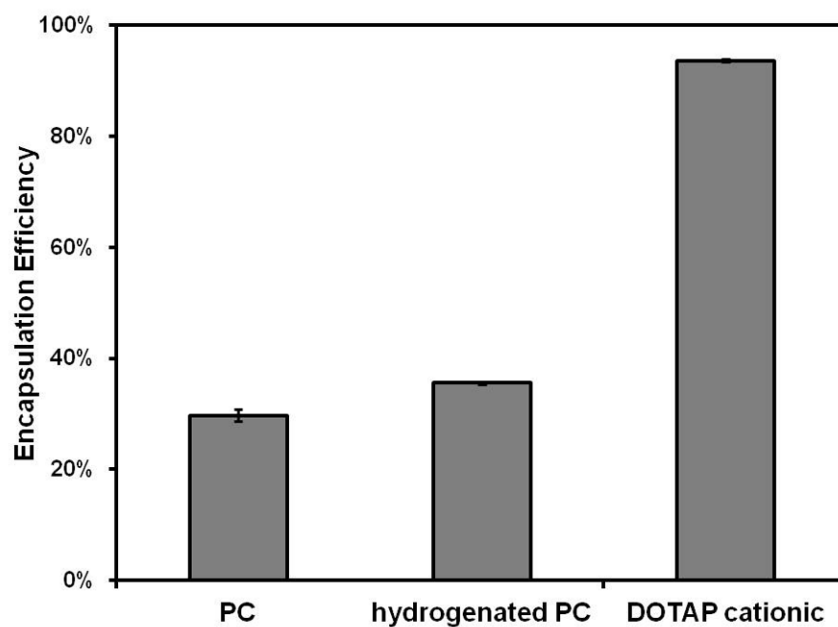


**Figure 5-2.** Encapsulation efficiency of FITC-BSA in PC liposomes, hydrogenated PC liposomes and DOTAP cationic liposomes. Data represents the average of three samples with standard deviation.

fact suggests DOTAP cationic liposomes as the most suitable type for double-encapsulation formulations. Zeta-potential values can reflect surface net charge of vesicles. By use of Zeta Potential Analyzer, zeta potential of DOTAP cationic liposomes used is  $21.89 \pm 3.12$  mV, which can indirectly explain the reason of high encapsulation efficiency of FITC-BSA in DOTAP cationic liposomes. Moreover, it has been proposed that cationic liposomes have an adjuvant effect on the activation of antigen-presentation cells [84], which may potentially facilitate the initiation of an immune response and enhance the efficiency of dermal immunization. The other main function is to protect the antigens from clearance in the body [132]. In addition, high skin-penetration ability has been reported since cationic liposomes can bind the negatively-charged skin cells and hair follicles and thus achieve a high local concentration [81]. Therefore, among the three types of liposomes studied, DOTAP cationic liposomes were selected to prepare double-encapsulation formulations.

### ***Microstructure Visualization of the Double-Encapsulation System***

Right after preparation, the cross-section of the double-encapsulation formulation was observed by high-resolution cryo-SEM. As shown in Figure 5-3A, a typical double-encapsulation globule is filled with several  $W_1$  droplets. Closer observation of one  $W_1$  droplet indicated that a large amount of liposomes are encapsulated within (Figure 5-3B), confirming that most liposomes survive the homogenization process during the first emulsification step and stay in the  $W_1$  phase after the second emulsification step.

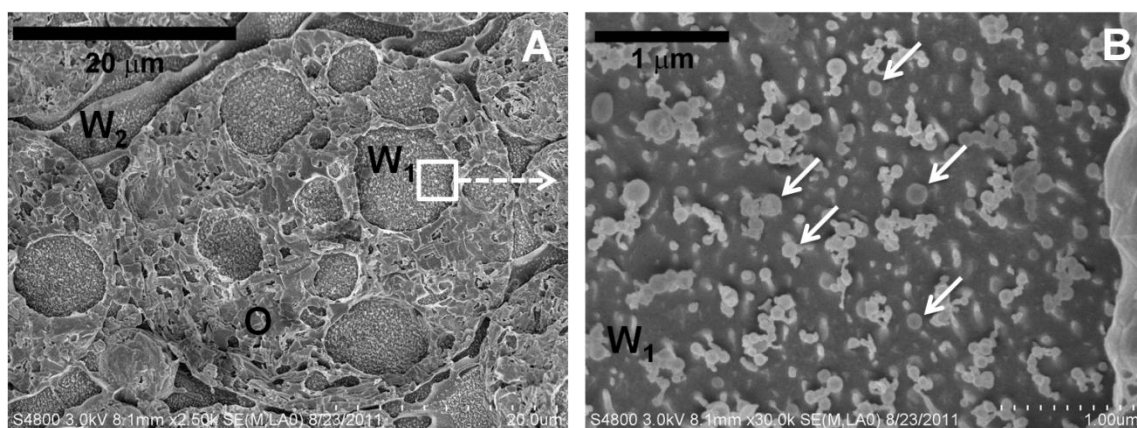


**Figure 5-3.** Cryo-SEM images of (A) the cross section of double-encapsulation formulation and (B) closer observation of one W<sub>1</sub> droplet shown in Figure 5-3A. Liposomes within the W<sub>1</sub> droplet are pointed by white arrows.

### ***Stability of Double-Encapsulation Formulations under Freeze-Thaw Treatment***

Freeze-thaw cycles have been reported as an approach to effectively trigger release of substances from double emulsions [40, 41]. It has been demonstrated that the stability of  $W_1/O/W_2$  double emulsions is maintained during and after freezing of the O-phase. On the other hand, breakdown of double emulsions occurs immediately after oil-thawing because the oil-soluble surfactant, expelled from the interfaces during the freezing process [133], cannot migrate back faster than the oil-melting rate. As shown in the control sample (Figure 5-4A), double emulsions undergo instant phase-separation upon freeze-thaw treatment, resulting in a creamy layer (top) and an aqueous layer (bottom). In accordance with previous studies [41], there were slight changes in the extent of phase separation after longer-time observations (up to 48 h).

Similar to the control double emulsion, freezing the oil phase of the double-encapsulation formulation (Figure 5-4B) at 5°C preserved stability. However, phase separation was not detected immediately after thawing at 35°C for 5 min. Instead, phase separation occurred slowly so that it took approximately 10 min to obtain a clear boundary between the creamy layer and the aqueous layer. After 48 h, the aqueous bottom corresponded to only 32.81% of the total volume of the double-encapsulation formulation (Figure 5-4C), while it was 40.05% for the control double emulsion under the same conditions. Consequently, presence of cationic liposomes in the  $W_1$  phase of the double-encapsulation formulation had a significant effect on the rate and extent of phase separation after oil thawing.

Optical-microscopy images taken with bright and fluorescent light indicated that both, the control double emulsions and the double-encapsulation formulation, contained

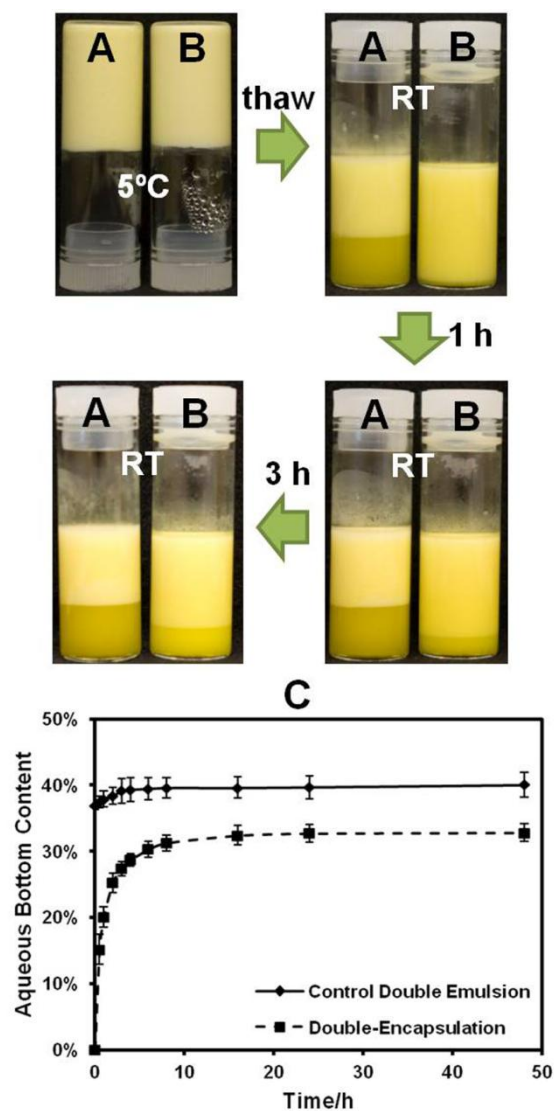


**Figure 5-4.** Visual comparison of the effect of the freeze-thaw treatment on phase separation of the control double emulsion (A) and the double-encapsulation formulation (B); Aqueous bottom content in the control double emulsion and the double-encapsulation formulation after freeze-thaw treatment (C).

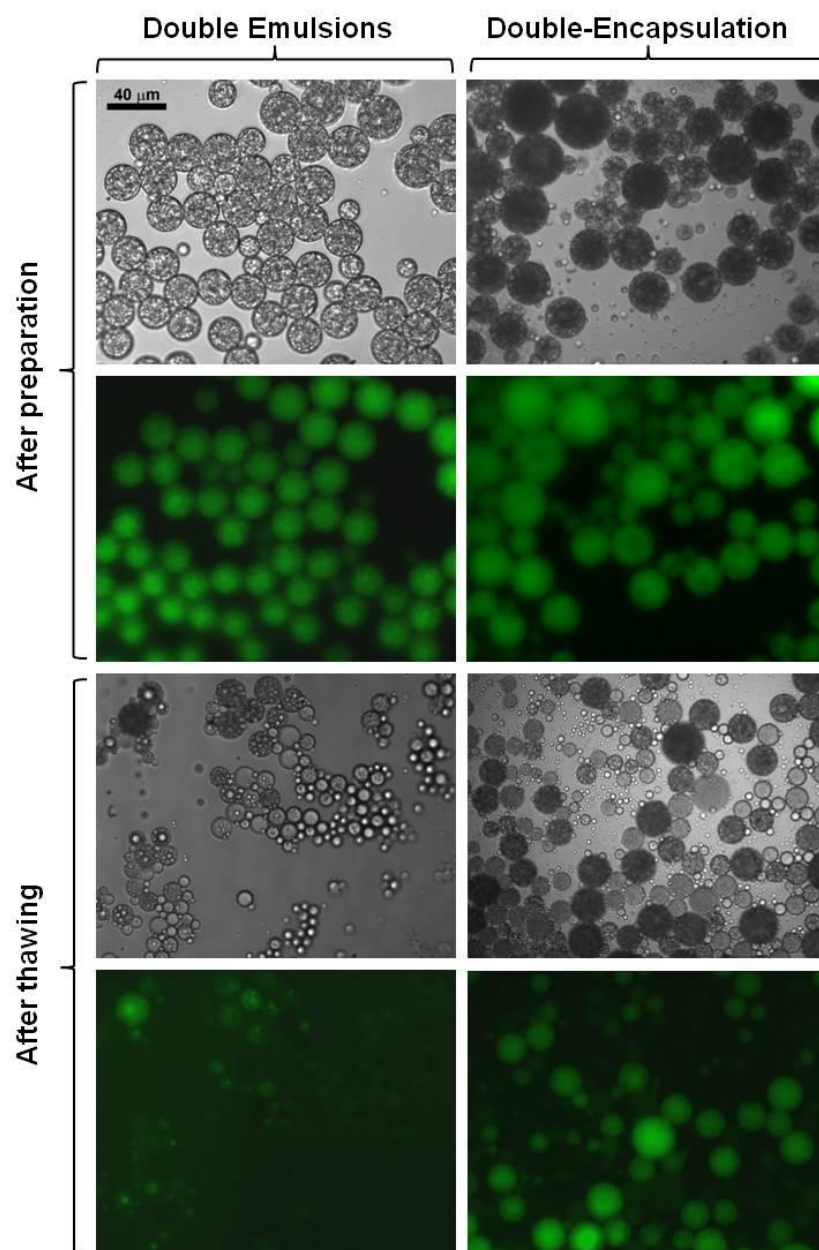


**Figure 5-5.** Microscopy observation of the top creamy layers of the control double emulsion and the double-encapsulation formulation after fabrication and freeze-thaw treatment. The scale bar is applicable to all images.

well-structured globules right after preparation, which were completely filled with many tiny  $W_1$  droplets (Figure 5-5). After thawing the control double emulsion, the top creamy layer was visualized under the microscope and it was found to consist of empty or nearly-empty oil globules, indicating that most FITC-BSA had been released from the  $W_1$  phase. In contrast, the top creamy layer of the thawed double-encapsulation formulation still contained many  $W_1$  droplets entrapped within the oil globules.

This finding demonstrates that presence of cationic liposomes in the  $W_1$  phase slows down the thaw-induced instability of double-encapsulation formulations, and consequently, liposomes and their contents are gradually – rather than instantly – released from the  $W_1$  phase. In fact, our previous experimentation inside glass microcapillaries [49] had indicated that presence of liposomes in the  $W_1$  phase is by itself a stabilizing factor for double emulsions. We then hypothesized that free PC lipids from destroyed liposomes adsorb onto the  $W_1/O$  interface and assist the stabilization effect of oil-soluble surfactant (Span 80) by increasing the overall surfactant concentration in the O-phase. Similarly, in W/O emulsions, liposomes destroyed by the emulsification procedure were seen to assist stabilization by donating the PC lipid [112]. What is more, simple emulsions stabilized by the PC lipid have also been reported to remain stable throughout the freeze-thaw treatment [134, 135], presumably because high-molecular-weight emulsifiers like lipids are less likely to diffuse between interfaces of emulsions. It was proposed that coalescence, induced by intermixing of the surface lipids among emulsion droplets, and subsequent merging of the monolayers within the interfaces, does not occur during freeze-thawing of lipid emulsions stabilized by PC lipid [135].

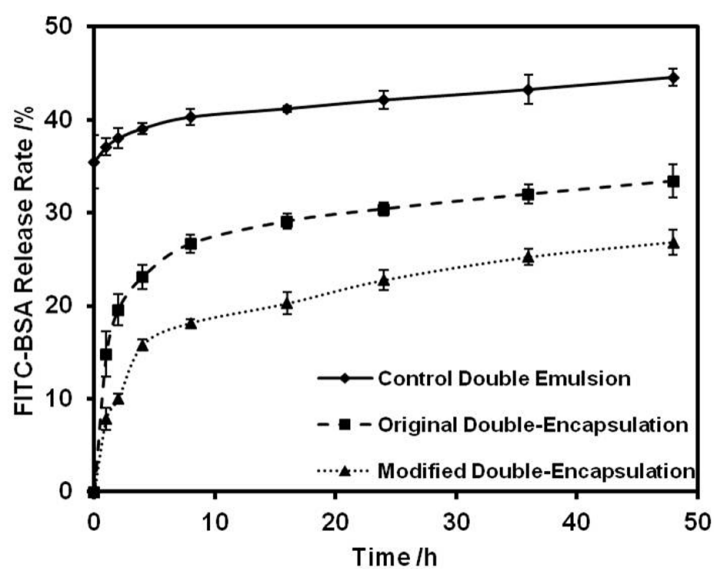


**Figure 5-6.** Release rate of FITC-BSA from the control double emulsion (◆), original double-encapsulation formulation (■) and modified double-encapsulation formulation (▲).

### ***Release Rate of FITC-BSA from the Double-Encapsulation System***

Absorbance analysis of the aqueous bottoms collected from the control double emulsion and the double-encapsulation formulation after freeze-thaw treatment revealed a significant effect of the PC lipid on the release rate of FITC-BSA. As shown in Figure 5-6, for the control double emulsion, 35.50% of FITC-BSA was recovered right after thawing, and this value increased to 44.56% after 48 h. For the double-encapsulation formulation, however, no FITC-BSA was obtained right after the freeze-thaw treatment since no aqueous bottom had formed at that time; FITC-BSA was then progressively released to reach 33.41% after 48 h. It is evident that the existence of cationic liposomes in the  $W_1$  phase delayed the release of FITC-BSA from the double-encapsulation formulation.

With the purpose of confirming the effect of PC lipid on the release rate of FITC-BSA, we fabricated another cationic liposome sample containing the same amount of DOTAP lipid but twice the amount of PC lipid as compared to the original cationic liposomes. The newly fabricated cationic liposomes were then incorporated into the  $W_1$  phase of a modified double-encapsulation formulation. As expected, increasing the content of PC lipid in the cationic liposomes further delayed the release of FITC-BSA, so that the amount of FITC-BSA recovered after 48 h dropped from 33.41% to 26.86%. Thus, we propose that the release rate of FITC-BSA may be tuned by adjusting the concentration of PC lipid in the cationic liposomes.

As suggested by previous work [105], the effective thickness of the layers that oil-soluble surfactants form to cover water/oil interfaces is directly related to the concentration of the oil-soluble surfactant. In general, a thick adsorbed layer leads to a

repulsive force between the  $W_1$  droplets and the  $O/W_2$  interface, while a thin adsorbed layer produces a net attractive force that leads to coalescence. For the modified double-encapsulation formulation, the additional PC-lipid molecules provide a thicker adsorbed layer and relatively-stronger repulsive force between the  $W_1$  droplets and the  $O/W_2$  interface, ultimately leading to delayed release of liposomes and FITC-BSA from the  $W_1$  phase. Additionally, in contrast to low-molecular-weight emulsifiers like Span 80, higher-molecular-weight emulsifiers such as proteins and lipids provide relatively thick interfacial membranes, resulting in a more stable system throughout the freeze-thaw treatment [136].

### ***Release Mechanism of the Double-Encapsulation System***

As mentioned above, the release of active substances from double emulsions is dominated by two main mechanisms: transport of active substances across the oil phase, and breakdown of double emulsions [31, 57, 109, 110]. During the storage of double-encapsulation formulations at 5°C, the release of FITC-BSA is suppressed by the frozen oil phase; after oil thawing, the release of FITC-BSA is mainly dominated by the breakdown of double-encapsulation formulations [40].

As illustrated in Figure 5-6, 14.79% of the FITC-BSA was released from the original double-encapsulation formulation after 1 h, which means that 14.79% of the  $W_1$  phase must have been released into the aqueous bottom. Assuming that the total volume of the double-encapsulation formulation is 100 mL, the original volumes of  $W_1$  phase,  $O$ -phase and  $W_2$  phase are 40 mL, 40 mL and 20 mL, respectively. Then, after 1h the aqueous bottom of the double-encapsulation formulation corresponded to 20.09 mL (Figure 5-4C), which is composed of 5.92 mL of  $W_1$  phase and 14.17 mL of  $W_2$  phase

according to our calculation. Finally, after 48 h the aqueous bottom contained 13.36 mL of  $W_1$  phase and 19.45 mL of  $W_2$  phase, indicating that almost all of the  $W_2$  phase was already present in the bottom aqueous layer.

It is known that a high concentration of Tween 80 in the  $W_2$  phase has a destabilizing effect on  $W_1/O/W_2$  double emulsions [109, 110]. In other words, the excess Tween 80 surfactant molecules form micelles that can dissolve some of the oil-soluble surfactant (Span 80), consequently inducing release of  $W_1$  droplets. Accordingly, the release of FITC-BSA from the double-encapsulation formulations was: (i) relatively faster during the earlier stages of the study (0-8 h), owing to the high concentration of Tween 80 in the  $W_2$  phase, and (ii) slower during the later stages (after 8 h) since most of the  $W_2$  phase was already in the aqueous bottom and fewer Tween 80 molecules were present at the top creamy layer.

Besides, since the  $W_1$  droplets were too small for external coalescence to be triggered by oil-thawing [40], internal coalescence followed by external coalescence is the release mechanism of the double-encapsulation formulation after the freeze-thaw treatment. In addition to this mechanism, liposomes in the  $W_1$  phase may have donated PC lipids to enhance the stabilization provided by the oil-soluble surfactant Span 80 [49]. As a result, coalescence took place gradually – rather than instantly – in the double-encapsulation formulation, and therefore a slower release of FITC-BSA was detected.

An interesting phenomenon was observed when we compared the diluted freshly-fabricated, double-encapsulation formulation to the control double emulsion. As shown in Figure 5-7, microscopy observation indicated that the double-encapsulation globule,

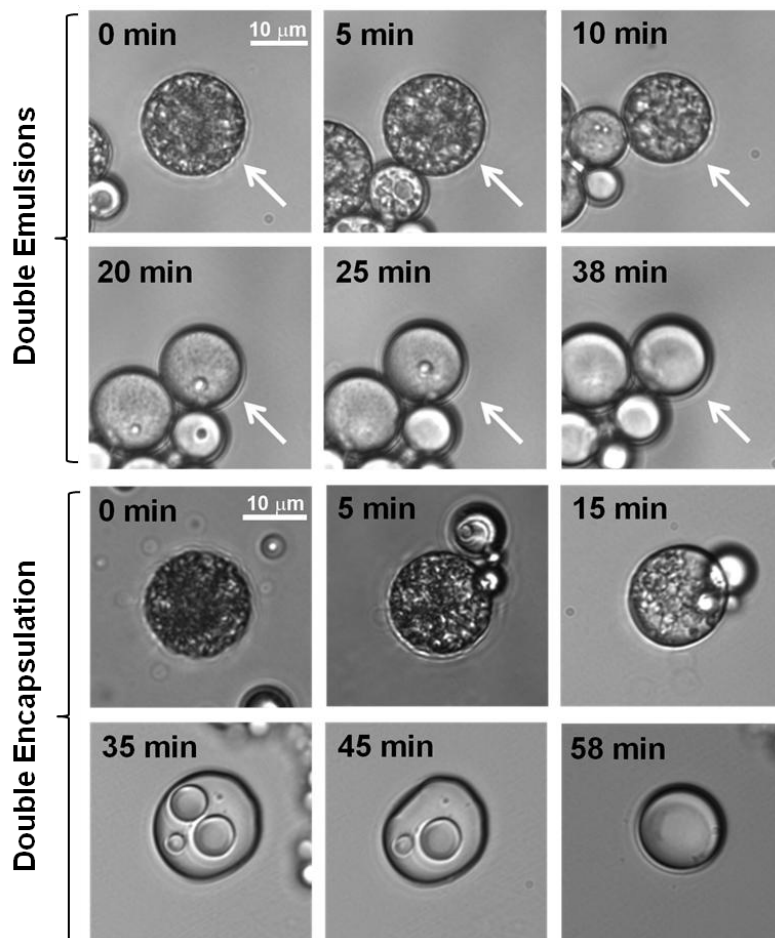


**Figure 5-7.** Real time observation of a typical double-emulsion globule right after preparation.  $W_1$  phase: 2 mg/ml FITC-BSA in PB buffer, O phase: 0.05 M Span 80 in *n*-hexadecane,  $W_2$  phase: 0.08 M Tween 80 in PB buffer; Real time observation of a typical double-encapsulation globule right after preparation.  $W_1$  phase: Cationic C liposomes containing 2 mg/ml FITC-BSA in PB buffer, O phase: 0.05 M Span 80 in *n*-hexadecane,  $W_2$  phase: 0.08 M Tween 80 in PB buffer.

like the control double-emulsion globule, initially contained many tiny  $W_1$  droplets. Subsequent internal coalescence progressively increased the average diameter of the  $W_1$  droplets and external coalescence took place upon reaching a certain threshold size. This observation is in agreement with findings by Pays et al. [108] and Villa et al. [110]. However, a key difference noticed in the present paper, is that external coalescence in double-encapsulation globules occurred for comparatively larger  $W_1$  droplets. This can be explained by considering the assumption that what leads to external coalescence and internal coalescence is the predominance of a Hamaker attraction over an electrostatic repulsion [105, 137]. An explanation may be that, as the donated PC lipids resulting from destroyed liposomes adsorb onto the  $W_1/O$  interface of the double-encapsulation globules, the effective surfactant concentration increases, thus leading to a greater effective thickness of the adsorbed layer. As a result, larger  $W_1$  droplets are needed to overcome the greater electrostatic repulsion.

## 5.2 Conclusions

Double-encapsulation formulations were fabricated by incorporating cationic liposomes loaded with the model active component FITC-BSA as the  $W_1$  phase of  $W_1/O/W_2$  double emulsions. In the present study, bulk double-encapsulation formulations were prepared using a two-step emulsification procedure, and subsequently stored at 5°C to obtain stable and cream-like formulations. With the purpose of exploring how active ingredients would be released from the proposed double-encapsulation system during it administered to the skin, phase separation and release rate were studied upon oil-thawing at skin temperature (35 °C). As expected, storing the double-encapsulation formulation at a temperature below the phase transition temperature of the O-phase

helped preserve stability while subsequent thawing of O-phase induced the release of liposomes and their contents.

Cryo-SEM images confirmed that most liposomes were well encapsulated within the  $W_1$  phase of the double-encapsulation formulation. As compared to the control double emulsions, the double-encapsulation formulation showed slower phase separation after freeze-thaw treatment due to the stabilizing effect of the PC lipid from the liposomes, which resulted in the gradual – rather than instant – release of liposomes and FITC-BSA from the  $W_1$  phase. Besides, control of the release of liposomes and FITC-BSA from the double-encapsulation formulation was proven feasible by varying the concentration of the PC lipid in the cationic liposomes. The release rate of the double-encapsulation formulation upon the freeze-thaw treatment is dependent on the amount of Tween 80 in the  $W_2$  phase, and consists of two stages, including initial fast release (0-8 h) and subsequent slow release (after 8 h).

## CHAPTER 6

### DISCUSSIONS AND FUTURE WORK

#### 6.1 Discussions

The studies presented in previous chapters [49, 51, 138] are part of our work to develop a vaccine formulation that will be applied dermally to facilitate the penetration of macromolecules across the skin.

In chapter 3, incorporation of liposomes in the  $W_1/O/W_2$  double-emulsion globules by use of capillary video-microscopy brought us a new delivery system, double-encapsulation system. The hypothesized model of a double-encapsulation delivery system indicated that active substances are encapsulated inside the liposomes, which are in turned entrapped inside the  $W_1$  phase of  $W_1/O/W_2$  double emulsions. Such system has the possibility to not only enhance the permeation of active substances across the skin due to the structural similarity of liposomal lipids with skin lipids, but also prevent the interaction of liposomes and their contents with unfavorable physicochemical conditions before they are administered to a specific target. From microcapillary-level experiments, the role of different types of surfactants on the stability of the double-encapsulation system was studied. More specifically, the effects of water-soluble surfactant, oil-soluble surfactant, as well as the presence of liposomes in the  $W_1$  phase on the stability of double

emulsions were evaluated. Investigating the stability of such double-encapsulation system and the role of surfactants in this system contributes to the knowledge of how to control the release from this system. External coalescence, defined here as coalescence between the  $W_1$  and  $W_2$  aqueous phases, was investigated as the mechanism for release of liposomes and their contents from the  $W_1$  phase to the  $W_2$  phase. It was concluded that a high oil-soluble surfactant concentration in the O phase corresponds to a thicker adsorbed layer that produces a greater repulsive force between the  $W_1$  phase and  $W_2$  phase to stabilize the double-emulsion globules; a high concentration of water-soluble surfactant in the  $W_2$  phase leads to the rupture of double emulsions and induces the rapid release of liposomes and their contents via external coalescence. The intrinsic effect liposomes may themselves have on the stability of double-emulsion globules was also investigated, which was accomplished by comparison of liposome-containing- $W_1$ -phase globules to pure-water- $W_1$ -phase globules. The major finding is that the mere presence of liposomes in the  $W_1$  phase extends the external-coalescence time for  $W_1/O/W_2$  double-emulsion globules due to the adsorption of free L- $\alpha$ -phosphatidylcholine molecules on the  $W_1/O$  interface.

As a non-invasive route, dermal vaccine delivery may provide improved convenience and compliance of patients over other traditional routes. However, cutaneous delivery is severely limited by the barrier effect imposed by the outmost layer of the skin, the *stratum corneum*. Based on whether an external source of energy is used for skin-permeation enhancement, passive and active methods were proposed to enhance the permeability of the *stratum corneum*. Due to the fact that passive methods can have a delivery time of up to several hours, we used the combination of passive and active

methods in Chapter 4. With the expectation that faster delivery of macromolecules through the skin would be accomplished, the combined use of microneedle skinroller with 200  $\mu\text{m}$  length needle and novel formulations, including liposomes, double emulsions and double-encapsulation formulation, was investigated *in vitro*, and their efficiency was compared. By combined use of microneedle perforation and novel formulation application, the dermal delivery of macromolecules was enhanced significantly when compared with passive method alone or microneedle skinroller-effected transport of aqueous solution of macromolecules. By use of confocal microscopy, it was observed that FITC-BSA in all formulations penetrated through the *stratum corneum* of porcine skin within 15 minutes after the microneedle skinroller perforation. Due to the encapsulation of liposomes in the  $W_1$  phase of double emulsions, FITC-BSA in double-encapsulation formulations shows greater penetration depth and diffusion ability as compared to FITC-BSA in aqueous solution or double emulsions. Such high diffusion ability is attributed to the structural similarity of phospholipids in liposomes with skin lipids. Because of the different transport coefficients of molecules in the *stratum corneum* and viable epidermis, the amount of FITC-BSA extracted from the viable epidermis is larger than that from the *stratum corneum*. Even though the combination of microneedle skinroller and double-encapsulation formulation shows encouraging results in *in-vitro* skin-permeation studies, further experiments, such as the selection of lipid in liposomes, should be considered.

The function of the liposomes is highly dependent on their physical-chemical characteristics. Particularly, the surface charge plays a great role on the adjuvant effect. Many *in-vivo* studies have demonstrated that cationic liposomes are more suitable for

vaccine delivery, compared with anionic and neutral liposomes [139, 140]. As a result, cationic liposomes are being used increasingly as efficient vaccine adjuvants. Cationic liposomes have been reported to have the ability to target antigens for endocytosis by antigen-presenting cells [141]. Other effect, such as the efficient interaction between cationic liposomes and the negatively charged molecules on the surface of antigen presenting cells, has been elucidated [132].

In chapter 5, three different liposomes, including PC liposomes, hydrogenated PC liposomes and DOTAP cationic liposomes, were fabricated and compared. Among several liposomes types, DOTAP cationic liposomes were selected based on the fact that they have (1) extremely high encapsulation capacity for negatively charged FITC-BSA, (2) high penetration ability across the skin and hair follicles, and (3) an adjuvant effect on the activation of antigen-presenting cells. Double-encapsulation formulations were prepared by the incorporation of cationic liposomes loaded with the model active component FITC-BSA as the  $W_1$  phase of  $W_1/O/W_2$  double emulsions. According to the cryo-SEM, liposomes are well encapsulated within the  $W_1$  phase, indicating that most liposomes remain intact during the homogenization step of formulation fabrication. After fabrication, double-encapsulation formulations were subsequently stored at 5°C to obtain stable and cream-like formulations, which can be applied on the skin in a same way as cosmetic formulations. Freezing the O phase of double-encapsulation formulations preserved their stability during the storage, and subsequent application of such system on the skin induced progressive release of liposomes and their contents. Different from the control double emulsions, the presence of cationic liposomes in the  $W_1$  phase slows down the thaw-induced instability of double emulsions, and consequently, liposomes and their

contents are gradually – rather than instantly – released from the  $W_1$  phase. The release mechanism upon the freeze-thaw treatment was internal coalescence followed by external coalescence. The role of phospholipid on the release rate of FITC-BSA was investigated, demonstrating that tuning the concentration of phospholipid in the cationic liposomes can control the release rate from double-encapsulation formulations.

## **6.2 Future Work**

The information gathered from this work gave us a better understanding of the double-encapsulation formulation. However, additional experiments are proposed in order to further investigate and test this system, thus achieving more successful applications. The follows list a few of them:

### ***Adding Penetration Enhancer in the Double-Encapsulation Formulation***

Double emulsions have the capacity to incorporate several ingredients in one compartment. Therefore, penetration enhancers are suggested to load to the O phase and/or  $W_2$  phase of this double-encapsulation formulation to facilitate the interaction of liposomes and their contents with the skin, thus enhancing the penetration of active components across the skin. The extent of skin-structure disruption can be evaluated by cryo-SEM and FTIR.

### ***In-Vitro Experiment***

*In-vitro* skin-permeation experiments using Franz-diffusion cells are a very effective and efficient method to study the amount of substances penetrated across the skin. To investigate the transdermal delivery efficiency of the optimized double-encapsulation system, *in-vitro* skin-permeation experiment will be conducted. The active

substance retained in the *stratum corneum* and viable epidermis at different time intervals will be extracted and analyzed. Besides quantitative analysis of substance retained in the skin, the penetration pathway of the optimized double-encapsulation formulation will be examined by use of confocal microscopy.

### ***In-Vivo Experiments***

*In-vivo* experiments offer valuable insights on the evaluation of the immune response when the model antigen is applied to the intact skin of mice. The immunogenicity of the model antigen FITC-BSA incorporated within double-encapsulation formulation will be determined; the adjuvanticity of cationic liposomes to stimulate the response of immune system will be assessed. By use of ELISA assay, IgG antibodies and antibodies with specificity against BSA will be detected. In addition, stain skin will be analyzed to look for recruitment of dendritic cells to the site of immunization and uptake of the fluorescent protein.

## LIST OF REFERENCES

- [1] Babiuk, S., M. Baca-Estrada, L.A. Babiuk, C. Ewen and M. Foldvari. 2000. Cutaneous vaccination: the skin as an immunologically active tissue and the challenge of antigen delivery. *Journal of Controlled Release*. 66(2-3): p. 199-214.
- [2] Barry, B.W. 2001. Novel mechanisms and devices to enable successful transdermal drug delivery. *European Journal of Pharmaceutical Sciences*. 14(2): p. 101-114.
- [3] Carrer, D.C., C. Vermehren and L.A. Bagatolli. 2008. Pig skin structure and transdermal delivery of liposomes: A two photon microscopy study. *Journal of Controlled Release*. 132(1): p. 12-20.
- [4] Michaels, A.S., S.K. Chandrasekaran and J.E. Shaw. 1975. Drug permeation through human skin: Theory and *in vitro* experimental measurement. *AIChE Journal*. 21(5): p. 985-996.
- [5] Eckert, R.L. 1989. Structure, function, and differentiation of the keratinocyte. *Physiological Reviews*. 69(4): p. 1316-1346.
- [6] Banga, A.K. 2011. Transdermal and intradermal delivery of therapeutic agents: Application of physical technologies. Taylor & Francis Group, LLC p. 219-233.
- [7] Paus, R., J.M. Schröder, K. Reich, K. Kabashima, F.T. Liu, *et al.* 2006. Who is really in control of skin immunity under *physiological* circumstances – lymphocytes, dendritic cells or keratinocytes? *Experimental Dermatology*. 15(11): p. 913-916.
- [8] Ada, G. 2001. Vaccines and Vaccination. *New England Journal of Medicine*. 345(14): p. 1042-1053.
- [9] Giudice, E.L. and J.D. Campbell. 2006. Needle-free vaccine delivery. *Advanced Drug Delivery Reviews*. 58(1): p. 68-89.
- [10] Nir, Y., A. Paz, E. Sabo and I. Potasman. 2003. Fear of injections in young adults: Prevalence and associations. *The American Journal of Tropical Medicine and Hygiene*. 68(3): p. 341-344.

- [11] Bos, J.D. and M.M.H.M. Meinardi. 2000. The 500 Dalton rule for the skin penetration of chemical compounds and drugs. *Experimental Dermatology*. 9(3): p. 165-169.
- [12] Arora, A., M.R. Prausnitz and S. Mitragotri. 2008. Micro-scale devices for transdermal drug delivery. *International Journal of Pharmaceutics*. 364(2): p. 227-236.
- [13] Warner, R.R., K.J. Stone and Y.L. Boissy. 2003. Hydration Disrupts Human Stratum Corneum Ultrastructure. *Journal of Investigative Dermatology*. 120(2): p. 275-284.
- [14] Williams, A.C. and B.W. Barry. 2004. Penetration enhancers. *Advanced Drug Delivery Reviews*. 56(5): p. 603-618.
- [15] Duracher, L., L. Blasco, J.-C. Hubaud, L. Vian and G. Marti-Mestres. 2009. The influence of alcohol, propylene glycol and 1,2-pentanediol on the permeability of hydrophilic model drug through excised pig skin. *International Journal of Pharmaceutics*. 374(1-2): p. 39-45.
- [16] Li, Y.-Z., Y.-S. Quan, L. Zang, M.-N. Jin, F. Kamiyama, *et al.* 2009. Trypsin as a novel potential absorption enhancer for improving the transdermal delivery of macromolecules. *Journal of Pharmacy and Pharmacology*. 61(8): p. 1005-1012.
- [17] Tan, G., P. Xu, L.B. Lawson, J. He, L.C. Freytag, *et al.* 2010. Hydration effects on skin microstructure as probed by high-resolution cryo-scanning electron microscopy and mechanistic implications to enhanced transcutaneous delivery of biomacromolecules. *Journal of Pharmaceutical Sciences*. 99(2): p. 730-740.
- [18] Hadgraft, J. 1999. Passive enhancement strategies in topical and transdermal drug delivery. *International Journal of Pharmaceutics*. 184(1): p. 1-6.
- [19] Kogan, A. and N. Garti. 2006. Microemulsions as transdermal drug delivery vehicles. *Advances in Colloid and Interface Science*. 123-126: p. 369-385.
- [20] Tahara, Y., S. Honda, N. Kamiya, H. Piao, A. Hirata, *et al.* 2008. A solid-in-oil nanodispersion for transcutaneous protein delivery. *Journal of Controlled Release*. 131(1): p. 14-18.
- [21] Kohli, A.K. and H.O. Alpar. 2004. Potential use of nanoparticles for transcutaneous vaccine delivery: Effect of particle size and charge. *International Journal of Pharmaceutics*. 275(1-2): p. 13-17.
- [22] Ackaert, O.W., J. Eikelenboom, H.M. Wolff and J.A. Bouwstra. 2010. Comparing different salt forms of rotigotine to improve transdermal iontophoretic delivery. *European Journal of Pharmaceutics and Biopharmaceutics*. 74(2): p. 304-310.

- [23] Herndon, T., S. Gonzalez, T.R. Gowrishankar, R. Anderson and J. Weaver. 2004. Transdermal microconduits by microscission for drug delivery and sample acquisition. *BMC Medicine*. 2(1): p. 12.
- [24] Henry, S., D.V. McAllister, M.G. Allen and M.R. Prausnitz. 1998. Microfabricated microneedles: A novel approach to transdermal drug delivery. *Journal of Pharmaceutical Sciences*. 87(8): p. 922-925.
- [25] McAllister, D.V., P.M. Wang, S.P. Davis, J.-H. Park, P.J. Canatella, *et al.* 2003. Microfabricated needles for transdermal delivery of macromolecules and nanoparticles: Fabrication methods and transport studies. *Proceedings of the National Academy of Sciences*. 100(24): p. 13755-13760.
- [26] Verbaan, F.J., S.M. Bal, D.J. van den Berg, W.H.H. Groenink, H. Verpoorten, *et al.* 2007. Assembled microneedle arrays enhance the transport of compounds varying over a large range of molecular weight across human dermatomed skin. *Journal of Controlled Release*. 117(2): p. 238-245.
- [27] Gill, H.S. and M.R. Prausnitz. 2008. Pocketed microneedles for drug delivery to the skin. *Journal of Physics and Chemistry of Solids*. 69(5-6): p. 1537-1541.
- [28] Qiu, Y., Y. Gao, K. Hu and F. Li. 2008. Enhancement of skin permeation of docetaxel: A novel approach combining microneedle and elastic liposomes. *Journal of Controlled Release*. 129(2): p. 144-150.
- [29] Badran, M.M., J. Kuntsche and A. Fahr. 2009. Skin penetration enhancement by a microneedle device (Dermaroller<sup>®</sup>) *in vitro*: Dependency on needle size and applied formulation. *European Journal of Pharmaceutical Sciences*. 36(4-5): p. 511-523.
- [30] Li, G., A. Badkar, S. Nema, C.S. Kolli and A.K. Banga. 2009. *In vitro* transdermal delivery of therapeutic antibodies using maltose microneedles. *International Journal of Pharmaceutics*. 368(1-2): p. 109-115.
- [31] Garti, N. and C. Bisperink. 1998. Double emulsions: Progress and applications. *Current Opinion in Colloid & Interface Science*. 3(6): p. 657-667.
- [32] Matsumoto, S., Y. Kita and D. Yonezawa. 1976. An attempt at preparing water-in-oil-in-water multiple-phase emulsions. *Journal of Colloid and Interface Science*. 57(2): p. 353-361.
- [33] Higashi, S., M. Shimizu, T. Nakashima, K. Iwata, F. Uchiyama, *et al.* 1995. Arterial-injection chemotherapy for hepatocellular carcinoma using monodispersed poppy-seed oil microdroplets containing fine aqueous vesicles of epirubicin. Initial medical application of a membrane-emulsification technique. *Cancer*. 75(6): p. 1245-1254.

- [34] Grossiord, J.L., M. Seiller and A. Silva-Cunha. 1998. Multiple emulsions: Structure, properties and applications. de Sante ed., Paris. p. 57-80.
- [35] Sugiura, S., M. Nakajima, K. Yamamoto, S. Iwamoto, T. Oda, *et al.* 2004. Preparation characteristics of water-in-oil-in-water multiple emulsions using microchannel emulsification. *Journal of Colloid and Interface Science*. 270(1): p. 221-228.
- [36] Florence, A.T. and D. Whitehill. 1981. Some features of breakdown in water-in-oil-in-water multiple emulsions. *Journal of Colloid and Interface Science*. 79(1): p. 243-256.
- [37] Gaiti, N., A. Aserin and Y. Cohen. 1994. Mechanistic considerations on the release of electrolytes from multiple emulsions stabilized by BSA and nonionic surfactants. *Journal of Controlled Release*. 29(1-2): p. 41-51.
- [38] Garti, N. and A. Benichou. 2001. Double emulsions for controlled-release applications-Progress and trends. Marcel Dekker, New York. p. 377-407.
- [39] Magdassi, S. and N. Garti. 1987. Formation of water/oil/water multiple emulsions with solid oil phase. *Journal of Colloid and Interface Science*. 120(2): p. 537-539.
- [40] Rojas, E.C. and K.D. Papadopoulos. 2007. Induction of instability in water-in-oil-in-water double emulsions by freeze-thaw cycling. *Langmuir*. 23(13): p. 6911-6917.
- [41] Rojas, E.C., J.A. Staton, V.T. John and K.D. Papadopoulos. 2008. Temperature-induced protein release from water-in-oil-in-water double emulsions. *Langmuir*. 24(14): p. 7154-7160.
- [42] Shima, M., M. Tanaka, T. Fujii, K. Egawa, Y. Kimura, *et al.* 2006. Oral administration of insulin included in fine W/O/W emulsions to rats. *Food Hydrocolloids*. 20(4): p. 523-531.
- [43] Qi, X., L. Wang and J. Zhu. 2011. Water-in-oil-in-water double emulsions: An excellent delivery system for improving the oral bioavailability of pidotimod in rats. *Journal of Pharmaceutical Sciences*. 100(6): p. 2203-2211.
- [44] Laugel, C., A. Baillet, M. P. Youenang Piemi, J.P. Marty and D. Ferrier. 1998. Oil-water-oil multiple emulsions for prolonged delivery of hydrocortisone after topical application: Comparison with simple emulsions. *International Journal of Pharmaceutics*. 160(1): p. 109-117.
- [45] Okochi, H. and M. Nakano. 2000. Preparation and evaluation of w/o/w type emulsions containing vancomycin. *Advanced Drug Delivery Reviews*. 45(1): p. 5-26.

- [46] Buyukozturk, F., J.C. Benneyan and R.L. Carrier. 2010. Impact of emulsion-based drug delivery systems on intestinal permeability and drug release kinetics. *Journal of Controlled Release*. 142(1): p. 22-30.
- [47] Bozkir, A. and G. Hayta. 2004. Preparation and evaluation of multiple emulsions water-in-oil-in-water (w/o/w) as delivery system for influenza virus antigens. *Journal of Drug Targeting*. 12(3): p. 157-164.
- [48] Bozkir, A., G. Hayta and O.M. Saka. 2004. Comparison of biodegradable nanoparticles and multiple emulsions (water-in-oil-in-water) containing influenza virus antigen on the *in vivo* immune response in rats. *Pharmazie*. 59(9): p. 723-725.
- [49] Wang, Q., G. Tan, L.B. Lawson, V.T. John and K.D. Papadopoulos. 2010. Liposomes in double-emulsion globules. *Langmuir*. 26(5): p. 3225-3231.
- [50] Jaimes-Lizcano, Y.A., L.B. Lawson and K.D. Papadopoulos. 2011. Oil-frozen W<sub>1</sub>/O/W<sub>2</sub> double emulsions for dermal biomacromolecular delivery containing ethanol as chemical penetration. *Journal of Pharmaceutical Sciences*. 100(4): p. 1398-1406.
- [51] Wang, Q., Y.A. Jaimes-Lizcano, L.B. Lawson, V.T. John and K.D. Papadopoulos. 2011. Improved dermal delivery of FITC-BSA using a combination of passive and active methods. *Journal of Pharmaceutical Sciences*. 100(11): p. 4804-4814.
- [52] Fechner, A., A. Knoth, I. Scherze and G. Muschiolik. 2007. Stability and release properties of double-emulsions stabilised by caseinate-dextran conjugates. *Food Hydrocolloids*. 21(5-6): p. 943-952.
- [53] Sapei, L., M.A. Naqvi and D. Rousseau. 2011. Stability and release properties of double emulsions for food applications. *Food Hydrocolloids*. 27(2): p. 316-323.
- [54] Gallarate, M., M.E. Carlotti, M. Trotta and S. Bovo. 1999. On the stability of ascorbic acid in emulsified systems for topical and cosmetic use. *International Journal of Pharmaceutics*. 188(2): p. 233-241.
- [55] Yan, J. and R. Pal. 2001. Osmotic swelling behavior of globules of W/O/W emulsion liquid membranes. *Journal of Membrane Science*. 190(1): p. 79-91.
- [56] Raghuraman, B., N. Tirmizi and J. Wiencek. 1994. Emulsion Liquid Membranes for Wastewater Treatment: Equilibrium Models for Some Typical Metal-Extractant Systems. *Environmental Science & Technology*. 28(6): p. 1090-1098.
- [57] Pays, K., J. Giermanska-Kahn, B. Pouligny, J. Bibette and F. Leal-Calderon. 2002. Double emulsions: How does release occur? *Journal of Controlled Release*. 79(1-3): p. 193-205.

- [58] Kita, Y., S. Matsumoto and D. Yonezawa. 1977. Viscometric method for estimating the stability of W/O/W-type multiple-phase emulsions. *Journal of Colloid and Interface Science*. 62(1): p. 87-94.
- [59] Colinart, P., S. Delepine, G. Trouve and H. Renon. 1984. Water transfer in emulsified liquid membrane processes. *Journal of Membrane Science*. 20(2): p. 167-187.
- [60] Wen, L. and K.D. Papadopoulos. 2000. Visualization of water transport in W<sub>1</sub>/O/W<sub>2</sub> emulsions. *Colloids and Surfaces A: Physicochemical and Engineering Aspects*. 174(1-2): p. 159-167.
- [61] Matsumoto, S., T. Inoue, M. Kohda and K. Ikura. 1980. Water permeability of oil layers in W/O/W emulsions under osmotic pressure gradients. *Journal of Colloid and Interface Science*. 77(2): p. 555-563.
- [62] Olivieri, L., M. Seiller, L. Bromberg, M. Besnard, T.-N.-L. Duong, *et al.* 2003. Optimization of a thermally reversible W/O/W multiple emulsion for shear-induced drug release. *Journal of Controlled Release*. 88(3): p. 401-412.
- [63] Mezei, M. and V. Gulasekharam. 1980. Liposomes - a selective drug delivery system for the topical route of administration I. Lotion dosage form. *Life Sciences*. 26(18): p. 1473-1477.
- [64] Baillie, A.J., A.T. Florence, L.R. Hume, G.T. Muirhead and A. Rogerson. 1985. The preparation and properties of niosomes—non-ionic surfactant vesicles. *Journal of Pharmacy and Pharmacology*. 37(12): p. 863-868.
- [65] Knepp, V.M., R.S. Hinz, F.C. Szoka Jr and R.H. Guy. 1988. Controlled drug release from a novel liposomal delivery system. I. Investigation of transdermal potential. *Journal of Controlled Release*. 5(3): p. 211-221.
- [66] Knepp, V.M., F.C. Szoka Jr and R.H. Guy. 1990. Controlled drug release from a novel liposomal delivery system. II. Transdermal delivery characteristics. *Journal of Controlled Release*. 12(1): p. 25-30.
- [67] Cevc, G. and G. Blume. 1992. Lipid vesicles penetrate into intact skin owing to the transdermal osmotic gradients and hydration force. *Biochimica et Biophysica Acta (BBA) - Biomembranes*. 1104(1): p. 226-232.
- [68] Dayan, N. and E. Touitou. 2000. Carriers for skin delivery of trihexyphenidyl HCl: Ethosomes vs. liposomes. *Biomaterials*. 21(18): p. 1879-1885.
- [69] Betz, G., R. Imboden and G. Imanidis. 2001. Interaction of liposome formulations with human skin *in vitro*. *International Journal of Pharmaceutics*. 229(1-2): p. 117-129.

- [70] Verma, D.D., S. Verma, G. Blume and A. Fahr. 2003. Particle size of liposomes influences dermal delivery of substances into skin. *International Journal of Pharmaceutics*. 258(1-2): p. 141-151.
- [71] Honeywell-Nguyen, P.L., G.S. Gooris and J.A. Bouwstra. 2004. Quantitative assessment of the transport of elastic and rigid vesicle components and a model drug from these vesicle formulations into human skin *in vivo*. *Journal of Investigative Dermatology*. 123(5): p. 902-910.
- [72] Ita, K.B., J. Du Preez, M.E. Lane, J. Hadgraft and J. du Plessis. 2007. Dermal delivery of selected hydrophilic drugs from elastic liposomes: Effect of phospholipid formulation and surfactants. *Journal of Pharmacy and Pharmacology*. 59(9): p. 1215-1222.
- [73] Dragicevic-Curic, N., D. Scheglmann, V. Albrecht and A. Fahr. 2008. Temoporfin-loaded invasomes: Development, characterization and *in vitro* skin penetration studies. *Journal of Controlled Release*. 127(1): p. 59-69.
- [74] Xu, P., G. Tan, J. Zhou, J. He, L.B. Lawson, *et al.* 2009. Undulating tubular liposomes through incorporation of a synthetic skin ceramide into phospholipid bilayers. *Langmuir*. 25(18): p. 10422-10425.
- [75] Dragicevic-Curic, N., S. Gräfe, B. Gitter, S. Winter and A. Fahr. 2010. Surface charged temoporfin-loaded flexible vesicles: *In vitro* skin penetration studies and stability. *International Journal of Pharmaceutics*. 384(1-2): p. 100-108.
- [76] El Zaafarany, G.M., G.A.S. Awad, S.M. Holayel and N.D. Mortada. 2010. Role of edge activators and surface charge in developing ultradeformable vesicles with enhanced skin delivery. *International Journal of Pharmaceutics*. 397(1-2): p. 164-172.
- [77] Cevc, G., A.G. Schätzlein, H. Richardsen and U. Vierl. 2003. Overcoming semipermeable barriers, such as the skin, with ultradeformable mixed lipid vesicles, Transfersomes, liposomes, or mixed lipid micelles. *Langmuir*. 19(26): p. 10753-10763.
- [78] Cevc, G., D. Gebauer, J. Stieber, A. Schätzlein and G. Blume. 1998. Ultraflexible vesicles, Transfersomes, have an extremely low pore penetration resistance and transport therapeutic amounts of insulin across the intact mammalian skin. *Biochimica et Biophysica Acta (BBA) - Biomembranes*. 1368(2): p. 201-215.
- [79] Cevc, G. and G. Blume. 2001. New, highly efficient formulation of diclofenac for the topical, transdermal administration in ultradeformable drug carriers, Transfersomes. *Biochimica et Biophysica Acta (BBA) - Biomembranes*. 1514(2): p. 191-205.
- [80] Cevc, G. and G. Blume. 2003. Biological activity and characteristics of triamcinolone-acetonide formulated with the self-regulating drug carriers,

Transfersomes®. *Biochimica et Biophysica Acta (BBA) - Biomembranes*. 1614(2): p. 156-164.

[81] Jung, S., N. Otberg, G. Thiede, H. Richter, W. Sterry, *et al.* 2006. Innovative liposomes as a transfollicular drug delivery system: Penetration into porcine hair follicles. *Journal of Investigative Dermatology*. 126(8): p. 1728-1732.

[82] Kitagawa, S. and M. Kasamaki. 2006. Enhanced delivery of retinoic acid to skin by cationic liposomes. *Chemical and Pharmaceutical Bulletin*. 54(2): p. 242-244.

[83] Touitou, E., N. Dayan, L. Bergelson, B. Godin and M. Eliaz. 2000. Ethosomes - Novel vesicular carriers for enhanced delivery: Characterization and skin penetration properties. *Journal of Controlled Release*. 65(3): p. 403-418.

[84] Yan, W., W. Chen and L. Huang. 2007. Mechanism of adjuvant activity of cationic liposome: Phosphorylation of a MAP kinase, ERK and induction of chemokines. *Molecular Immunology*. 44(15): p. 3672-3681.

[85] El Maghraby, G.M., B.W. Barry and A.C. Williams. 2008. Liposomes and skin: From drug delivery to model membranes. *European Journal of Pharmaceutical Sciences*. 34(4-5): p. 203-222.

[86] Ganesan, M.G., N.D. Weiner, G.L. Flynn and N.F.H. Ho. 1984. Influence of liposomal drug entrapment on percutaneous absorption. *International Journal of Pharmaceutics*. 20(1-2): p. 139-154.

[87] Kato, A., Y. Ishibashi and Y. Miyake. 1987. Effect of egg yolk lecithin on transdermal delivery of bunazosin hydrochloride. *Journal of Pharmacy and Pharmacology*. 39(5): p. 399-400.

[88] Kirjavainen, M., A. Urtti, I. Jääskeläinen, T. Marjukka Suhonen, P. Paronen, *et al.* 1996. Interaction of liposomes with human skin *in vitro* - The influence of lipid composition and structure. *Biochimica et Biophysica Acta (BBA) - Lipids and Lipid Metabolism*. 1304(3): p. 179-189.

[89] Cevc, G., A. Schätzlein and H. Richardsen. 2002. Ultradeformable lipid vesicles can penetrate the skin and other semi-permeable barriers unfragmented. Evidence from double label CLSM experiments and direct size measurements. *Biochimica et Biophysica Acta (BBA) - Biomembranes*. 1564(1): p. 21-30.

[90] Torchilin, V.P. 2005. Recent advances with liposomes as pharmaceutical carriers. *Nature Reviews Drug Discovery*. 4(2): p. 145-160.

[91] Huang, Y.-Z., J.-Q. Gao, W.-Q. Liang and S. Nakagawa. 2005. Preparation and characterization of liposomes encapsulating chitosan nanoparticles. *Biological & Pharmaceutical Bulletin*. 28(2): p. 387-390.

- [92] Maurer, N., K.F. Wong, M.J. Hope and P.R. Cullis. 1998. Anomalous solubility behavior of the antibiotic ciprofloxacin encapsulated in liposomes: A  $^1\text{H}$ -NMR study. *Biochimica et Biophysica Acta (BBA) - Biomembranes*. 1374(1-2): p. 9-20.
- [93] Sułkowski, W.W., D. Pentak, K. Nowak and A. Sułkowska. 2005. The influence of temperature, cholesterol content and pH on liposome stability. *Journal of Molecular Structure*. 744-747: p. 737-747.
- [94] Klibanov, A.L., K. Maruyama, V.P. Torchilin and L. Huang. 1990. Amphipathic polyethyleneglycols effectively prolong the circulation time of liposomes. *FEBS Letters*. 268(1): p. 235-237.
- [95] Moghimi, S.M. and J. Szebeni. 2003. Stealth liposomes and long circulating nanoparticles: Critical issues in pharmacokinetics, opsonization and protein-binding properties. *Progress in Lipid Research*. 42(6): p. 463-478.
- [96] Boyer, C. and J.A. Zasadzinski. 2007. Multiple lipid compartments slow vesicle contents release in lipases and serum. *ACS Nano*. 1(3): p. 176-182.
- [97] Dai, C., B. Wang, H. Zhao, B. Li and J. Wang. 2006. Preparation and characterization of liposomes-in-alginate (LIA) for protein delivery system. *Colloids and Surfaces B: Biointerfaces*. 47(2): p. 205-210.
- [98] Yoshioka, T., N. Skalko, M. Gursel, G. Gregoriadis and A.T. Florence. 1995. A non-ionic surfactant vesicle-in-water-in-oil (v/w/o) system: Potential uses in drug and vaccine delivery. *Journal of Drug Targeting*. 2(6): p. 533-539.
- [99] Bromberg, L.E. and A.M. Klibanov. 1995. Transport of proteins dissolved in organic solvents across biomimetic membranes. *Proceedings of the National Academy of Sciences*. 92(5): p. 1262-1266.
- [100] Lopes, L.B., E. Furnish, P. Komalavilas, B.L. Seal, A. Panitch, *et al.* 2008. Enhanced skin penetration of P20 phosphopeptide using protein transduction domains. *European Journal of Pharmaceutics and Biopharmaceutics*. 68(2): p. 441-445.
- [101] Ding, Z., S. Bal, S. Romeijn, G. Kersten, W. Jiskoot, *et al.* 2011. Transcutaneous immunization studies in mice using diphtheria toxoid-loaded vesicle formulations and a microneedle array. *Pharmaceutical Research*. 28(1): p. 145-158.
- [102] Peltonen, L., J. Hirvonen and J. Yliruusi. 2001. The behavior of sorbitan surfactants at the water-oil interface: Straight-chained hydrocarbons from pentane to dodecane as an oil phase. *Journal of Colloid and Interface Science*. 240(1): p. 272-276.
- [103] Hou, W. and K.D. Papadopoulos. 1997.  $W_1/O/W_2$  and  $O_1/W/O_2$  globules stabilized with Span 80 and Tween 80. *Colloids and Surfaces A: Physicochemical and Engineering Aspects*. 125(2): p. 181-187.

- [104] Wen, L. and K.D. Papadopoulos. 2001. Effects of osmotic pressure on water transport in  $W_1/O/W_2$  emulsions. *Journal of Colloid and Interface Science*. 235(2): p. 398-404.
- [105] Hou, W. and K.D. Papadopoulos. 1996. Stability of water-in-oil-in-water type globules. *Chemical Engineering Science*. 51(22): p. 5043-5051.
- [106] Csóka, I. and I. Erős. 1997. Stability of multiple emulsions: I. Determination of factors influencing multiple drop breakdown. *International Journal of Pharmaceutics*. 156(1): p. 119-123.
- [107] Santini, E., L. Liggieri, L. Sacca, D. Clausse and F. Ravera. 2007. Interfacial rheology of Span 80 adsorbed layers at paraffin oil-water interface and correlation with the corresponding emulsion properties. *Colloids and Surfaces A: Physicochemical and Engineering Aspects*. 309(1-3): p. 270-279.
- [108] Pays, K., J. Giermanska-Kahn, B. Pouligny, J. Bibette and F. Leal-Calderon. 2001. Coalescence in surfactant-stabilized double emulsions. *Langmuir*. 17(25): p. 7758-7769.
- [109] Ficheux, M.F., L. Bonakdar, F. Leal-Calderon and J. Bibette. 1998. Some stability criteria for double emulsions. *Langmuir*. 14(10): p. 2702-2706.
- [110] Villa, C.H., L.B. Lawson, Y. Li and K.D. Papadopoulos. 2003. Internal coalescence as a mechanism of instability in water-in-oil-in-water double-emulsion globules. *Langmuir*. 19(2): p. 244-249.
- [111] Kabalnov, A. and H. Wennerström. 1996. Macroemulsion stability: The oriented wedge theory revisited. *Langmuir*. 12(2): p. 276-292.
- [112] Muderhwa, J.M., S.W. Rothwell and C.R. Alving. 1998. Emulsification of liposomes with incomplete Freund's adjuvant: Stability of the liposomes and the emulsion. *Journal of Liposome Research*. 8(2): p. 183-194.
- [113] Muderhwa, J.M., G.R. Matyas, L.E. Spitler and C.R. Alving. 1999. Oil-in-water liposomal emulsions: Characterization and potential use in vaccine delivery. *Journal of Pharmaceutical Sciences*. 88(12): p. 1332-1339.
- [114] Wu, J., J.B. Li, J. Zhao and R. Miller. 2000. Dynamic characterization of phospholipid/protein competitive adsorption at the aqueous solution/chloroform interface. *Colloids and Surfaces A: Physicochemical and Engineering Aspects*. 175(1-2): p. 113-120.
- [115] He, Q., Y. Zhang, G. Lu, R. Miller, H. Möhwald, *et al.* 2008. Dynamic adsorption and characterization of phospholipid and mixed phospholipid/protein layers at liquid/liquid interfaces. *Advances in Colloid and Interface Science*. 140(2): p. 67-76.

- [116] Lawson, L.B. and K.D. Papadopoulos. 2004. Effects of a phospholipid cosurfactant on external coalescence in water-in-oil-in-water double-emulsion globules. *Colloids and Surfaces A: Physicochemical and Engineering Aspects*. 250(1-3): p. 337-342.
- [117] McConnell, H.M. 1991. Structures and transitions in lipid monolayers at the air-water interface. *Annual Review of Physical Chemistry*. 42(1): p. 171-195.
- [118] Cheng, J., J.-F. Chen, M. Zhao, Q. Luo, L.-X. Wen, *et al.* 2007. Transport of ions through the oil phase of  $W_1/O/W_2$  double emulsions. *Journal of Colloid and Interface Science*. 305(1): p. 175-182.
- [119] Tojo, K. 1987. Mathematical modeling of transdermal drug delivery. *Journal of chemical engineering of Japan*. 20: p. 300-308.
- [120] Haq, M., E. Smith, D. John, M. Kalavala, C. Edwards, *et al.* 2009. Clinical administration of microneedles: Skin puncture, pain and sensation. *Biomedical Microdevices*. 11(1): p. 35-47.
- [121] Sandby-Møller, J., T. Poulsen and H.C. Wulf. 2003. Epidermal thickness at different body sites: Relationship to age, gender, pigmentation, blood content, skin type and smoking habits. *Acta Dermato-Venereologica*. 83(6): p. 410-413.
- [122] Altin, J.G. and C.R. Parish. 2006. Liposomal vaccines — Targeting the delivery of antigen. *Methods*. 40(1): p. 39-52.
- [123] Christensen, D., E.M. Agger, L.V. Andreasen, D. Kirby, P. Andersen, *et al.* 2009. Liposome-based cationic adjuvant formulations (CAF): Past, present, and future. *Journal of Liposome Research*. 19(1): p. 2-11.
- [124] Bhowmick, S., T. Mazumdar, R. Sinha and N. Ali. 2010. Comparison of liposome based antigen delivery systems for protection against *Leishmania donovani*. *Journal of Controlled Release*. 141(2): p. 199-207.
- [125] Dubey, V., D. Mishra, A. Asthana and N.K. Jain. 2006. Transdermal delivery of a pineal hormone: Melatonin via elastic liposomes. *Biomaterials*. 27(18): p. 3491-3496.
- [126] Gillet, A., A. Grammenos, P. Compère, B. Evrard and G. Piel. 2009. Development of a new topical system: Drug-in-cyclodextrin-in-deformable liposome. *International Journal of Pharmaceutics*. 380(1-2): p. 174-180.
- [127] Loan Honeywell-Nguyen, P., H.W. Wouter Groenink and J.A. Bouwstra. 2006. Elastic vesicles as a tool for dermal and transdermal delivery. *Journal of Liposome Research*. 16(3): p. 273-280.

- [128] van den Bergh, B.A.I., J.A. Bouwstra, H.E. Junginger and P.W. Wertz. 1999. Elasticity of vesicles affects hairless mouse skin structure and permeability. *Journal of Controlled Release*. 62(3): p. 367-379.
- [129] Verma, D.D., S. Verma, G. Blume and A. Fahr. 2003. Liposomes increase skin penetration of entrapped and non-entrapped hydrophilic substances into human skin: A skin penetration and confocal laser scanning microscopy study. *European Journal of Pharmaceutics and Biopharmaceutics*. 55(3): p. 271-277.
- [130] Malzert-Fréon, A., J.-P. Benoît and F. Boury. 2008. Interactions between poly(ethylene glycol) and protein in dichloromethane/water emulsions: A study of interfacial properties. *European Journal of Pharmaceutics and Biopharmaceutics*. 69(3): p. 835-843.
- [131] Kuntsche, J., J.C. Horst and H. Bunjes. 2011. Cryogenic transmission electron microscopy (cryo-TEM) for studying the morphology of colloidal drug delivery systems. *International Journal of Pharmaceutics*. 417(1-2): p. 120-137.
- [132] Christensen, D., K.S. Korsholm, I. Rosenkrands, T. Lindenstrøm, P. Andersen, *et al.* 2007. Cationic liposomes as vaccine adjuvants. *Expert Review of Vaccines*. 6(5): p. 785-796.
- [133] Herhold, A.B., D. Ertas, A.J. Levine and H.E. King, Jr. 1999. Impurity mediated nucleation in hexadecane-in-water emulsions. *Physical Review E*. 59(6): p. 6946-6955.
- [134] Zhang, F. and A. Proctor. 1997. Rheology and stability of phospholipid-stabilized emulsions. *Journal of the American Oil Chemists Society*. 74(7): p. 869-874.
- [135] Saito, H., A. Kawagishi, M. Tanaka, T. Tanimoto, S. Okada, *et al.* 1999. Coalescence of lipid emulsions in floating and freeze-thawing processes: Examination of the coalescence transition state theory. *Journal of Colloid and Interface Science*. 219(1): p. 129-134.
- [136] Thanasukarn, P., R. Pongsawatmanit and D.J. McClements. 2004. Influence of emulsifier type on freeze-thaw stability of hydrogenated palm oil-in-water emulsions. *Food Hydrocolloids*. 18(6): p. 1033-1043.
- [137] Sengupta, A.K. and K.D. Papadopoulos. 1992. van der Waals interaction between a colloid and the wall of its host spherical cavity. *Journal of Colloid and Interface Science*. 152(2): p. 534-542.
- [138] Wang, Q., E.C. Rojas and K.D. Papadopoulos. 2012. Cationic liposomes in double emulsions for controlled release. *Journal of Colloid and Interface Science*. 383(1): p. 89-95.

- [139] Latif, N. and B. Bachhawat. 1984. The effect of surface charges of liposomes in immunopotential. *Bioscience Reports*. 4(2): p. 99-107.
- [140] Nakanishi, T., J. Kunisawa, A. Hayashi, Y. Tsutsumi, K. Kubo, *et al.* 1997. Positively charged liposome functions as an efficient immunoadjuvant in inducing immune responses to soluble proteins. *Biochemical and Biophysical Research Communications*. 240(3): p. 793-797.
- [141] Smith Korsholm, K., E.M. Agger, C. Foged, D. Christensen, J. Dietrich, *et al.* 2007. The adjuvant mechanism of cationic dimethyldioctadecylammonium liposomes. *Immunology*. 121(2): p. 216-226.

## **BIOGRAPHY**

Qing Wang was born on November 24, 1980 in Shandong Province, People's Republic of China. The author received her Bachelor degree in Chemical Engineering from Shandong Polytechnic University, China in 2003. Her Master degree in Chemical Engineering, specializing in drug delivery, was received in 2006 from Beijing University of Chemical Technology, China. There she developed a nanoparticle-based pesticide formulation with controlled release property. She enrolled in the Ph.D. program of the Department of Chemical Engineering at Tulane University in the spring of 2007, where she was presented the "American Institute of Chemists Award" in 2011 and the "Distinguished Graduate Student Awards" in 2009, 2011 and 2012.